

**UNIVERSITA' DEGLI STUDI DI ROMA**

**“LA SAPIENZA”**

**FACOLTA' DI SCIENZE MATEMATICHE, FISICHE E NATURALI**

**DOTTORATO DI RICERCA IN SCIENZE CHIMICHE - CICLO XVII**

**Chimica Macromolecolare e Biologica**

***SYNTHESIS OF MOLECULES WITH POTENTIAL  
ANTIAGGREGATION ACTIVITY OF  $\beta$ -AMYLOID IN  
ALZHEIMER'S DISEASE***

**Dottoranda**

**Diana CELONA**

**Matricola 010619**

**Relatori**

**Prof. Armandodoriano Bianco**

**Dott.ssa Maria Ornella Tinti**

**Dott.ssa Patrizia Minetti**

**Coordinatore**

**Prof. Pasquale De Santis**

Anno Accademico 2001/2002

Dipartimento di Chimica, Dipartimento di Scienze Biochimiche  
R&D Department Sigma-Tau Industrie Farmaceutiche Riunite S.p.A.

# INDEX

## 1. Introduction

I. <u>Alzheimer and Amyloid</u>	pag. 3
• Alzheimer's Disease (AD)	pag. 3
• Symptomatology and Clinical Features	pag. 4
• Causes	pag. 5
• AD Genetics	pag. 6
II. <u><math>\beta</math>-Amyloid</u>	pag. 7
• The Structure of $\beta$ -Amyloid ( $A\beta$ )	pag. 7
• The Amyloid Precursor Protein (APP)	pag. 7
• Protolysis of the APP	pag. 8
• The $A\beta$ Hypothesis of Alzheimer's Disease	pag. 11
• Fibrillogenesis and Aggregation Process	pag. 12
III. <u>Current Discovery Targets – Potential Strategies</u>	pag. 16
• Inhibition of $A\beta_{1-42}$ and $A\beta_{1-40}$ fibrillogenesis and Aggregation	pag. 17
• Fibrillogenesis Studies Techniques	pag. 19
• Staining Identification Methods of Amyloid	pag. 20
• Thioflavin Test ThT	pag. 21
• Assay Method	pag. 24
IV. <u>Molecular Modelling</u>	pag. 26
• $A\beta$ Model Building	pag. 26
• Interaction of $A\beta$ Model 12-42 with Inhibitors	pag. 29
V. <u>Diagnostic Target</u>	pag. 31

## 2. Results and Discussion

I. <u>Chemistry</u>	pag. 35
• The Pamoic Acid Derivatives	pag. 35
• The Set Up of Non-Labelled 1,1'-methylene-2-naphthol (ST1859) Synthesis	pag. 37
• Ether and Ester Derivatives of 1,1'-methylene-2-naphthol	pag. 39
• Halide Derivatives of 1,1'-methylene-2-naphthol	pag. 42

• Aliphatic and Aryl Derivatives of 1,1'-methylene-2-naphthol	pag. 49
• 1,1'-methylene- $\alpha$ -naphthol Compound	pag. 52
• 1,1'-binaphthalene Compounds	pag. 52
• 1-(2-hydroxybenzyl)-2-naphthol Compound	pag. 53
• Amino Bis-Naphthol Derivatives	pag. 54
• Diaryloximethane Compounds as Models for 1,1'-methylene-2-naphthol Derivatives	pag. 57
• Benzoamide Tetraline Compounds	pag. 60
II. <u>Biology and SAR Analysis</u>	pag. 63
III. <u>The Solubility Issue</u>	pag. 71
<b>3. Conclusions</b>	pag. 72
<b>4. Experimental Section</b>	pag. 74
I. <u>Chemistry</u>	pag. 74
II. <u>Biology</u>	pag. 124
<b>5. Bibliography</b>	pag. 127

# 1. Introduction

## I. Alzheimer and Amyloid

Elderly age makes behavioural changes that, normally, do not completely upset the quality of life. Changes come from cerebral structure variations which are due to the alteration of brain weight and the loss of its proteic content.

The number of neuronal cells decreases or becomes smaller in subcortical zone. These changes are the reason for sleep, appetite and memory loss, and motor activity upset, all of which are typical signs of elderly age.

“Dementia” does not mean elderly age, and it is not directly linked to it. Many people keep their intellectual capacity intact throughout life.

“Dementia” appears in people of about 45 years of age, it is rare from 45 to 65. Many geriatric diseases are due to a neurological collapse that results in different degrees of dementia. Alzheimer’s disease (AD) accounts for about half of known dementia diseases. AD is currently the fourth leading cause of dementia. Twenty –five million people worldwide, including 4 million Americans, are estimated to suffer from AD.

- Alzheimer’s disease (AD)

Alzheimer’s disease was first described by a German physician Alois Alzheimer in 1906<sup>1</sup>. He first demonstrated the typical microscopic changes in the autopsy of a woman in her 50’s who had suffered what seemed to be a mental illness. Through a microscope he observed brain cells filled with twisted strands of fiber, surrounded by dense deposits. However, the exact biochemical nature of these structures remained elusive for almost 80 years, until protein chemical and molecular biological studies showed their main components. For many years AD was considered a rare pre senile dementia form. In the 70’s it was classified as just another senile pathology because of its common symptomatology and some pathological aspects described by Alzheimer. Now day 70% of dementia is AD, and it is well known that it is a fatal, progressive neurodegenerative disorder characterized by memory loss, cognitive deficits and behavioral changes. Morphologically, the disease is characterized by neuropathological loss of cerebral neurons from particular regions of the brain accompanied by the presence of

neurofibrillary tangles and senile plaques. These two pathognomic histologic features of the disease consisted and still consist of i) tangles, that is, filaments of the microtubule-associated protein tau; ii) of senile plaques, whose main protein component is the amyloid  $\beta$ -protein (A $\beta$ ). These features are the hallmarks of Alzheimer's disease. The average course of the disease, from the time it is recognized to death, is about 6 to 8 years, but it may range from under 2 years to over 20 years.

A very small minority of Alzheimer patients are under 50 years of age, while most are over 65. The prevalence of dementia doubles with each 5 years' increase in age, from 3 % among all those aged 60, to 4-5 % among all aged 65 and 30-40 % among those over the age of 80 years. In 1998 twenty-five million people world wide were estimated to suffer from AD. Over 75 % of all people with dementia in the world live in the developing countries, mainly India , China, and Latin America.

In the absence of a cure, extrapolation of current statistics shows that by the 2040 the number of AD patients will quintuple.

- Symptomatology and Clinical Features<sup>2</sup>

Significant disturbances in social behaviour, mood and appraisal of reality occur in most patients and constitute a major source of impaired quality of life for patients and their caregivers. The earliest symptom of AD is usually an insidiously progressive disorder of memory, followed by disturbances of judgement, which occur frequently and at times can lead to disastrous personal and financial losses.

Gross behavioural disturbances may occur, like suspiciousness, progressing to frank paranoia. The patients suffer hallucinations, both visual and auditory, delusions, dysphoria and depression, fearfulness, disturbances of motor activity , wandering, purposeless movements, inappropriate acts, aggressiveness, which may be verbal and physical. Other behavioural symptoms are restlessness/hyperactivity, apathy, resistance to intervention for hygiene, nutrition, and personal safety. Other classical symptoms are the reversal of day and night and wandering during the night.

The later stage of the disease is characterized by unexplained phobias and anxieties, to the point of incontinence of urine and stool.

A small percentage of AD patients develop myoclonus and seizures.

Some patients may develop symptoms of Parkinson's disease such as bradykinesia, rigidity, hypokinetic speech, slow shuffling gait. In recent years many advances have been made and much is known about this disease. It is now possible to diagnose the disease with as much as 90-percent certainty, and identify three progressively worsening stages: mild, moderate and severe, but even a century after the discovery of the first symptoms, there are still no definite answers to many questions, and still no cure. The key to confronting and treating AD could be understanding its etiology and pathobiology.

- Causes

Attention was focused on the senile plaque (also known as dense core or neuritic plaque) as a key feature of the neuropathology of AD. It has been known since 1968 that the density of the senile plaques found in brain post-mortems shows a significant correlation with the severity of the clinical dementia measured in life. The senile plaque, some 50mm in diameter is a complex lesion of the cortical neuropil. A central deposit of extracellular amyloid fibrils (the core) is surrounded by dystrophic neurites and by activated microglia, a type of brain inflammatory cell, and reactive glial cells, called astrocytes. The major protein component of the amyloid core is the 40-42 amino acid residue  $\beta$ -amyloid protein ( $A\beta$ ) although a number of other proteins are also associated with senile plaques<sup>3</sup>. In AD, amyloid deposits represent a starting point to formulate a strategy in order to discover the etiology of the disease. Amyloid deposits present a variety of morphologies; three general forms may be defined on the basis of their gross morphology, anatomical site, and fibrillar characteristics<sup>1</sup>:

1. Senile plaques, which are areas of damaged neuropil containing fibrillar deposits of  $A\beta$ , often in the form of dense plaque-cores, as well as reactive astrocytes, activated microglia and varying amounts of dystrophic neurites at the periphery;
2. Diffuse plaques, less dense, are not associated with dystrophic neurites, activated microglia, or reactive astrocytes. They are found throughout the neuropil, in areas of the brain generally not implicated in clinical AD; they contain an amorphous, cotton candy-like appearance, little or no fibrillar  $A\beta$  and are not associated with obvious neuropil damage. Moreover these diffuse plaques are often found in

abundance in elderly, cognitively normal people, leading to the suggestion that these may be the precursor to pathogenic dense plaques.

3. Vascular deposits, which are found in the walls of small cerebral blood vessels and contain accumulations of fibrillar A $\beta$ .

Neurofibrillary tangles are found in the brain regions critical to higher brain function. Biochemical analysis reveals that the filamentous form of the Tau protein found in these tangles is hyperphosphorylated. Tau hyperphosphorylation renders insoluble this otherwise highly soluble cytosolic protein, and this modified form of Tau is also found in many plaque-associated dystrophic neurites. Interestingly, Tau containing neurofibrillary tangles are found in a number of other, uncommon neurodegenerative diseases, while the amyloid-containing neuritic plaques are unique to AD.

Despite the intriguing similarity between the otherwise dissimilar neurodegenerative disorders (such as Parkinson, Huntington, prion and amyotrophic diseases), the central question of whether the associated abnormal protein aggregates themselves cause disease or are simply byproducts of the disease process has not been definitely settled. Are the amyloid plaques and neurofibrillary tangle lesions causative, or are they merely “tombstones” or markers of regions that have degenerated due to pathogenic events not yet clearly defined? As reported below, the identification of genes associated with AD clearly demonstrates that alterations in the proteolytic processing that produces amyloid- $\beta$  protein can cause AD. Thus A $\beta$  is either the molecular culprit or an intimately linked epiphenomenon<sup>3</sup>.

- AD Genetics<sup>3</sup>

Three genes have been clearly identified as causative and one gene as a risk factor in AD<sup>4</sup>. The first identified FAD (familial AD or FAD)-causing mutation<sup>5-6</sup> is found in the gene that encodes the amyloid  $\beta$ -precursor protein ( $\beta$ -APP), on chromosome 21. It is relative to A $\beta$  phenotype: A $\beta$  or A $\beta$ 1-42. It has been individualized through making studies of families suffering from autosomal dominant, early-onset forms of AD (familial AD or FAD). Apart from the fact that FAD is clearly hereditary and manifests itself at earlier ages (<60 years), it is impossible to distinguish it from the sporadic form of AD; but also it is correlated to the Down Syndrome<sup>7-8</sup>, where patients carry an extra copy of the APP gene, located on chromosome 21, and they produce more A $\beta$  from

birth and develop amyloid plaques as early as the age of 12. Especially thanks to this last consideration, the observance of A $\beta$ 1-42 specific diffuse plaques suggests that these could be the precursors of the dense, neuritic plaques found in an AD brain.

Missense mutations, in the gene for presenilin -1, relative to chromosome 14 and in the gene relative to the encoding of presenilin-2 related to chromosome 1, are the other two genetic factors that have to be found out<sup>9-10</sup>. Both of them are related to A $\beta$ 1-42 phenotype, and are strictly related to FAD.

Considerable efforts have been made to identify the genes associated with the more common late-onset, sporadic form of AD. These attempts have succeeded in finding in the apoE gene the possible cause<sup>11</sup>. ApoE is a lipid transport protein that comes in three allelic variants: E2, E3, and E4. The ApoE4 allele is the major risk factor for late-onset AD, that is, those who carry one or two copies of this allele may not necessarily develop AD, but these carriers are at substantially increased risk. This factor is related to A $\beta$  plaques and vascular deposits such as phenotype. More recently, studies<sup>12</sup> with transgenic mice have demonstrated that ApoE is required for amyloid formation and glial activation caused by FAD-mutant APP.

## II. $\beta$ -Amyloid

- The Structure of  $\beta$ -Amyloid (A $\beta$ )

The amyloid  $\beta$  (A $\beta$ ) is a 4KD, a peptide derived from proteolytic cleavage of the amyloid precursor protein (APP)<sup>13</sup>. It is constituted by 40-43 aa and the sequence is (1)DAEFRHDSGYEVHHQKLVFFAEDV(25)GSNKGAIIGL(35)MVGGVVIAT(43)

The beta AP sequence is usefully divided into two regions. Residue 1-28 comprises a hydrophilic domain with a high proportion of charged residue (46%). In APP this domain is presumed to be extracellular. The C-terminal residue 29-42 comprise a richly hydrophobic domain with a high proportion of beta branched amino acids; in APP this domain is associated with the cell membrane<sup>14</sup>.



- The Amyloid Protein Precursor (APP)

The APP gene, located on chromosome 21, codes for multiple isoforms of a glycoprotein containing a single membrane spanning sequence, a long N-terminal extracellular region and a short C-terminal cytoplasm tail (Figure1). Alternative mRNA splicing results in the formation of APP<sub>770</sub>, APP<sub>751</sub>, APP<sub>714</sub>, APP<sub>695</sub>, APP<sub>863</sub> and APP<sub>865</sub>, where the number gives the total number of amino acids in each protein. The two latter isoforms do not contain an A $\beta$  domain within their sequence<sup>15</sup>. APP expression occurs ubiquitously throughout the body and the primary APP isoform varies according to cell and tissue type<sup>16</sup>. Human neurons express high levels of APP<sub>695</sub> together with lesser amounts of APP<sub>781</sub>, and are responsible for the majority of the APP produced in the brain<sup>17</sup>. Other brain cell types such as meninges and glial cells produce predominantly the longer APP isoforms, APP<sub>770</sub>, APP<sub>751</sub> and APP<sub>714</sub>. Each of these, unlike APP<sub>695</sub> contain a Kunitz protease inhibitor domain which is known to confer resistance to proteolysis by trypsin and chymotrypsin<sup>18-19</sup>.

APP has a large extracellular domain, a transmembrane domain which spans the plasma membrane once, and a small cytoplasmic domain. Its amino terminus lies within the extracellular space, and its carboxyl terminus is situated within the cytoplasm. A $\beta$  occupies a region spanning the extracellular and transmembrane domains of APP; 28 residues are found in the extracellular domain and 11-14 residues are located within the plasma membrane.

The following domains for APP<sub>695</sub> have been described. At its N-terminus, APP has a 17 residue signal peptide for transport into the endoplasmic reticulum. This is followed by a region rich in cysteine residues. The next one hundred amino acids include many glutamic and aspartic acid residues (negatively-charged), as well as a stretch of seven uninterrupted threonine residues. Two consensus sequences<sup>20</sup> for N-linked glycosylation exist at positions 467 – 469 and 496 – 498.

- Proteolysis Of The APP

Proteolytic cleavage of APP occurs in two distinct manners via either the  $\alpha$ -secretase pathway or the  $\beta$ -secretase pathway. The former pathway involves neuronal secretion of sAPP $_{\alpha}$ , by a putative  $\alpha$ -secretase enzyme which precludes the formation of full-length

A $\beta$ , as cleavage occurs between residues 612 and 613 of APP<sub>695</sub> corresponding to A $\beta$  residues 16 and 17 (Figure1). The 10-KDa C-terminal APP fragment generated by  $\alpha$ -secretase cleavage can be further processed by a putative  $\gamma$ -secretase enzyme which cleaves APP<sub>695</sub> between residues 637 and 638 or residues 639 and 640 yielding A $\beta$ <sub>17-40</sub> or A $\beta$ <sub>17-42</sub>.

Traditionally the  $\alpha$ -secretase pathway has been called the non amyloidogenic pathway since full-length A $\beta$  is not formed. Full-length A $\beta$  is generated by the  $\beta$ -secretase or amyloidogenic pathway (Figure1), whereby APP<sub>695</sub> is enzymatically cleaved by a  $\beta$ -secretase protease between residues 596 and 597. This yields a secret APP species denoted sAPP $\beta$  and a membrane bound peptide containing the intact A $\beta$  domain (C-100). C-100 has been demonstrated to be highly amyloidogenic and neurotoxic to cultured neurons *in vitro*. Further proteolysis of C-100 by  $\gamma$ -secretase generates full-length A $\beta$ . Interestingly, the  $\gamma$ -secretase cleavage occurs within the transmembrane domain of APP. APP metabolism by the  $\beta$ -secretase pathway was initially suggested as being an abnormal proteolytic processing event specific to, and with a causative role in AD.

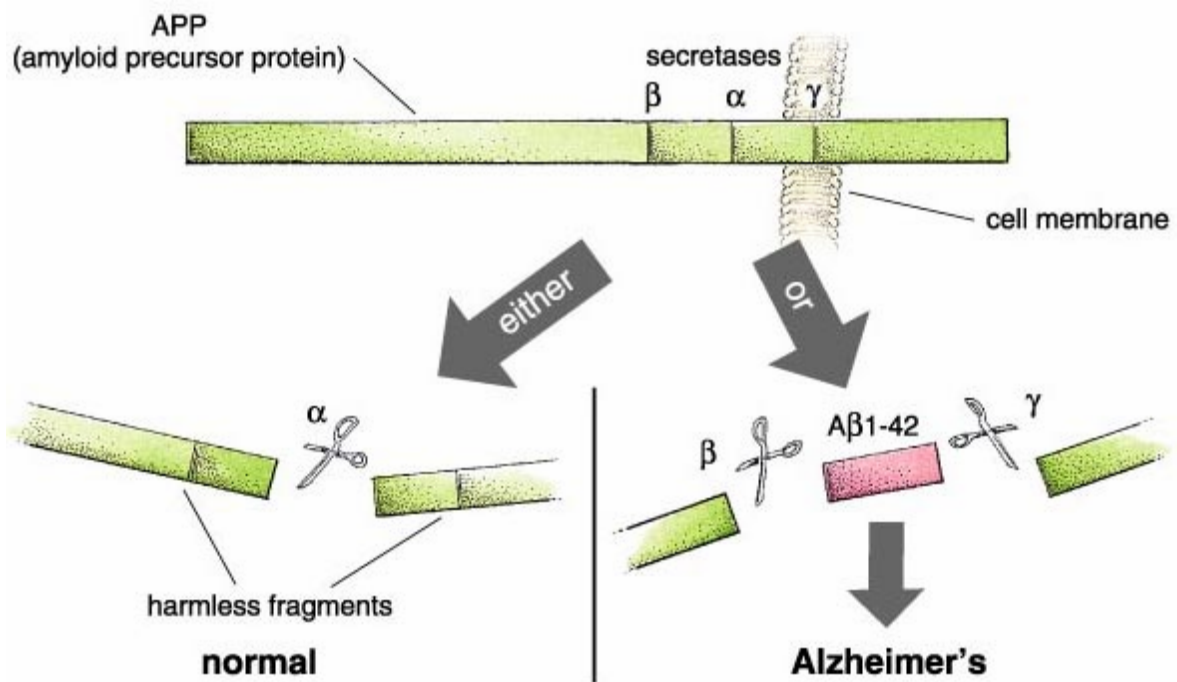


Fig.1 Citron et al., *Proc. Natl. Acad. Sci. USA*, **93**, 13170-13175, 1996

However, proteolysis of APP via the  $\beta$ -secretase pathway has been found to be a normal process which occurs ubiquitously in both AD and non-demented individuals.

Proteolysis of APP by  $\beta$  – and  $\gamma$ -secretase was initially thought to occur in late endosomal or lysosomal compartments. However, other reports have demonstrated activity of both secretases in the endoplasmic reticulum and the Golgi. Although the  $\beta$ -secretase cleavage is probably specific there are a number of N-terminally modified and truncated forms found in the brain. N-terminal truncation is probably a result of non-specific proteolysis subsequent to release of full-length  $A\beta$ .  $A\beta$  truncated at position 3 ( $A\beta_{3pE}$ ) and position 11 ( $A\beta_{11pE}$ ) is particularly abundant in the brain. The N-terminal glutamic acid residues of these peptides are post-translationally modified to form pyroglutamyl species, making these peptides less susceptible to further proteolysis. This resistance to proteolysis probably explains the high abundance of  $A\beta_{9pE}$  and  $A\beta_{11pE}$  relative to other N-terminal truncated  $A\beta$  forms.

There is also significant heterogeneity inherent in the  $\gamma$ -secretase cleavage site, with the C-terminus of  $A\beta$  varying between amino acids 39 and 43. Whereas the 40 amino acid form of  $A\beta$  ( $A\beta_{1-40}$ ) accounts for approximately 90% of all  $A\beta$  normally released from cells, it appears to contribute only to later phases of the pathology. In contrast, the longer more amyloidogenic 42-residue form ( $A\beta_{1-42}$ ), accounting for only 10% of the remaining secreted  $A\beta$ , is deposited in the earliest phase of AD and remains the major constituent of most amyloid plaques throughout the disease. This heterogeneous cleavage can be explained by  $\gamma$ -secretase, actually being multiple enzymes, or by  $A\beta$  generation occurring in different cellular sites where conditions affect enzymic specificity.

$A\beta_{1-42}$  production has been demonstrated in neuronal endoplasmic reticulum and nuclear envelope, whereas  $A\beta_{1-40}$  production has been observed in the trans-Golgi membrane. However, different sensitivity to cleavage at position 40 and 42 has been shown by studies with protease inhibitors, supporting the multiple enzyme hypothesis. A combination of the two hypotheses whereby different enzymes reside in separate cellular compartments is also possible.

Studies indicate that the product of a gene associated with early onset AD, presenilin-1 (PS-1), is required to enable normal  $\gamma$ -secretase activity. Furthermore, it has been

proposed that PS-1 is itself a  $\gamma$ -secretase. It is possible to anticipate that A $\beta$  itself is not toxic, it becomes toxic to neuronal cells once it has aggregated into amyloid fibrils.

A $\beta_{1-40}$  and A $\beta_{1-42}$  are the most amyloidogenic fragments. As it will be explained more precisely in the following chapters, they are involved principally in the AD process, because of their clear capacity to form filamentous aggregates (amyloid fibrils and consequently amyloid plaques), characterized principally by a characteristic green birefringence in Circular Dichroism studies, also by a strong insolubility and proteolytic resistance.

- The A $\beta$  Hypothesis of Alzheimer's Disease<sup>3 and 13</sup>

The common theme of A $\beta$  production and deposition has bolstered the amyloid hypothesis of AD pathogenesis, which states that production and deposition of A $\beta$  in the form of fibrils leads to neuronal cell death and eventually to the clinical presentation and progression of AD. The hypothesis that A $\beta$  amyloid formation and deposition is a cause factor in AD<sup>21</sup> is supported by the observation that mutations which increase the secretion and the aggregation propensity of A $\beta$ , such as the Swedish double mutation of APP (where is reported a significant increase in A $\beta$  secretion compared with cells expressing wild type APP), Down's Syndrome, the dutch cerebral haemorrhage and presenilin mutations, cause symptomatically severe early onset forms of AD (see AD genetic section). In an attempt to obtain an animal model of AD transgenic mice which over-express either mutant or wild-type human APP have been produced and these animals have been found to develop AD-like pathology. The fact that A $\beta_{1-42}$  is increased in all these forms is very intriguing because this form of A $\beta$  is particularly prone to fibril formation, and A $\beta$  fibrils are toxic to cultured neurons<sup>3 and 22-23</sup>, (*in vitro* studies of A $\beta_{1-40}$  and A $\beta_{1-42}$  confirm this hypothesis, and reported that aged solution of these species are toxic to cultured neurons and the aggregation propensity of A $\beta$  has been correlated with neurotoxicity<sup>24</sup>).

Moreover, A $\beta_{1-42}$  fibrils can serve as templates that induce fibrillization of other A $\beta$  species that would otherwise remain soluble. Moreover, human neurons in AD vulnerable brain regions specifically accumulate A $\beta_{1-42}$ , suggesting that intracellular A $\beta_{1-42}$  accumulation is an early event in neuronal dysfunction .

- Fibrillogenesis and Aggregation Process

Since the beginning of AD studies, searching for the cause(s) of AD<sup>1</sup> has meant working backwards from the clinical presentation of dementia to specific, correlative neuroanatomic features (plaques, tangles, and synaptic and neuronal loss) and then to the morphologic and biochemical characterization of amyloid deposits. Once decided to follow the amyloid hypothesis and on the consequence, established that the predominant protein component of amyloid deposits is the A $\beta$ , which exhibits a variety of different structures, continuing in our exploration of AD nature to individuate a possible target which come in, the questions to face up are why and how A $\beta$ , which normally circulates in a soluble form in the plasma and cerebrospinal fluid, should form insoluble deposits. To answer these questions, the structure of A $\beta$  within amyloid deposits has to be examined.

The answer is in the fibrous nature of A $\beta$ , or more specifically in the fibrillization process of this protein.

The fibrillization process appears to initiate a cascade of events producing neuronal cell death and resulting in the cognitive and behavioural decline characteristic of A $\beta$ .

The fibrous nature of amyloid was first established in 1959 by Cohen and Calkins<sup>25</sup> in electron microscopic studies. Subsequent electron microscopy by Terry et al. , Kidd<sup>26</sup>, and many others has demonstrated that A $\beta$  exists in a fibrillar form within amyloid plaques in the AD brain. Later high ultrastructural studies of fibrils have revealed a more complex subfibrillar organization. Shirahama and Cohen<sup>25</sup> suggested the following model of fibril organization: fibrils were composed of one or more 75-80 Å diameter filaments, which were in turn composed of a pentagonal array of laterally associated 25-35 Å diameter protofibrils. Each protofibril was composed of 2-3 subprotofibrils, each of which was 10-15 Å wide. Subsequent electron microscopic studies of a variety of amyloids have revealed structures consistent with this model of fibril organization.

Initial inferences to the secondary structure of A $\beta$  fibrils have come from studies of the tinctorial properties of amyloid deposits in the brain parenchyma and vasculature. Senile plaques exhibit a green birefringence when stained with Congo Red and

examined using polarized light. This is a defining characteristic of amyloid deposits and is due to the presence of protein polymers possessing  $\beta$ -sheet structure. To examine further the secondary and higher order structure of the  $A\beta$  fibril, X-ray diffraction analysis of unoriented senile plaque cores was done by Kirschner et al<sup>27</sup>. These studies showed prominent reflections of 4.76 Å and 10.6 Å. In oriented samples, each of these reflections, instead of appearing as rings, appeared as diametrically opposed arcs and each set of arcs was oriented orthogonally to each other.

Interpreting their data in the context of Pauling and Corey's model of the pleated  $\beta$ -sheet (See figure 2), concluded that the protein components of the amyloid fibril were arranged in a cross- $\beta$  pleated sheet. In this model,  $A\beta$  molecules form an anti-parallel  $\beta$ -sheet oriented orthogonally to the fibril axis. Hydrogen bonding between the  $\beta$ -strands accounts for a 4.7 Å meridional reflection (parallel to the fibril axis). Face-to-face stacking of multiple  $\beta$ -sheets produces a  $\sim 10\text{Å}$  equatorial reflection (perpendicular to the fibril axis).

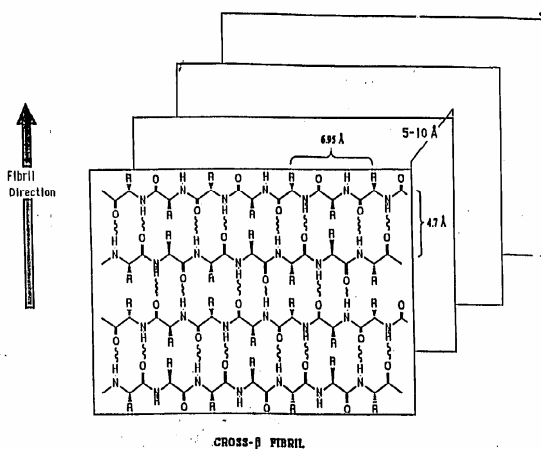


FIGURE 1: Schematic depiction of Pauling's cross- $\beta$  fibril model (Marsh et al., 1955). This model is generally accepted to represent all amyloid. The point of this review is to emphasize that this structure may represent one member of a structural class. The antiparallel arrangement of the peptide chains and the resultant linear hydrogen-bonding network are shown for the front sheet. Another model has been proposed in which the interstrand orientation ( $\Delta z = 0.6 \text{ Å}$ , as opposed to  $0 \text{ Å}$  in the Pauling cross- $\beta$  fibril), and hence the hydrogen bond geometry, differs (Arnott et al., 1967). The intersheet distance will vary, depending on the side chains involved. The major reflections in the X-ray fiber diffraction pattern which are considered to be diagnostic of this structure are the interstrand distance of 4.7 Å along the meridian and the variable intersheet distance (5-10 Å) along the equator.

## Figure 2

How does the cross- $\beta$  pleated sheet secondary structure element relate to the quaternary structure in the mature amyloid fibril?

Among amyloids, the highest resolution structural information obtained to date has been from transthyretin (TTR) fibrils, components of the amyloid associated with familial

amyloidotic polyneuropathy (FAP). Thus it has to turn to the TTR fibril for answers to the question above. Integrating the TTR models with the high resolution electron microscope structures of Shirahama and Cohen<sup>25</sup> yields the following quaternary organization of A $\beta$  amyloid fibrils. A $\beta$  molecules self-associate form extended  $\beta$ -sheet helices, subprotofilaments, 10-15Å in diameter. Multiple subprotofilaments pack face-to-face to form helical superstructures 25-35 Å in diameter termed protofilaments. Protofilaments associate laterally to form rotationally symmetric arrays 75-80 Å in diameter termed filaments. The original terms subprotofibril and protofibril have been replaced by subprotofilament and protofilament to emphasize the precursor-product relationships among these structures. Amyloid fibrils are composed of one or more filaments. Multiple filaments may be wound around one another to form super-helical structures. It should be emphasized that the formation, association, and assembly of subfibrillar structures into fibrils occurs as a concerted process, not as a linear chain of events. One of the most interesting and intriguing aspects of the  $\beta$ -sheet helix model of amyloid fibril is its ability to explain how peptides and proteins which differ so dramatically in size (e.g. 20-200 amino acids) can produce polymers of such similar structure, the explanation comes from the basic structure of the  $\beta$ -sheet which, in most proteins, is composed of  $\beta$ -strands varying in length from 3-10 amino acids. In the formation of the extended  $\beta$ -sheet helix, in this way, a similar core structure is produced by a variety of diverse polypeptides. This folding process, and the resulting assembly of protofilaments and fibrils, are critical steps in a common pathway of fibrillogenesis<sup>1</sup>.

It is clear from the prior discussion that A $\beta$  fibrillogenesis is a complex process<sup>1and 13</sup> which at a minimum involves changes in A $\beta$  conformation and the self-association of A $\beta$  to form cross- $\beta$  plated sheet, subprotofilaments, protofilaments, and filaments. Although it is unlikely that each subfibrillar structure first forms completely then assembles in a filament, in studying the kinetics of fibrillogenesis it is helpful to conceptualize the process in terms of a series of discrete structural stages. Kinetically<sup>1and 13</sup>, A $\beta$  fibrillogenesis may be viewed as a nucleation –dependent polymerization process. As such , two key assembly steps are involved, nucleation and elongation. Nucleation is a thermodynamically unfavourable process requiring assembly of multiple

protein monomers to form an organized structure, the nucleus. Indeed this first step can occur not only through homogeneous nucleation, as previously discussed, but also: micellization, where at sufficiently high concentration, A $\beta$  spontaneously forms micelles, from which nuclei are released and seeding by A $\beta$  aggregates or non A $\beta$ -structures. Subsequent addition of monomers to the nucleus elongates the polymer chain. It has to be highlighted also that the A $\beta$  molecules that form nuclei and micelles and which add to fibril ends in the elongation steps are likely either monomer or dimeric. During the fibrillogenesis process, the intermediate (protofibrils) are formed with morphologies distinct from those of the mature amyloid  $\beta$ -type fibrils. At sufficiently high fibril concentrations and lengths, diffusion can result in enmeshing of fibrils to produce gels and precipitates. In the case of amyloid fibrillogenesis, morphological and biophysical studies have shown that there are additional steps also prior to nucleation, and concurrently or following polymer extension<sup>1</sup>. What is it possible to conclude? There is surely a link between amyloid fibril formation and AD, as shown through genetic, neuropathologic, and biochemical evidence<sup>13 and 28</sup>. Neurotoxicity associated with A $\beta$  is highly dependent on its conformation, it is not related to its primary but quaternary structure (See Corey's model) and the morphology of the aggregates formed. Monomeric A $\beta$  is thought to be not neurotoxic, whereas both protofibrillar and fibrillar species of A $\beta$  exhibit neurotoxicity in cell based assays. Recent reports suggest that monomeric A $\beta$  act as a natural antioxidant and protect neurons against metal-induced oxidative damage, whereas aggregated A $\beta$  act as a free radical generator, implying an aggregation-dependent biological function of A $\beta$ <sup>28</sup>. In conclusion, because the weight of evidence from pathology, genetics, cell biology and molecular biology that heavily favour the amyloid hypothesis, it becomes an important therapeutic target interfering with small molecules in the fibrillogenesis and aggregation process, trying to inhibit the nucleus formation, or the packaging of fibrils' sheets, or in the kinetic aspect of the process, slowing the formation of aggregates, and modulating the production, deposition and toxicity of A $\beta$ .



### III. Current Discovery Targets - Potential Strategies<sup>29-30</sup>

Although the aetiology of AD is nowadays not yet fully understood, several therapeutic strategies have become evident, to arrest or reverse the progression of AD. Potential targets could be summarized in the following points:

1. Decreasing A $\beta$  production by effecting  $\beta$ APP processing.
2. Preventing or reducing A $\beta$  aggregation and plaque maturation or improving clearance of A $\beta$  (e.g. through microglia or ApoE).
3. Inhibiting neurotoxic effects of A $\beta$ (e.g. restoring calcium homeostasis, reducing oxidative damage or decreasing inflammation)
4. Decreasing cellular response to injury.

Clearly, the formation and maturation of neuritic plaques are central events in AD pathology. In the light of all these considerations, the following potential strategies could be:

- inhibition of A $\beta_{1-42}$  or A $\beta_{1-40}$  production and/or secretion, with or without concomitant stimulation of APPs secretion (increasing  $\alpha$ -secretase, decreasing  $\beta$  or  $\gamma$  secretase).
- inhibition of A $\beta_{1-42}$  or A $\beta_{1-40}$  aggregation
- inhibition or prevention of amyloid fibril formation
- blocking or limiting direct neurotoxic effects of A $\beta$  (restoring Ca<sup>2+</sup> homeostasis)
- resolubilisation of plaques
- stimulation of A $\beta$  clearance
- prevention or limitation damage of brain inflammatory response(preventing free radical toxicity)
- correction of copper and zinc imbalances
- blocking the cellular response to injury by inhibiting neuronal apoptosis.

Actually, Federal Drugs Administration(FDA) has approved two drugs that fight Alzheimer's:Tacrine (Cognex) and Donezepil (Aricept), but they prevent the breakdown of acetylcholine, a brain chemical needed for normal memory and learning. They frequently produce a modest improvement in symptoms, but do not significantly alter the course of the disease. They are followed by several side effects. There are also

studies that have suggested that prolonged use of NSAID decreases the average rates of the disease. There is a list of other drugs that enter in to several of the points explained above, but we would like to focus our attention on those drugs that could inhibit fibrillogenesis and aggregation of A $\beta$ , our final target. In past times, a number of small molecules have been reported to interfere with the *in vitro* aggregation of A $\beta$  peptides:  $\beta$ -cyclodextrin and rifampicin are the first compounds that showed they inhibited fibril formation of A $\beta$  peptides; Congo Red (CR), chrysamine G and other sulphonate dyes were found to display the same activity and recently nicotine and iododoxorubicin, estrogens, melatonin, benzofuran were reported to act as aggregation inhibitors as well<sup>31</sup>. Most of these molecules can be considered tools and some of them have been regarded as structural hits in the search for more active and pharmacologically useful compounds, as in our case.

- Inhibition of A $\beta$ <sub>1-42</sub> Or A $\beta$ <sub>1-40</sub> Fibrillogenesis and Aggregation<sup>31-33</sup>

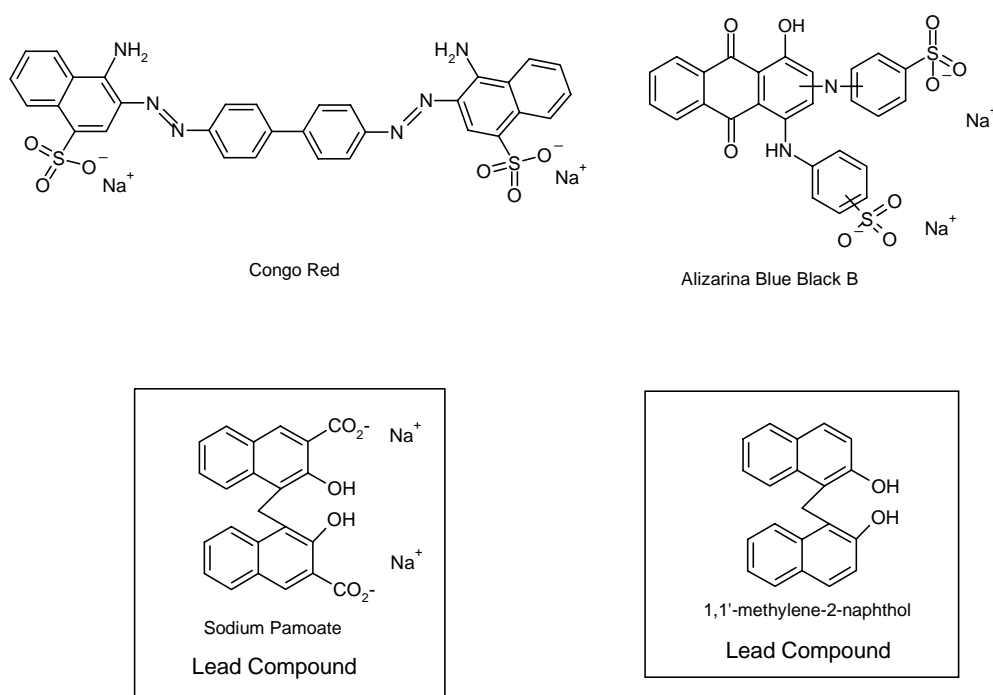
Unlike neuritic plaques, diffuse plaques can not be visualised using amyloid-staining dyes like Congo red or thioflavin S. Within these deposits, A $\beta$  molecules assume a  $\beta$ -pleated sheet conformation and self-associate into loosely-bound aggregates, but they do not assemble into fibrils. Fibril assembly does occur in neuritic plaques; once formed, these fibril pack into a cross- $\beta$  conformation to form amyloid. Thus, amyloid is an orderly arrangement of peptid molecules. Substitution of a single amino acid in the A $\beta$  sequence can significantly alter the electrostatic and hydrophobic interactions mediating fibril assembly. A $\beta$  aggregation is dependent on pH, concentration and length of incubation in aqueous media. A $\beta$  exists in a random conformation at low pH, a  $\beta$ -pleated sheet conformation at pH4-7 and in a random conformation at high pH. The effect of pH on A $\beta$ 's secondary structure indicates that the assembly of  $\beta$ -strands is influenced by the ionisation state of key residues. Histidine-aspartic acid/glutamic acid salt bridges have been proposed to stabilise  $\beta$ -pleated sheets, facilitating fibril assembly. At pH 7.4, A $\beta$ <sub>1-42</sub> is highly insoluble in water, due to the presence of a hydrophobic C-terminal sequence extending from residues A $\beta$ <sub>29</sub>-A $\beta$ <sub>42</sub>. Supersaturated solutions of A $\beta$  contain A $\beta$  aggregates and exhibit kinetic, as opposed to thermodynamic, solubility. In

other words, supersaturated A $\beta$  solutions can appear to be completely soluble when in fact precipitation will occur eventually. Nucleation, i.e., the formation of a specific-size A $\beta$  oligomer, will cause an A $\beta$  solution that is not at thermodynamic equilibrium to precipitate rapidly. Nucleation is the rate-limiting step in the formation of amyloid. Lag time (i.e. the time until an A $\beta$  solution exhibiting kinetic solubility precipitates) is directly-related to the oligomer size required for nucleation and inversely-related to protein concentration. The ability of A $\beta$  to assume a  $\beta$ -pleated sheet conformation and form fibrils is dependent on a hydrophobic sequence of amino acids stretching in a particular region of full-length A $\beta$ . Given these facts, it might be possible to hinder plaque formation by introducing an A $\beta$  ligand that could inhibit the self-association of A $\beta$ . Low molecular weight molecules are candidate A $\beta$  ligands for this purpose and are thought to facilitate the transformation of diffuse plaques into neuritic plaques. Obviously, a therapeutically useful drug must increase the clearance of fibrillated A $\beta$  and cross the blood-brain barrier.

According to literature data, the Congo Red is the most common dye that binds specifically with amyloid fibrils. This specific interaction leads to an amyloidogenic fibrils birefringent enhancement and a characteristic circular dichroism. In literature several attempts to correlate CR binding to  $\beta$ -sheet amyloid structure have been reported. There are two main interaction models<sup>34</sup> of CR with the fibrils. The first shows the CR as intercalary agent, whose principal axis lies parallel to the strands in to the anti parallel  $\beta$ -sheet fibrils. In the second hypothesis, the dye is always an intercalary agent but its axis lies perpendicular to the  $\beta$ -strand direction, so that the every five peptidic chains the distance between positively charged residues (Lysine 16, 28) is about the two CR sulphonilic groups one (19Å). This is the most credited interaction model; based on these considerations, the pharmacophoric model construction has been made by CAMD(Computer Aided Molecular Design ) using sulphonate and polysulphonate dyes, with known activity as reported in literature in order to discriminate chemical activity classes. In order to validate this pharmacophoric model, many sulphonate, polysulphonate dyes and alternative compounds containing different negative charged functional groups have been selected (e.g. orthohydroxyl benzoic acids, phosphoric ones) from a commercial molecule set. Among those compounds that validated the

model, the most active dye was the Alizarina Blue Black B (ABBB an available commercial Aldrich product, which has been tested as mixture as HPLC isolated products), the alternative charged functionalized compounds, the Pamoic Acid<sup>35</sup> has been found. Among no validating model compounds, the 1,1'-methylene-2-naphthol (bis-naphthol)<sup>35</sup>, completely structurally similar to pamoic acid, was however tested and showed to have better activity both *in vitro* and *in vivo* as highlighted by IC50 values and autoradiographic results, respect to Pamoic acid. As will be explained in the molecular modelling section, it has been found to interact following a different model with respect to the pharmacophoric model related to negative charged functional groups. Our biological and chemical interest has been and will be pointed out re. Pamoic acid, and bis-naphthol, at present our lead compounds (See Scheme 1).

Scheme 1



- Fibrillogenesis Studies Techniques<sup>36-37</sup>

Powerful methodologies like NMR, Circular Dichroism (DC) or FTIR studies are of limited use in the characterization of the A $\beta$  protein (and its related structures), a cause of its insolubility in aqueous solution, as it is often necessary to add some cosolvents to

maintain its minimal solubility, but that could also alter the aggregation process. It is difficult to obtain detailed structural information about the fibrillogenesis process with conventional techniques alone because of its different aggregation characteristics, related to pH conditions, concentration and as a consequence the lack of a crystallographic structure of A $\beta$ . However, investigation of  $\beta$ -amyloid peptide and also the fibrillogenesis process have been reported and executed by solid NMR, HPLC method, coupled with Electron Spray Ionization Mass Spectrometry, DC. Several other techniques, such as X-ray-crystallography, light scattering, fluorescence spectrometry, size exclusion chromatography, atomic force microscopy have been employed in studies of amyloid proteins.

CD spectroscopy can provide qualitative and semi quantitative information about the secondary structure of proteins and peptides in solution (in general, it can be applied for A $\beta$  structure too), by the different absorption of the left and right handed components of circularly polarized light by chiral molecules in solution. An adequate representation of the CD spectra of globular protein, (this similitude makes this technique useful for A $\beta$  identification), is possible if considering them as a combination of CD spectra for pure  $\alpha$ -helix,  $\beta$ -sheet and random coil determined using poly-L-lysine. Considering all spectra as a combination of these curves, it is possible to estimate the amount of these secondary structures in a given protein using curve fitting algorithms.

Electron microscopy (EM) offers an available technique for the ultrastructural characterization of preprotofilaments, protofilaments and mature fibrils forming during *in vivo* fibrillogenesis. Atomic Force microscopy (AFM) has recently been used as an attractive imaging technique in the amyloid field. It is an excellent alternative to EM because of its nanometer level resolution, a relatively simple specimen preparation. It is able to resolve numerous distinct A $\beta$  assemblies. It is also a simple technique for studying fibrillogenesis and aggregation as it is based on a staining identification.

- Staining Identification Methods of Amyloid<sup>38</sup>

The staining reaction due to the interaction of amyloid and iodine<sup>39</sup> was often used in the earlier studies of amyloidosis; nowadays amyloid is still identified by its characteristic histological staining reactions. The histological staining methods are

crucial for the diagnosis of amyloidosis and are also commonly used in amyloid research.

Amyloid was first recognized by tinctorial properties elicited when amyloid –laden tissues were treated with iodine at the autopsy table (Virchow 1855). The evidence is based on the presence of minor carbohydrate moieties in the amyloid deposits.

In the presence of the same carbohydrate components, the staining properties of amyloid with rosoline dyes (e.g. methyl violet and cresyl violet), the main staining methods for Amyloid before Congo Red using in 1920, was based.

Because of their low sensitivity and complete lack of specificity, these methods are abandoned, and staining with Congo Red became, and is nowadays, the most universally used method to demonstrate amyloid. Congo Red is a fluorescent dye<sup>40</sup>, so the alkaline CR methods for studies in ordinary light is also useful for fluorescence studies if mounting is performed in a non fluorescent medium.

However this fluorescence is not as specific for amyloid as is the green birefringence observed with polarized light. The fluorescence of Congo Red in tissue sections may be used in the quantitation of amyloid in tissue and the staining is easier to recognize . Thioflavine staining is currently popular for amyloid studies, not only for the detection of amyloid in tissue sections but also for the study of fibrillogenesis “in vitro”.

- Thioflavin Test ThT<sup>41-43</sup>

Thioflavin S and Thioflavin T are sulfur-containing compounds’, only Thioflavin T seems to be fully characterized chemically. While Thioflavin S is a mixture of several components with different properties, Thioflavin T is a small, positively charged benzothiazole compound with a formula weight of 319.

The histologic dyes Thioflavin S and T, under the appropriate conditions, selectively stain amyloid structures in a number of pathological settings as does the diazobenzidine sulfonate dye, Congo Red, which is also birefringent when bound to fibrils, phorwhite BBU, Sirius Red, and several other fluorescent and nonfluorescent aromatic molecules also show this property.

Investigation of the amyloid fibril formation process requires not only the ability to distinguish the characteristic amyloid  $\beta$ -sheet structure from amorphous aggregates of the monomer or nonamyloid fibril form of the precursor protein, but quantitation of the

amyloid form as well. Congo red and Thioflavin T undergo characteristic spectral alterations on binding to a variety of amyloid fibrils that do not occur on binding to the precursor polypeptides, monomers, or amorphous aggregate of peptide. Both dyes are available for in vitro test of amyloid fibril formation. The Thioflavin S is unsuitable for quantitative analysis in solution, because binding to amyloid fibrils enhances the emission intensity of it but with no change in the excitation or emission spectra, which means a high background fluorescence in solution. Using ThT, amyloidogenic A $\beta$  synthetic peptides derived from the major protein of the AD senile plaque protein give rise to a large fluorescence excitation spectral shift that means selective excitation of the amyloid fibril-bound ThT. The binding of ThT to amyloid is not known, but studies in vitro concerning fibrils, derived from purified amyloid proteins or synthetic peptides show that the dye interacts with the specific quaternary structure of the  $\beta$ -plated sheet fibril and not the monomeric peptides. So the binding is not due to a link with any specific amino acid sequence. However, the binding motif is not present in all synthetic amyloid – like fibrils. The binding of the ThT to amyloid fibrils creates a characteristic 120nm red shift of its excitation spectrum<sup>42</sup>. The biophysical mechanism by which amyloid fibrils induce this hypochromic shift is not clear. One hypothesis suggests that the ground state of the chromophore is altered by binding to amyloid fibrils rather than the excited state, which is usually related to the emission spectrum<sup>43</sup>. This theory is supported by two observations: the pronounced excitation spectral changes and the lack of an effect on the emission spectrum. The difference absorption spectrum for ThT in the presence of A $\beta$  (1-40) fibrils shows a maximum around 440, clearly shifted from both the free dye absorbance (400nm) and the fluorescence excitation maximum (335nm). A $\beta$ (1-42) creates the same spectral changes. There is no spectral evidence for ThT dimerization in solution at concentration up to 10mM. Explanations due to dye rotational restriction or environmental dielectric constant are cut off by a lack of a solvent viscosity spectral effect on the excitation spectrum, and low dielectric solvents enhance only the emission intensity. The characteristic excitation maximum of amyloid fibril-bound ThT is showed at the presence of high concentrations of polyhydroxy solvents. The explanation is that the dye binding site may have similar hydrogen bonding characteristics.

Because fluorescence depends on binding site number, affinity and quantum yield, it is really difficult to obtain an exact relationship between ThT fluorescence and absolute amyloid fibril concentration. The ThT test is the most common, high sensitivity staining method to study the complex system of amyloid fibrils, particularly where the complexes are unknown. It is useful to be able to infer something from the repeating  $\beta$ -sheet structure of the fibrils and to distinguish them from the irregular aggregates. The apparent affinity of ThT for different amyloid fibrils depends on the identity of the fibril building block, ranging from 0.033 $\mu$ M to 11 $\mu$ M [A $\beta$ (1-40)]. It has been shown that the affinity of ThT to A $\beta$  increases at high pH values, probably a cause of its quaternary positively charged benzothiazole ring nitrogen<sup>38</sup>. At high pH values, there is the probability of a depolymerization of the fibrils, so the test is made at pH 7.4 (see the experimental section). The stability of the fibrils also depends on the identity of the peptide subunits, so the measurements have to be made rapidly, after the dilution of the sample in the solution. In our assays (see the experimental section), the A $\beta$ (1-42) has been chosen as peptide monomer, because it is more toxic and close to the real aggregate condition. The formation of A $\beta$ (1-40), also A $\beta$ (1-42) fibrils can be measured either by taking aliquots of a reaction mixture incubated under appropriate conditions and reading the fluorescence after dilution into ThT containing buffer or by running multiple small volume reactions and quenching with ThT containing buffer<sup>41</sup>. It is necessary to have a fluorescence plate reader and small volume reactions. The reaction time required depends on the state of the peptide used, temperature, stirring, ionic strength, by side pH condition assay. Usually, a detectable reaction is obtained between 3 and 6 h under the available conditions, and reaches the equilibrium overnight. Particularly A $\beta$ (1-40) fibril formation is very sensitive to temperature, the rate increase deep between 25°C and 37°C. When the reaction is terminated, it is possible to read the amyloid specific fluorescence in a regular fluorimeter, after removing the sealing film and by the addition of a ThT solution. Storage at either temperature the peptide seeds spontaneously over a period of weeks to several months<sup>41</sup>.

If the fresh unopened lyophilized peptide or peptide not aggregated is treated using trifluoroacetic acid, formic acid, HFIP, the lag phase is prolonged before fibril formation is apparent.



Different batches of peptide from the same suppliers and material from various suppliers can lead to different kinetic fibril formation. The irreproducibility is due to the conformational ambiguity of A $\beta$  peptide<sup>41</sup>.

Fibrils formed from other amyloidogenic A $\beta$  peptides such as 1 – 28, 1 – 42, 12 – 28 and 25-35 yield different ThT fluorescence signal intensities, without a drastically altered stoichiometry of ThT binding, which means the ThT fluorescence depends dramatically on the nature of the subunit fibril. ThT measurement of A $\beta$  fibril formation can be used to assess whether an added component could interfere or potentiate amyloid fibril formation. In such applications, the question is if the effect is on the maximal extent of fibril formation or on the rate of fibril formation, that is, if the effect is kinetic or thermodynamic.

In the search for inhibitors, this is an important distinction as kinetic inhibition of an intermediate step in fibril formation will eventually be overcome by the overwhelming thermodynamic stability of the fibril. Also all fluorescent probes, apparent inhibitors or potentiators could affect either the quantum yield or the number of ThT molecules bound to the amyloid fibril without changing the percentage of fibril formation. All this information, coming from literature data, has been fundamental both in the choice of the technique to use to study the capacity of our compounds to inhibit the fibrillogenesis and aggregation process, both in the application of a ThT test, once chosen as a more suitable test, to reach our aim (see experimental section II). In conclusion, based on this information, the ThT test has been chosen by our group to study the anti-aggregant capacity for our compounds, because it has been shown to be the most suitable, for its practicality and widespread strength.

- Assay Method<sup>44-45</sup>

The fluorescent yield of ThT is relatively low for most amyloid fibrils, necessitating the use of microgram quantities of fibril for detection.

Fibril formation is frequently measured in aliquots of a fibril forming reaction.

To evaluate and discriminate among our drugs, varying the potencies of the potential amyloid inhibitors, it has been necessary to test them in ThT assay, which can be

executed following two different methodologies that are related to the three different phases of A $\beta$  aggregation<sup>44</sup>:

- 1) Nucleation
- 2) Extension
- 3) Polymerization

The A $\beta$ <sub>1-42</sub> is dissolved in an appropriate buffer solution under conditions where it is initially in a non polymerized state. Under controlled stirring conditions, there is a period during which no polymerization is detected, whereas prefibrillar or soluble, but highly ordered, forms of amyloid are formed. As soon as enough prefibrillar material has formed in the sample, fibril formation starts rapidly, continuing until the unpolymerized peptide is completely consumed. The  $\beta$ A fibrillogenesis is defined as nucleated polymerization process<sup>1</sup>, based on these three characteristics: 1) time period during which nucleation occurs but fibril formation is not observed; 2) the rate of the fibrillogenesis reaction once fibrillogenesis has started; 3) the level of fibril formation at the end of polymerization process.

The assay conditions, applied by our team, enabled us to study our drug inhibition potency using the second and third characteristic of the process, hypothetically interfering in post nucleation aggregation and in amyloid deposits formation steps. Mario Negri Institute is a research group that collaborates with us in the common aim to determinate the inhibition potency of the compounds. Parallely, Mario Negri Institute's assay permitted the study of the inhibition drug capacity in the first step of the process, in protofibril formation (the Mario Negri experimental process will not be reported in the experimental section and has been only touched upon in this context to point out and understand the difference of target which our compounds are related to among all potential inhibitors. It is possible to affirm that to underline this different interest, the difference between the two tests is not in the methods but closely related to their different experimental procedure; as it will be evident in the experimental section, in our test the drug is incubated in soluble A $\beta$  and aggregated moiety in order to evaluate the drug's interference not only with the A $\beta$  aggregated but also with the A $\beta$  in aggregation process, on the contrary in the test of Mario Negri, it is incubated in soluble

one). Inhibitory potency may be expressed by the ratio of the nuclear formation in the presence of the inhibitors on the nucleation in the absence of test compound.

An inhibitor of polymerization thus has a ratio or lag greater than one; it can also reduce the amount of polymerization observed at the end of the assay. The final polymerization level can be expressed as the percentage of aggregation better than polymerization. We use this parameter to judge the inhibition of our drugs(see the experimental section).

In the extension phase, the preformed amyloid is combined with monomeric A $\beta$  to seed the monomer so that it will be incorporated immediately into fibrils.

This is a first order kinetic model for the addition of A $\beta$  onto the ends of existing fibrils. In this case, the effect of an inhibitor is to slow down the rate of fibrillogenesis; it may display also alternative effects binding differentially with various forms of A $\beta$ . If an inhibitor binds preferentially to nuclei, it may delay the polymerization, but still allow a normal rate of polymerization once initiated. It could be useful to report some practical information, found in literature<sup>45</sup>, which is generally in ThT test and in its application. The robustness of one's assay depends on the quality of A $\beta$  used. Reliable commercial sources of A $\beta$  (1-42) that now exist, have to be checked by RP-HPLC analysis, to discern between "good" or "bad" lots of A $\beta$ . Highest quality ones show a single peak with limited tailing; on the contrary an observably broader rear shoulder appears, a cause of the impurities presence such as deletion peptides. An example of decreasing A $\beta$  quality can be inferred from decreasing lag times in a nucleation assay, incomplete solubility, and increasing back ground toxicity of "monomeric" A $\beta$ . In practice, the ultimate test of a lot of A $\beta$  is if it performs well in an assay in which the performance of high-quality A $\beta$  is well characterized.

#### IV. Molecular Modelling

- $\beta$ A Model building

Experimental evidence on aggregational properties and secondary structure of  $\beta$ A was utilized to build a model of  $\beta$ A fibril, as reported below:

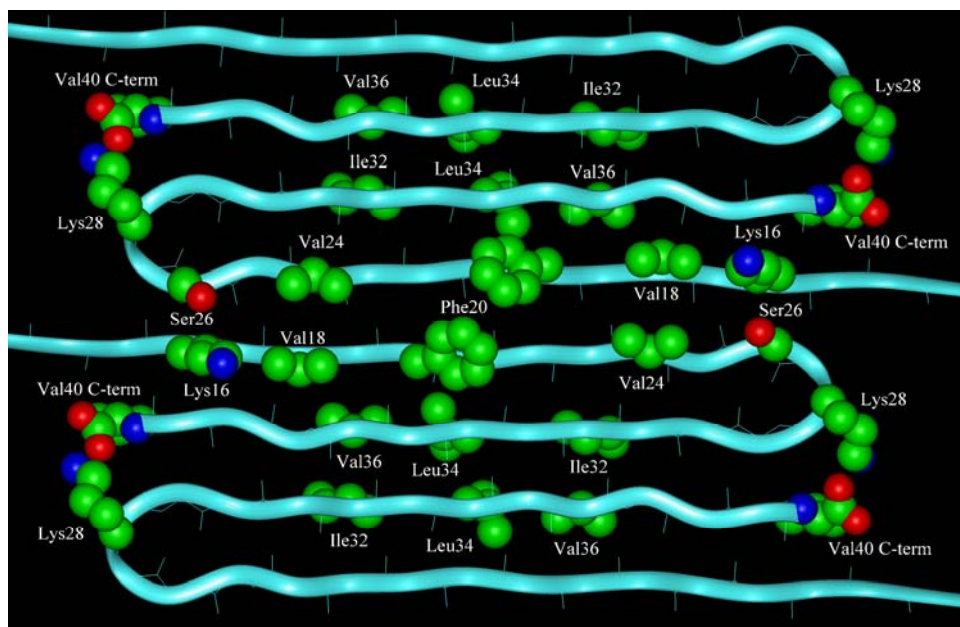
▲ A comparison of amino-terminally truncated  $\beta$ A peptides identified a peptide spanning residues 10 to 43 as a prototype for amyloid  $\beta$ A. Infrared spectroscopy of  $\beta$ A peptides in the solid state showed that their secondary structure consists of a beta-turn flanked by two strands of antiparallel beta-pleated sheet. Analog peptides containing a disulfide bridge were designed to stabilize different putative beta-turn positions. Limited proteolysis of these analogs allowed a localization of the central beta-turn at residues 26 to 29 of the entire sequence<sup>46</sup>.

▲ The secondary structure and the aggregation of fragment 25-35 of the beta-amyloid protein (beta AP(25-35)OH) under a variety of conditions was studied using circular dichroism spectroscopy<sup>47</sup>. The random coil $\leftrightarrow$ beta-sheet transition is shifted completely toward beta-structured fibrils at pH 7.4 where the Met-35 carboxyl group is fully charged. In contrast, removal of the charged carboxy terminus by amidation locks the equilibrium in the random coil conformation. Model calculations suggested an antiparallel beta-sheet structure involving residues 28-35 which is stabilized at both ends of the beta-sheet by ion pairs formed between Lys-28 and Met-35.

The role of lysine 28 can be maintained also in other aggregating peptides e.g. 1-40 or 1-42 where COOH group of the C-terminal aminoacid is involved. This condition means that a unique model of fibril couldn't exist depending on the length of the involved peptide.

So two different models of  $\beta$ A were built, one relative to a 12-40 sequence and another relative to a 12-42 one, both having a  $\beta$ -turn between 26-29 aa. Figure 3 shows a tetrameric aggregate of the two strands 12-40 (A) and 12-42  $\beta$ A (B) where are pointed out the differences between the two above mentioned models. In particular, it can be noted that a shift between two contiguous monomers exists, necessary to find the right ion-pair interaction between Lys28 and C-terminal COOH. The result is a different facing of charged and hydrophobic aminoacids. This hypothesis takes in account also the major propensity of the 1-42 peptide to aggregate in respect to the 1-40 one.

A)



B)

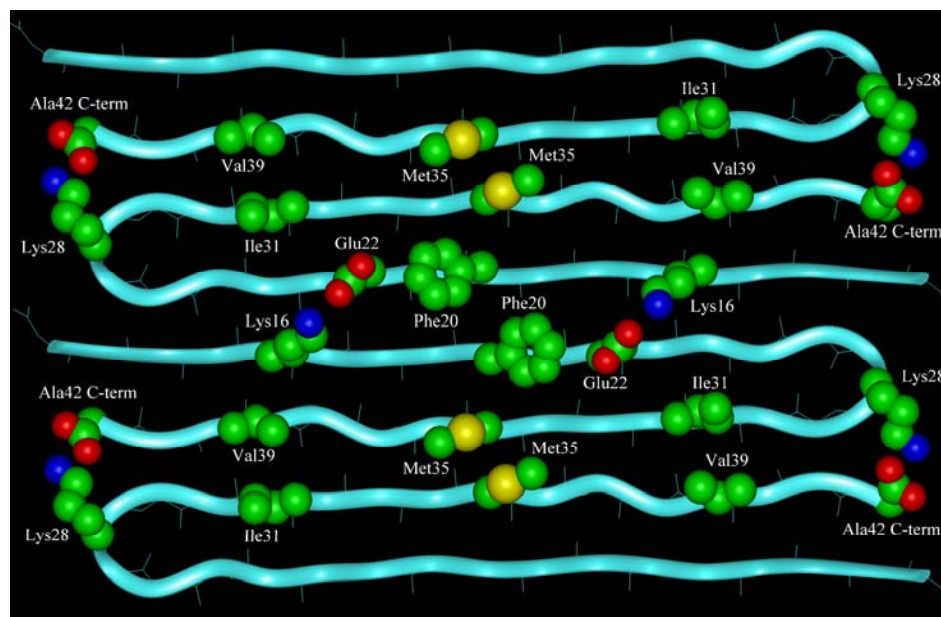


Fig 3 : A) Tetrameric model of protofibril 12-40 B) Tetrameric model of protofibril 12-42 Both of them are stabilized by Lys28-COOH C-term and only 12-42 model also by Lys16-Glu22 ion-pair. In CPK are shown the most representative polar and hydrophobic aminoacids involved in the interface stabilization.

- Interaction of  $\beta$ A model 12-42 with inhibitors

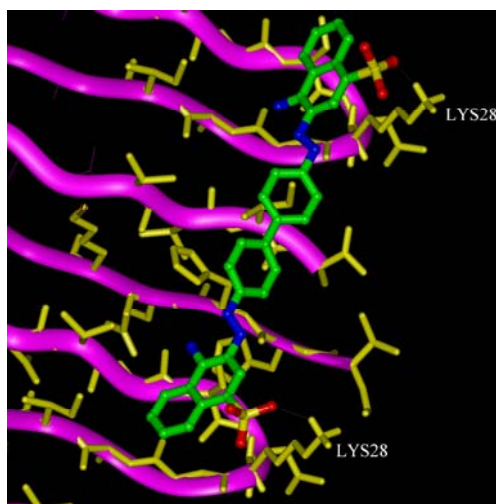
Different hypotheses are reported in literature to explain how Congo red (CR) binds to  $\beta$ A and inhibits its aggregation. Klunk W.E. et al (*J. Histochem Cytochem* **37(8)**: 1273-1281 (1989); *Neurobiol Aging* 15(6) 691-698 (1994)<sup>34and49</sup> work was taken as a reference that quantitatively examined CR bond to beta-sheet conformation of both insulin fibrils and poly L-lysine. Their conclusion hypothesized bonds between the two negatively charged sulfonic acid groups of CR and two positively charged amino acid residues of two separate protein molecules which are properly oriented by virtue of the beta-pleated sheet conformation of the peptide backbone.

In house docking results, based on the model B of protofibril, confirm as a possible solution the involvement of two Lys28 at a distance of 19 Å as counterions of sulphonate groups of CR.

Similar conclusions are retrieved using dyes with acidic groups as alizarine BBB

Fig. 4 shows the details of this mode of interaction for the sulphonate dyes.

A)



B)

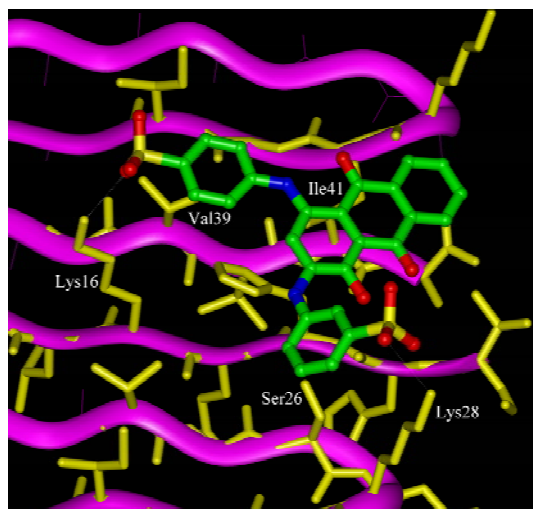


Fig. 4: A) Docking solution of CR (ion-pair interaction with two Lys28);  
 B) Docking solution of Alizarine BBB (ion pair interaction with Lys16 and Lys28)

The ion-pairing between Lysine and the inhibitor can destabilize the mechanism of aggregation, resulting in a diminution of neurotoxicity. To maximize the binding it is also important the lipophilic moiety of the inhibitor structure and the spatial localization with regard to the position of the acidic groups. These spatial parameters were

determined and used as a pharmacophoric model to discriminate active from inactive compounds in a series of different dyes (POSTER 60: 12<sup>o</sup> European Symposium on Structure-Activity Relationship Agosto 1998 – Copenhagen (Denmark))

Pamoic acid has different characteristics due to lack of planarity of the aromatic moieties, common to other dyes; nevertheless it is an active compound and a possible docking solution is reported where only one of the carboxy group is involved in an ion-pair interaction, the other one forms a H-bond with Ser26. Indeed the naphthol group interacts with hydrophobic aminoacids Ile31 and Val24.

The unexpected activity of bis naphthol in inhibiting 1-42 fibrillogenesis, as reported in tab. can be also explained using the 12-42 model of  $\beta$ A. In Fig 5 is shown the comparison between the mode of interaction of pamoic acid and bis naphthol. The second compound is embedded in a hydrophobic environment represented principally by Phe20 and Met35 and maintains a H-bond interaction between one of the phenolic groups and Glu22.

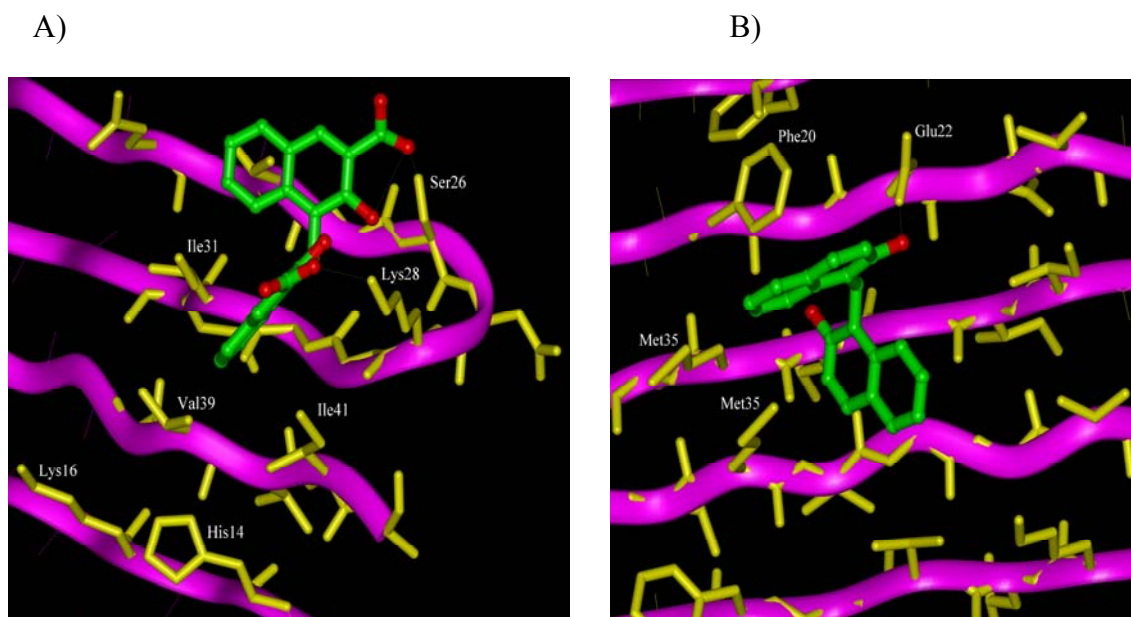


Fig. 5: A) A docking solution of Pamoic acid (ion-pair interaction with Lys28 and H-bond with Ser26); B) A docking solution of bis naphthol (H-bond with Glu22 and hydrophobic interaction with Phe 20 and the two Met 35)

Then the pharmacophore model of the two classes of compounds, pamoic acid and bis naphthol derivatives, proves to be very different, showing a net preference in orienting the acidic structures towards the external portion of the protofibril, where are localized the positively charged aminoacids and the hydroxilic structures towards the internal and more hydrophobic part, although both of them destabilize important interface contacts.

#### V. Diagnostic target

At the present time, diagnostic confirmation and visualization of the plaques in the brains of Alzheimer's patients can occur only after death, during postmortem autopsy.

The strategy to treat Alzheimer's disease (AD) involves the use of drugs designed to decrease or eliminate the formation of waxy extracellular clumps, or amyloid plaques, that appear in the brains of AD patients. It is those plaques that are believed to contribute to the inevitable decline in neurological function of these patients. No method currently exists that permits physicians to visually monitor changes in the plaque formations of the brains of living patients. Such monitoring would require the development of a probe, or dye-like compound, capable of not only crossing the blood-brain barrier(BBB) but subsequently binding to the plaque formations so that visualization of the amyloid clumps could occur using imaging methods (for example, positron emission tomography PET).

Researchers at the University of Pennsylvania School of Medicine have created a stealth-like molecule, called BSB, that can effectively breach the blood-brain barrier in mouse models and bind to specifically and sufficiently the resident plaque formations so that they can be visualized by existing imaging techniques. Their work, which represents the first time that Alzheimer-like plaques have been visualized *in vivo* in living animals, sets the stage for the refinement of this dye-like compound so it may be used to diagnose and monitor the treatment of patients with Alzheimer's disease. This research is an enormously important step towards developing an imaging method that could pinpoint the tell-tale signs of plaque development associated with Alzheimer's disease in a living brain. This tool could help clinicians peer into a person's brain and monitor amyloid levels in response to treatment<sup>50</sup>. We are presently involved not only in the study of molecules able to interfere with the  $\beta A$  aggregation process, but also in finding a diagnostic target to use in PET analysis, like the other research teams. Based on molecular modelling studies and *in vitro* biological results (see biological



experimental section, ThT test results), suggesting a possible interaction between the  $\beta$ -amyloid fibrils and our lead compounds, Pamoic acid and 1,1'-methylene-di-2-naphthol<sup>35</sup>, ST1859, have undergone BBB crossing studies. To attain our aim, the synthesis of the [<sup>14</sup>C]-Pamoic acid and 1,1'-[<sup>14</sup>C]-methylene-di-(2-naphthol)<sup>52</sup> has been developed in order to obtain a radiolabelled probe. They have been used to study the blood-brain-barrier(BBB) crossing and the accumulation in acute amyloidosis, in animal studies, using autoradiographic techniques. To understand how the BBB crossing has been evaluated, the method relative to ST1859 can be touched upon for example. Several experiments have been executed using <sup>14</sup>C-ST1859, by the Sigma-Tau biological Department. The labeled drug has been administered to male rats at different doses and checked after 30min and after 2h and 30min. The BBB crossing of ST 1859 can be expressed by a value related to radioactivity registration, made using a  $\beta$ -counter and reported as DPM/g (Decadiments per minutes/g) Brain BB in fresh tissue. These values are: 35643 after 30min., and 12365 after 2h and 30min. These studies show ST1859 ability to cross the BBB, with respect to Pamoic acid probably due to its uncharged structure. Based on these results, it is conceivable to use our lead compound (ST1859) for evaluating its binding with amyloidic deposits in the cerebral tissue from AD patients, *in vivo* studies. Due to the ability of bis-naphthol to bind to  $\beta$ 1-42, it could be also possible, by using the labelled molecule, to evaluate its binding competition with other non labelled compounds, putative intercalators during  $\beta$ -amyloid aggregation. To cope with *in vivo* studies, we have had to set the non- labelled reaction, following the fundamental characteristic<sup>53-57</sup> for the preparation of a PET drug, a radiopharmaceutical drug. It is well known, in the synthesis of a radiolabelled drug, the first step is the radioisotope production by a nuclear reaction<sup>53</sup>. This means the nucleus transformation by hitting it with particles, having enough energy. The most common used particles are the proton, deuteron and He nucleus, in order to obtain radioisotopes. These nuclei receive an acceleration inside a particle accelerator (e.g. a cyclotron) and are sent to the target that undergoes the reaction. These particles have a million electron volt-energy to combat the nucleus repulsion force and to be able to get inside the target, causing a variation in the ratio neutrons/ protons in order to generate the radionuclide. The particle energy is about 20 MeV. The hit nucleus can react following two ways: by

emission of a particle like the incident one, or by a decomposition, based on a real nuclear reaction with an emission of a different particle or a  $\gamma$  radiation. As soon as the molecule that has to be labelled has been chosen, it is very important to decide the radionuclide to use, which chemical form, which position to be labelled and the method to use to purify the labelled molecule. Choosing the radionuclide and the labelled position comes from the structure of the drug and from the synthetic pathway, formed of as few steps as possible, to introduce the radionuclide. Obviously the drug metabolic pathway influences the labelled position. Labeling a molecule means following some fundamental rules:

1. Reaction and purification time within the short half-life ( $T_{1/2}$ ) of the radionuclide. A finished PET drug product is typically administered to patients within a few minutes to a few hours following the preparation.
2. The radio synthesis has to be fast, reproducible and with high yield because it will be used in human studies. In general, a radiochemical synthesis at high specific radio activity has to be carried out in a simple way and its performance has to fit with the best yield of the product. In this context an important point of the radiosynthetic procedure is the isolation and purification of the product.
3. The starting material, which has to be labelled, has to be in large quantity to the labelled reagent.
4. The  $T_{1/2}$  has to be chosen according to study-time.
5. The radionuclide must decay by positron ( $\beta^+$ ). Others decay by EC (electronic capture), but these radiations are not useful in PET imaging formation, a PET drug exhibits a spontaneous disintegration of the unstable nuclei by the emission of positrons and it is used for the purpose of providing dual photon positron emission tomographic images. In consequence the decision to use  $^{11}\text{C}$  as radionuclide ( $T_{1/2} = 20.4$  min). Radiopharmaceutical drug labelled with  $^{11}\text{C}$  are widely used in nuclear medical imaging. Non- carrier- added-  $^{11}\text{C}$  is usually produced by proton bombardment of natural nitrogen gas via the  $^{14}\text{N}(\text{p},\alpha)^{11}\text{C}$  reaction. The ST1859 preparation is available to radio synthesis necessities. It has been prepared by a diarylation reaction, that involves the formaldehyde (well known radiolabeled reagent) using, as will be explained more deeply in the results and discussion

chemistry section. Non carrier- added-  $^{11}\text{C}$  can be extracted from the irradiated target in the form of  $^{11}\text{C}$  carbon dioxide. Many procedures have been established to produce ( $^{11}\text{C}$ )-formaldehyde. This method involves two steps, based on the reduction of target –produced  $^{11}\text{C}$  carbon dioxide to ( $^{11}\text{C}$ )-methanol and the subsequent oxidation of ( $^{11}\text{C}$ )-methanol to ( $^{11}\text{C}$ )-formaldehyde on metallic converters and catalyst. Because of target necessity, formaldehyde solution has been used in our laboratory, to set the reaction. At present our protocol is going to be carried out by a research team of Medical Vienna University Department of Clinical Pharmacology, on volunteer patients.

## 2. Results and Discussion

### I. Chemistry

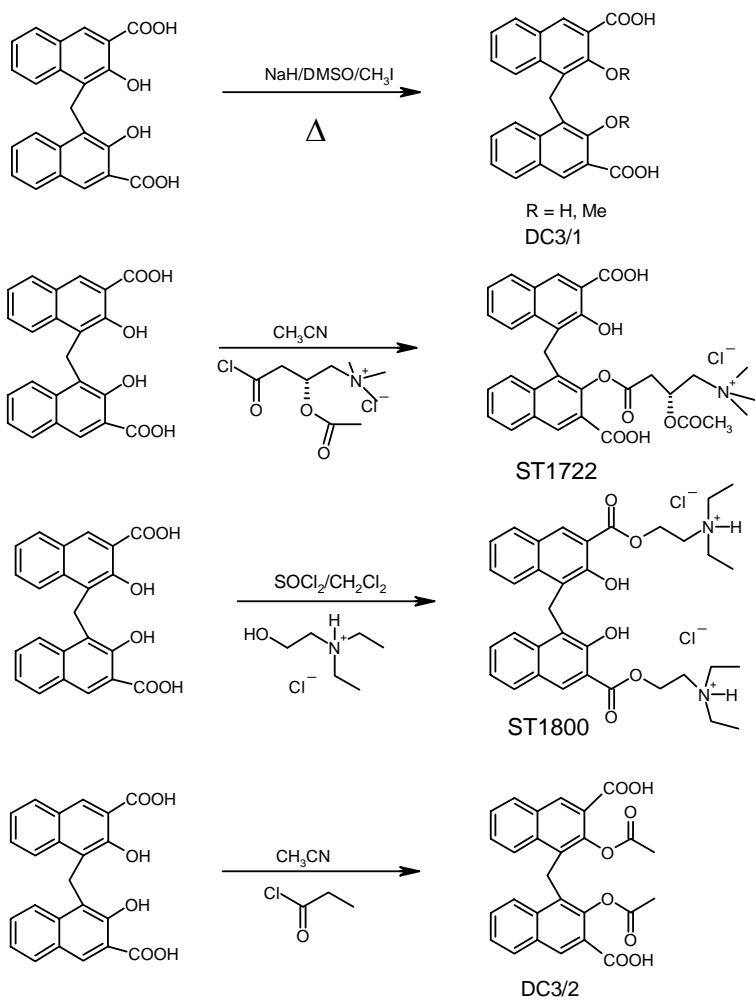
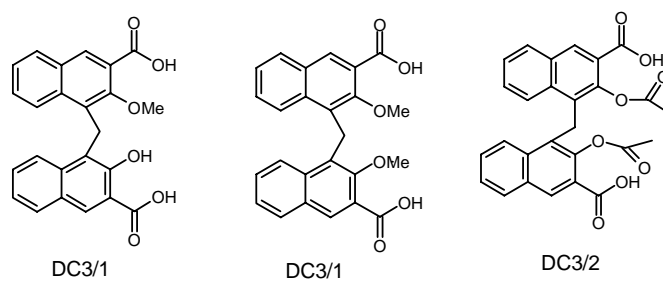
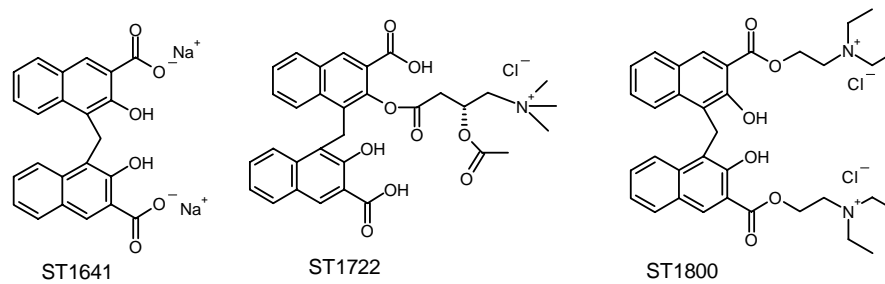
Our item consisted in synthesizing potential inhibitors of A $\beta$  aggregation, which have been tested in ThT test aggregation assay (see experimental section biology). Our biological and chemical interest has been focused on Pamoic acid and ST1859, based on molecular modelling and preliminary biological assay results, and therefore on the synthesis of their derivatives<sup>35</sup>.

- The Pamoic Acid Derivatives<sup>35</sup>

In pamoic acid, a commercially available product, the biaryl structure has been maintained with respect to CR by two naphthalen rings, bind at C-1 by a methylene bond, that let the carboxylic groups, that have substituted the sulphonilic ones, respects the charged groups distance established by the pharmacophoric model (see Molecular Modelling section). Some of its derivatives have been synthesized, to collect experimental data in order to cope with a structure-activity relationship (SAR).

The first one was sodium Pamoic salt (ST1645), which is also commercial. Following the same aim but also to obtain as much structural information as possible and obtain also a probable prodrug, some ether and ester derivatives of Pamoic Acid have been synthesized (See Scheme A). The groups that were introduced at first were L-acetyl carnitine (ST1722)<sup>35</sup> and diethylethanolamine (ST1800)<sup>35</sup>, successively simple methyl ester of the phenolic hydroxilic group, by simple esterification reactions. Other methyl ether derivatives at the phenolic groups have been obtained in low yield by simple etherification reactions but they were recognized with difficulty only by ESI-MS because of their complicated purification process.

Scheme A



- The Set Up of Non-Labelled 1,1'-methylene-2-naphthol (ST1859)<sup>35</sup> synthesis

The ST 1859 is a commercially available product, characterized by two naphthol rings, bound at C-1 by a methylene group, which breaks the system planarity by its  $C_{SP^3}$  hybridization. It has also been chosen to become the possible probe in autoradiographic ( $^{14}C$  animals studies)<sup>52</sup> and scintigraphic process ( $^{11}C$ -PET) for *in vivo* studies. Our item, satisfactorily reached, consisted in settling the reaction for the preparation of ( $^{11}C$ ) ST 1859 for PET studies, respecting the radiosynthesis necessities (see Diagnostic Target section). The synthesis of ST 1859 is a diarylation reaction<sup>58</sup>, whose time and yield have been improved to succeed in our aim.

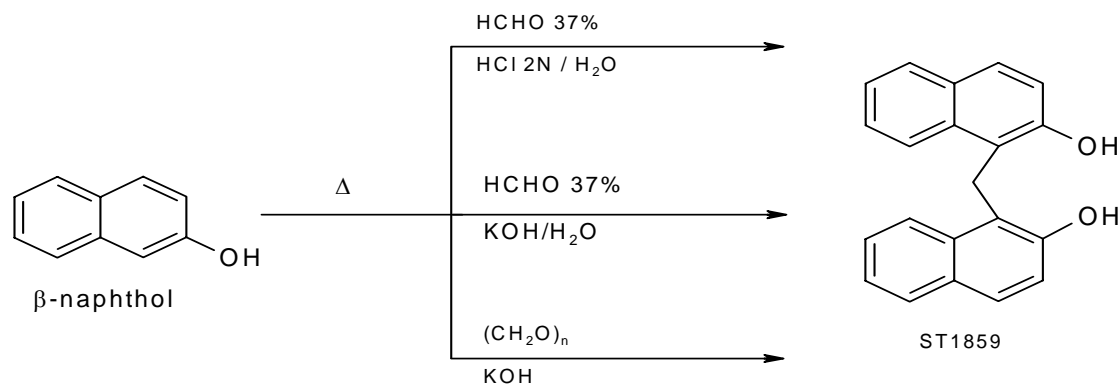
In alkaline condition catalysis, the reaction comes in two steps; the first one is like aldolic condensation: the  $\beta$ -naphthol is activated as phenolate ion, which leads to carbanion, which becomes the nucleophilic agent. This nucleophile attacks the carbonylic function of the formaldehyde. The second step consists in the addition of the other phenolate to a methylene cyclo esadienone, formed by a desidratation reaction of the intermediate. This reaction calls to mind the condensation of aromatic rings with aldehydes (or ketones) particularly the hydroxymethylation of phenols with formaldehyde, called the Lederer-Manasse reaction<sup>59</sup>. The diarylation reaction is especially common with phenols, in our case it was adapted to naphthols. It can be alkaline or acid catalysed.

This reaction must be carefully controlled, since it is possible for both C-1 and both C-3 positions to be activated and rearylated, so that a polymeric structure could be produced, even though the C-1 is more reactive than the C-3 position.

In acid catalysis the attacking species is the carbocation ( $RR'OHC^+$ ) formed from the aldehyde (or ketone).

These general mechanism and conditions have been applied in the synthesis of ST 1859(See Scheme **B**), trying to use both acid and alkaline catalysis in order to choose the best synthetic conditions to guarantee the highest yield of reaction, by 25 minutes (half time of  $^{11}C$ ).

Scheme B



The problems that we faced, were related not only to the choice of catalytic conditions, but also the formaldehyde reagent form to use, the molar ratio between the  $\beta$ -naphthol and the formaldehyde, the possibility to work by half time of  $^{11}\text{C}$ , obtaining the product in high yield and quickly or easily to purify.

Like aldehyde, the solid formaldehyde and the formaldehyde 37% solution have been used.

Generally, in PET studies liquid targets are preferred to solid ones, a cause of their minor hazard employment, also the preparation of  $[^{11}\text{C}]\text{-HCHO}$  leads to a solution because of the isotope species and the reagents used<sup>53-57</sup>. As a consequence, in order to prepare a reproducible chemical protocol for the radio synthetic laboratory, we have preferred the formaldehyde 37% solution to the solid one, even though we obtained the same yield in both cases. Re. molar ratio between  $\beta$ -naphthol and the condensing reagent (HCHO 37%), principally two different ratios were used the 1:1 and 2:1 to respect the radio synthesis necessary to work with soft excess of the  $\beta$ -naphthol to the labeled reagent. In aqueous alkaline conditions, using the molar ratio of 2:1,  $\beta$ -naphthol to HCHO 37% solution, the reaction was complete; using the acid catalysis, by HCl 2N,

molar ratio 1:1, the final product is fifty to fifty with starting material, within 1h, as highlighted by TLC. The purification was settled by the analytical group. It was used a C-18 symmetry column and CH<sub>3</sub>CN / H<sub>2</sub>O 70 : 30 as eluent. Choice of this elution mixture is not only due to the best condition of separation between the final product and the eventual starting material not reacted, but also for the easy decomposition of ST1859 in solvent like MeOH. The ST1859 has to be handled with care, because it is light and air sensitive; it undergoes oxidation process, like all phenols, this oxidation process is favoured by standing just for 1h dissolved in solvent like as AcOEt , CH<sub>2</sub>Cl<sub>2</sub> (sparling soluble), also MeOH, and especially if the sample is air and light exposed<sup>60-63</sup>. Preparing ST 1859 and its derivatives means working quickly under argon in dark vessels, avoiding as possible air contact, also in purification process too.

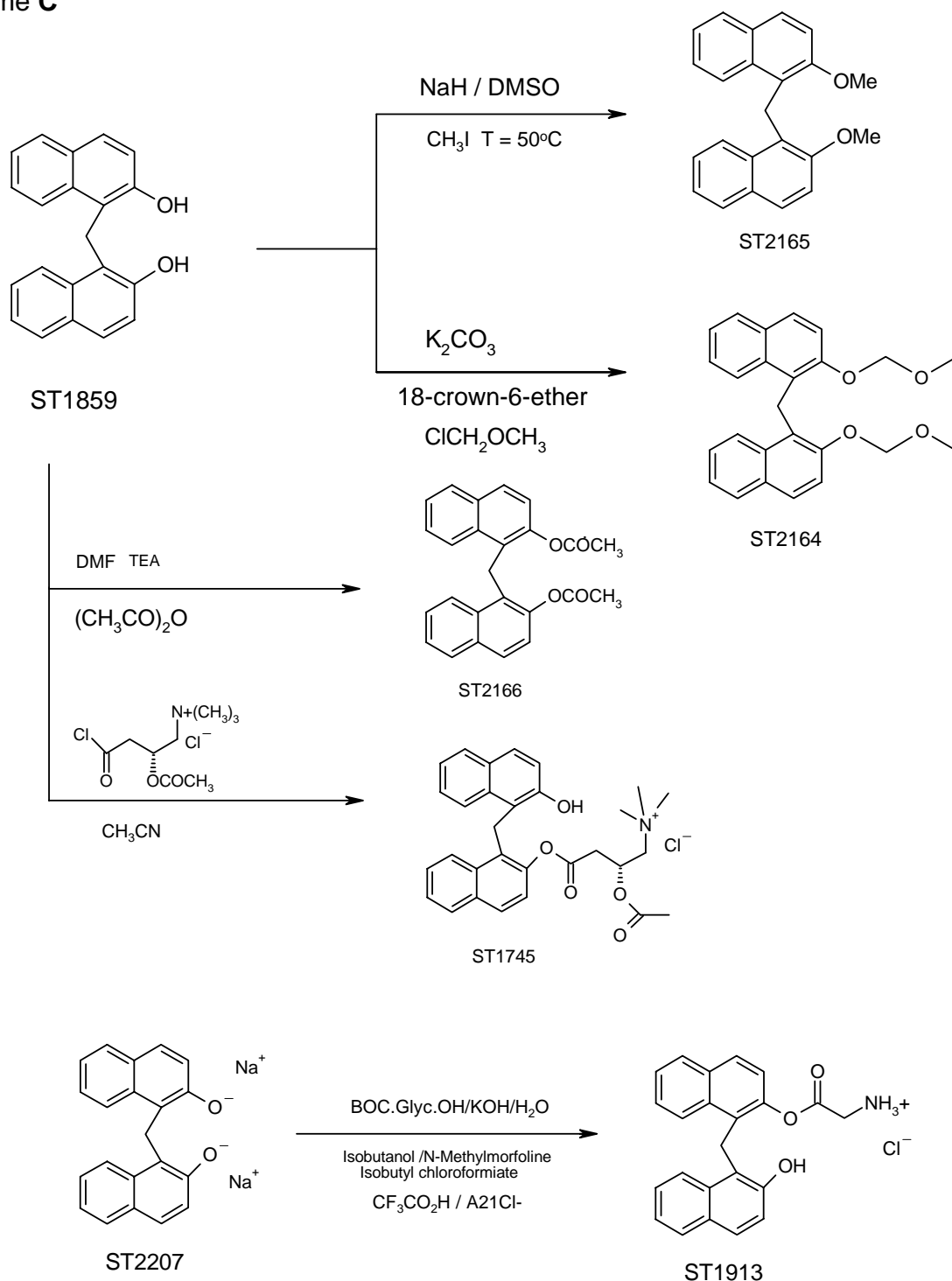
In order to enhance the low solubility of the product in aqueous solution (medium of the ThT test), as just done for pamoic acid, the sodium salt (ST 2207) was prepared, by an alkaline hydrolysis. Different bases have been employed to obtain the relative salt, (NaHCO<sub>3</sub>, KOH, Mg(OH)<sub>2</sub>, and NaOH). The salification difficulties were probably due to the pKa and electron withdrawing characteristics, related to the phenolic groups; particularly after the salification of the first phenolic hydroxyl group, the second one is less reactive for its enhanced acidity a cause of the resonance stabilization of the negative charge just formed; salification was finally obtained by an excess of NaOH. To eliminate the NaOH excess a recrystallization by isopropanol was necessary. The resulting salt has been identify by NMR characterization as highlighted by the evident disappearance of OH – proton signal at 10.18ppm in d-DMSO.

- Ether and Ester Derivatives of 1,1'-methylene-2-naphthol

To enhance the lypophilic characteristic of our lead compound, to obtain more structural information useful to SAR, and eventually thinking of a pro drug , the ST1859 has been derivatized at the phenolic hydroxyl groups by etherification and esterification reactions (SCHEME C).



Scheme C



The first simple ether derivative was the ST2165<sup>35</sup>, 1,1'-methylene-2-dimethoxynaphthalene, obtained by etherification of the two phenolic hydroxyl groups, activating by the use of NaH excess; the resulting phenolate ion is the nucleophile, which gives substitution to the methylene iodine at 50 °C under anhydrous conditions,

in a closed vessel, under stirring. The large amount of NaH and CH<sub>3</sub>I was used to carry on the reaction up to a quantitative yield, but as showed by TLC evidence (hexane/AcOEt 9 : 1) a small moiety of starting material compound always remained. The same reaction has been reproduced influencing the kinetic of the reaction, left overnight, without obtaining any improvement.

The product was identified by <sup>1</sup>H-NMR and <sup>13</sup>C spectroscopy. Its formation was clearly evident by the appearance of OCH<sub>3</sub> singlet signal at 3.98ppm, and the consequent absence of broad singlet relative to the phenolic group at 10.18ppm; looking at <sup>13</sup>C spectrum, the signal relative to 2xOCH<sub>3</sub> was highlighted at 56.3ppm. The diether derivative ST2164<sup>35</sup> was synthesized in order to better understand the importance of the phenolic free groups and also to study the influence of a spacer longer than a methylene at phenolic group at C-2,2' derivative in Aβ interaction. It was prepared using different experimental conditions respect to the ST2165<sup>35</sup>. A soft activating agent of the phenolic protons, like as K<sub>2</sub>CO<sub>3</sub> was used, but in order to enhance the nucleophilic power of phenolate ion formed at alkyl halide(ClCH<sub>2</sub>OCH<sub>3</sub>) a crown ether (18-crown-6) was employed under anhydrous conditions.

The ST2164<sup>35</sup> has been obtained in a quantitative yield, without any further purification.

The ST2166<sup>35</sup> is the founder of ester derivatives of ST1859 (See Scheme C). It was synthesized by a simple classic esterification reaction of ST1859. The phenolate ions, formed by triethylamine hydrolysis, gives substitution at the acetic anhydride in anhydrous conditions.

The ST2166 was directly obtained as white solid, without any further purification; it was characterized by <sup>1</sup>H-NMR in DMSO, where it is evident the -CH<sub>3</sub> singlet signal appearance at 1.90ppm.

The synthesis of ST1913<sup>35</sup> was faced up to obtain an ester with an higher solubility in aqueous solution. In order to obtain the ST1913<sup>35</sup>, an esterification reaction was always used, just a little bit longer in execution time for the preparation of the reagents. The ST2207 was derivatized by bocglycine in KOH at 180°C activated, by its treatment with isobutyl chloroformate and N-methyl morpholine in isobuthanol. The resulting product was submitted to an acidic hydrolisis and finally obtained by passing it on A/21 resine (See Scheme C).

The ST1745<sup>35</sup> has been synthesized having in mind the possibility to form a product that included in itself different characteristics: it could cross the BBB, for its lipophilicity due to bis-naphthol scaffold, it could be derivatized by a chiral agent at C-2 to study its weight on the A $\beta$  interaction, and it could be soluble enough in aqueous solution due to the quaternary ammonium. Furthermore there was the possibility to let the acetyl carnitine eventually pass the BBB, using the bis-naphthol moiety as carrier, but even though is possible a cause of its charged nature and also a cause of the probable hydrolysis of esterases, it could be interesting to exploit the known protecting neurotoxic damage effects of acetyl carnitine<sup>35</sup> in other mental disorders (all synthesized esters could be seen as pro drug). Looking at this ambitious item, the chloridrate L-acetyl carnitine (previously prepared and isolated from its enantiomer)<sup>35</sup> was treated with SOCl<sub>2</sub> in CH<sub>2</sub>Cl<sub>2</sub> to obtain the acyl chloride derivative, which was the object of the nucleophilic substitution of ST 1859 phenolate ion formed by an alkaline reaction. The mono ester derivative (ST1745) was isolated by purification and characterized by <sup>1</sup>H-NMR data (See Scheme C).

There is a multiplet at 2.00ppm relative to the CH<sub>2</sub> of ester to naphthol and the shift at low field (8.40ppm) of H-3' proton, probably due to the deshielding effect of the carbonylic group of ester formed at C-2.

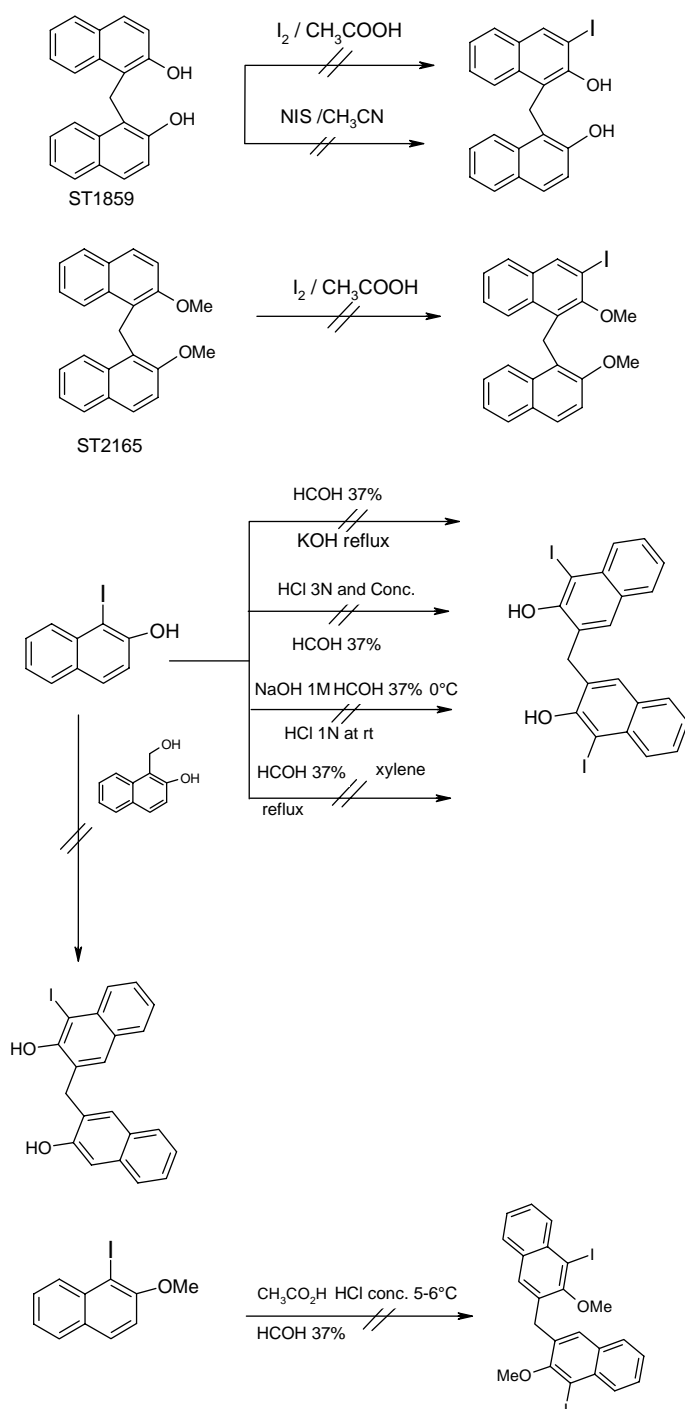
Obviously there are the signals relative to the remaining L-acetyl carnitine structure: the singlet of -N(CH<sub>3</sub>)<sub>3</sub> at 3.10ppm, the singlet of CH<sub>3</sub>CO<sub>2</sub> at 3.40ppm, the multiplets relative to the CH<sub>2</sub>-N at 3.60-4.00 and the coupled stereogenic H at 5.60ppm.

- Halide Derivatives of 1,1'-methylene-2-naphthol

Our interest was also in finding out the consequence of an halogen introduction on the biphenolic structure of our lead compound, not only for the SAR studies but also to create a possible probe molecule to use in scintigraphic investigation, alternatively to the [<sup>13</sup>C] 1,1'-methylene-2-naphthol, which had been just settled and employed.

Our item was to have an iodine derivative, because I<sup>125</sup> can be used in scintigraphic process, so it was important to find a strategic pathway that let us to introduce or obtain easily a iodine derivative. Different synthetic approaches were faced (See Scheme D).

Scheme D

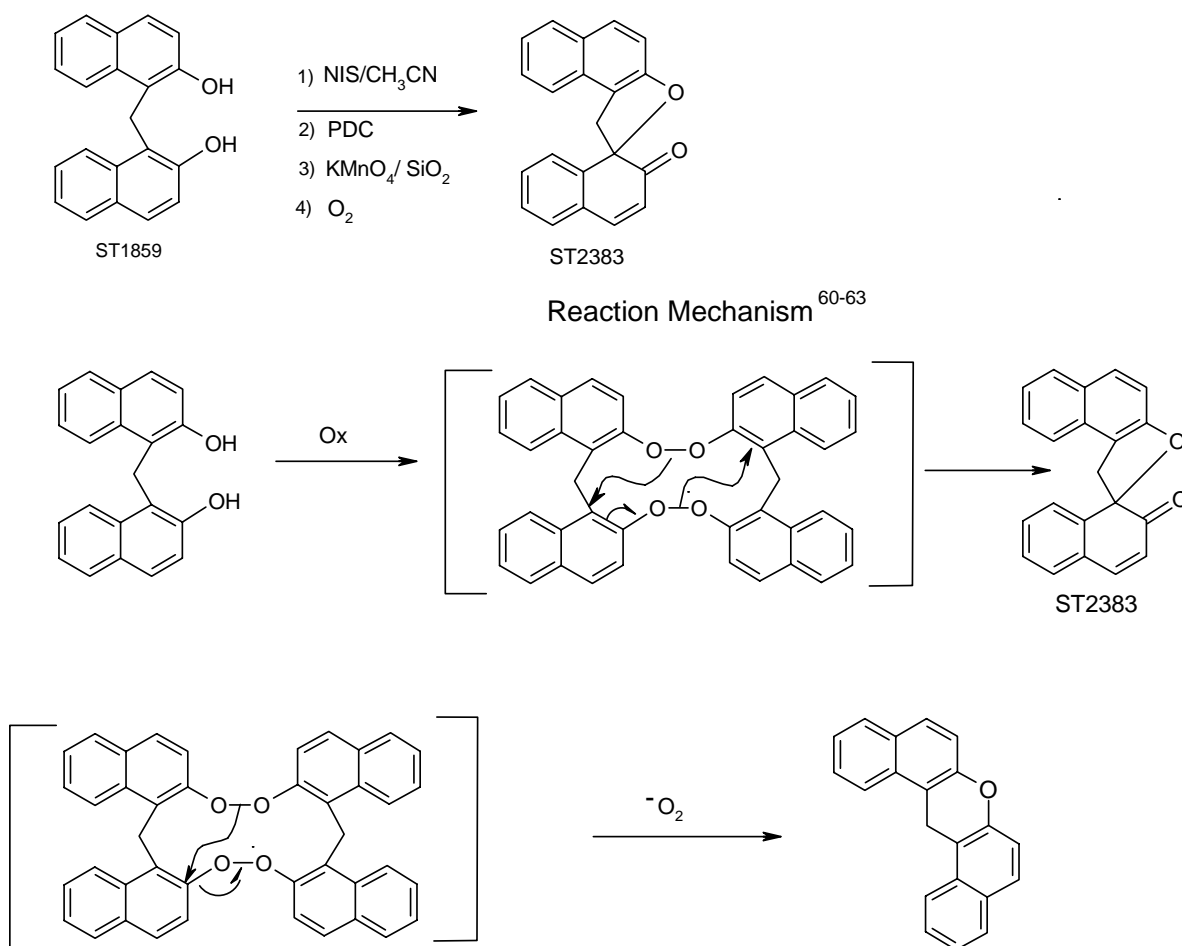


All attempts made to introduce Iodo directly on the two biphenyl structures of ST 1859 or ST2165<sup>64-67</sup> failed (see scheme D), however the use of NIS reagent, gave interesting results; the starting material (ST1859), added of NIS in CH<sub>3</sub>CN, both at room

temperature and at 80°C, trying to make the iodination reaction start, gave the same result: the spiro derivative compound (ST2383)<sup>62</sup>.

Its formation could be probably due to an oxidative characteristic component of NIS, and its radical action mechanism well known in the iodination of double bond. In our case both these two factors: a radical initiator supported by oxidative conditions led to the initiation of a radical oxidative intramolecular coupling of phenolic hydroxyl groups; this hypothesis is confirmed by other experimental data, collected directly from oxidation of ST1859, by using PDC and MnO<sub>4</sub> on SiO<sub>2</sub>, in CH<sub>2</sub>CL<sub>2</sub> solution at room temperature<sup>60-63</sup> (see Scheme E).

Scheme E



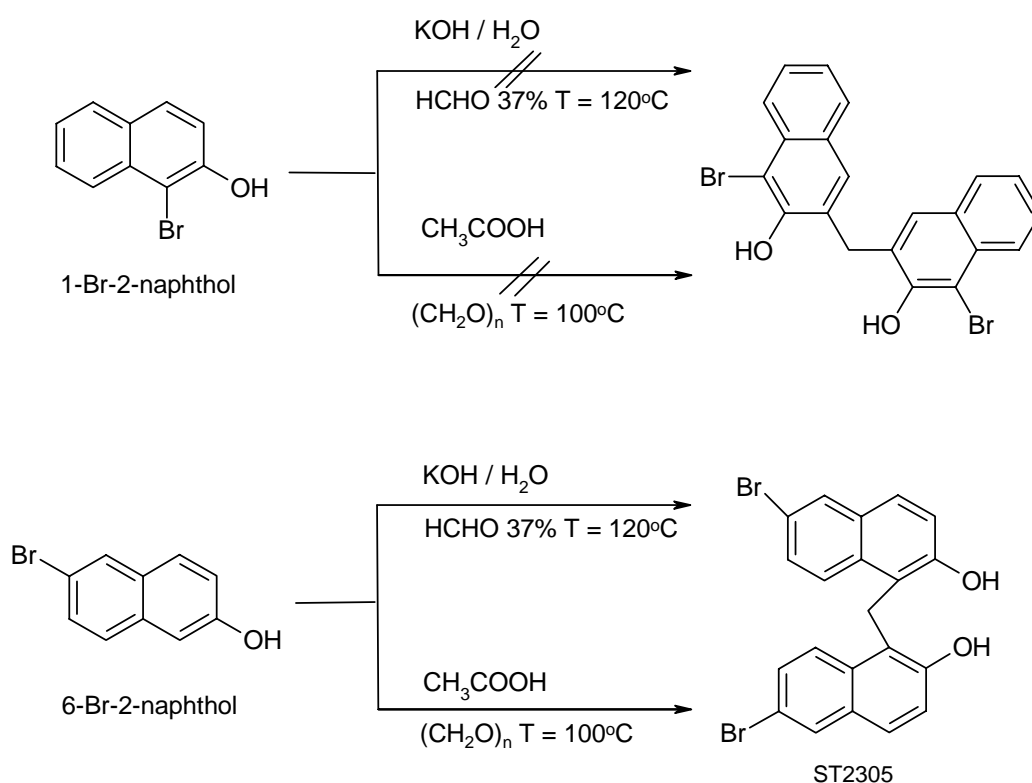
The only result obtained has been the same spiro compound derivative, as confirmed by the <sup>1</sup>H-NMR and <sup>13</sup>C data. It is possible to highlight that the singlet relative to the methylene of ST1859 splits in a double doublet.

In the spiro structure this signal shifts from 4.80 to 3.50 and 4.00 ppm at highfields; the splitting of the singlet to a double doublet can be due to a non magnetic and chemical environmental equivalence of the two protons. They become a non magnetic and chemical equivalent because they are not yet linked to a symmetric structure, as before. The methylene protons become enantiotopic and connected to a stereogenic chiral center (C-1'). There has been a shift of H-3' of ST1859 to high field (6.29ppm), because in the "spiro" structure this proton belongs to an  $\alpha$ - $\beta$  insaturated system, instead of an aromatic one. From  $^{13}\text{C}$ -NMR analysis the characteristic carbonyl signal is that one that allows us to identify the hypotised structure and it is highlighted at 186.5ppm.

It is also possible to recognize the C-2 at 153.2ppm and C-1' at 100.1ppm. Another synthetic pathway was followed to reach our item; in order to obtain the iodo derivative, we attempted to exploit the acid or base coupling reaction using commercial iodo naphthol and methoxy derivative as starting material<sup>68-70</sup> (See Scheme **D**); no results were obtained, probably a cause of the disactivated starting naphthols for stereo electronic reasons. In fact the iodo at C-1 with its electron withdrawing power could diminish the possibility to form phenolate and in consequence diminish nucleophilic power of C-3, in alkaline conditions, even though it has to be considered that the diarylation should however be expected at C-3 (for the characteristics of the substituent groups) position.

To reach our goal, consisting in introducing anyway and at any position a Iodine onto the skeleton of the lead compound (but also any other halogen for the SAR studies), it was thought to obtain a bromide derivative of the ST1859, to turn to indirect iodination by lithiation of the corresponding bromide, followed by treatment with iodine<sup>71-75</sup> (See Scheme **F** and **G**).

## Scheme F



In order to obtain the bromide derivative, several direct bromination attempts of ST1859 and ST2165 had been tried, but did not lead to satisfactory results. To reach our goal, it was hypothesized to use commercially available starting materials like 1-Br-2-naphthol and 6-Br-2-naphthol, (SCHEME F) that had to undergo the diarylation synthesis method<sup>58</sup> settled for the preparation of ST 1859(See SCHEME F).

Using the 1-Br-2-naphthol by acid or alkaline catalysis, with HCHO 37% (easier to use) but also solid one, did not lead to the hypothesized result; both reactions failed to start, probably due to stereo electronic reasons. In fact, the bromide electron withdrawing capacity at C-1 position, decreases the nucleophilic power of the phenolate ion formed in alkaline conditions, or of the phenolic hydroxyl group in acid catalysis, to the formaldehyde carbonyl. This hypothesis has been supported by the successful

completing reaction of the 6- Br – 2 naphthol, which let us obtain ST2305 (SEE SCHEME F). The naphthol has been activated by alkaline catalysis.

As coupling agent we chose the HCOH 37% (1 : 1) at reflux, under stirring. The reaction was complete within 3h with high yields (56% to naphthol, low yield was obtained by acid catalysis). The formation of a bromo derivative has been confirmed by <sup>1</sup>H-NMR and <sup>13</sup>C analysis.

The first important signal that has to be highlighted, it is the singlet at 4.62 ppm, relative to the formation of methylene bridge between two naphthol structures.

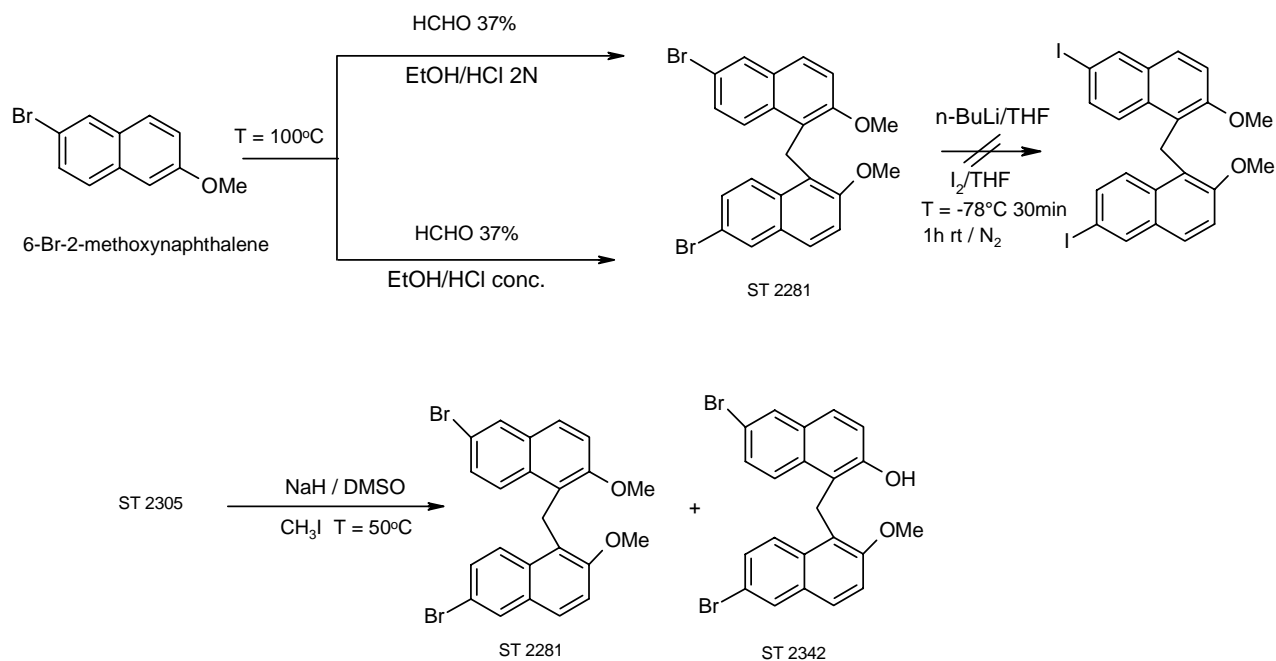
From <sup>13</sup>C-NMR analysis the CH<sub>2</sub> appears at 28.3ppm. The structure has been confirmed by IS analysis for negative infusion that puts in evidence the molecular peak at 457 m/z; the peak shows the typical isotopic abundance of two bromo containing structure. Electron withdrawing hindrance can explain the good result of this reaction respect to that one done with 1-Br-2naphthol.

The different position of the Bromo on the naphthol ring in the starting material occupies the C-6 position simply furthest respect to phenolate ion and means that the electron with drawing power of Bromo has a minor impact on the nucleophilicity of phenolate ion at H-2, and on its consequent rearrangement and activation of the C-3 carbanion attacking position.

Following this synthetic success, the coupling reaction was applied on other Bromo derivative naphthol in order to obtain bisnaphthol structure with different functionalization at phenolic hydroxyl groups. The diarylation conditions<sup>58</sup> have been adapted to the 6 – Br – methoxynaphthalene and let us obtain ST 2281(See SCHEME G).



## Scheme G



Its coupling has been executed by acid catalysis: using HCl 2N in EtOH as reaction solvent, without altering the other experimental conditions (reaction time and temperature), and also by HCl conc.

By soft acid catalysis, the product was obtained with a low yield, by HCl conc. the reaction was quantitative (54% to naphthalene) the ST2281 formation was confirmed by IS analysis that showed the molecular peak at 487m/z positive infusion, with the characteristic isotopic abundance aspect due to the two bromo on the scaffold. The ST 2281 structure was definitively assigned by <sup>1</sup>H-NMR and <sup>13</sup>C analysis. In <sup>1</sup>H-NMR, the singlet signal, relative to the methylene protons, appears at 4.80ppm, which can be also identified at 28.3ppm in <sup>13</sup>C analysis. The ST2281 was used as intermediate in order to obtain the iodo derivative by lithiation of the corresponding dibromide, followed by treatment with iodine<sup>71-75</sup>. All attempts led to a decomposed reaction mixture where the product of our interest, as highlighted by IS studies, was not present.

In order to obtain more possible information to use about SAR, it has been thought to synthesized a bromo bis naphthalene derivative that maintains one phenolic hydroxyl group protection free (See Scheme G).

ST2305 has been exploited as the intermediate for the partial functionalization of the phenolic hydroxyl group by simple methoxylation reaction, which had been used in ST2165 preparation.

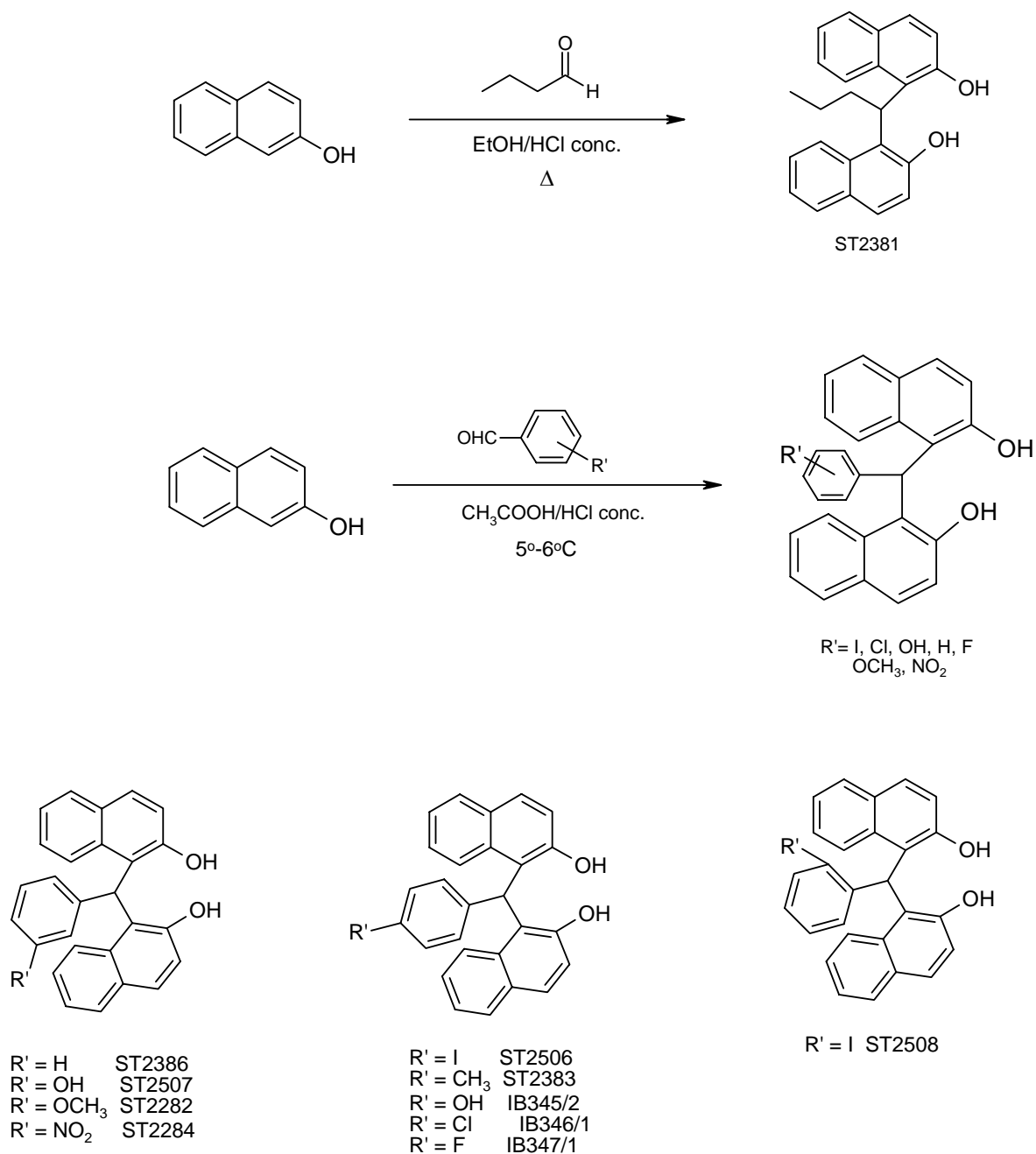
The methoxylation reaction has been utilised in the same experimental condition described for ST2165, but using a stoichiometric CH<sub>3</sub>I amount to obtain the monomethoxylated derivative.

The reaction mixture obtained highlighted the mono-, di – methoxylated derivative and the starting material; the dimethoxylated product (ST2281) with very low yields (8%), the product of our interest (ST2342) with satisfactory yield(67%) both confirmed by IS analysis, which shows the molecular peak at 471 in negative infusion, because of the hydroxyl free at C- 2. Its structure has been confirmed by <sup>1</sup>H-NMR and <sup>13</sup>C analysis; there is a shift of the methylene protons signal to low yields starting from 4.62ppm relative to ST2305 to 4.78ppm relative ST2342, due to the deshielding effect of the methoxygroup, at C-2; there is a singlet at 4.10ppm that shows an area of only 3H, relative to OCH<sub>3</sub> and the presence of one phenolic hydroxyl group at 8.20ppm as broad singlet. This free phenolic hydroxyl should enhance the solubility of the product in water solution.

- Aliphatic and Aryl Derivatives of 1,1'-methylene-2-naphthol

In order to functionalize the scaffold of Lead compound furthermore, we hypothesized and synthesized the aryl and aliphatic derivatives of ST1859 at methylene bridge. To reach our goal, an acid catalysed condensation<sup>76-77</sup> was chosen and applied, using different acids relative to the nature of the aldehyde (See SCHEME H)

## Scheme H



In order to obtain an aliphatic derivative at methylene conjunction, drawing one's inspiration from literature, but having cross C-C coupling methodology at our disposal, we thought to apply the acid catalysed condensation of previously described products.

Mild conditions were used with respect to those in literature<sup>76-77</sup>. From data reported in literature<sup>76-77</sup>, of several acids tested in this condensation, the best results were obtained using a catalytic amount of trifluoromethanesulfonic acid (TFOH), as a very strong acid, and the 3kbar pressure, but this synthetic method was efficient for C-C cross coupling of phenols, of some reactive naphthols with aromatic aldehydes. In the same reaction, using an aliphatic aldehyde (in literature propanal) fairly low yield of the coupled product was observed. The lower product yields might be ascribed to the unavoidable side reactions under these hard conditions. Furthermore no reaction has been observed when pivaldehyde had been used as an aliphatic aldehyde. Based on these results, our choice using a mild acid cross coupled reaction grew much stronger.

ST2381 was synthesized; following the standard procedure the 2-naphthol attacked the activated carbocation of butiraldehyde, by HCl conc. catalysis, at 60°C under stirring for 3 hours. The reaction mixture showed several by side products, also the starting material.

The final product (ST2381) has been obtained with low yield (4.1%). The propionaldehyde derivative has not been obtained in the same reaction. The ST2381 formation has been determined by IS analysis; there is a molecular peak at 341.0 m/z per negative infusion.

By <sup>1</sup>H-NMR analysis the structure is assigned; the splitting of the methylene singlet signal to the triplet one's that appears at 5.78ppm, has been highlighted.

The low fields shift and the coupled signal are due to the aliphatic chain introduction at the methylene as also confirmed by methyl triplet at 0.9, the H-2'' quartet at 1.42 and the H-3'' singlet at 2.5ppm.

Our goal consisted also in obtaining aromatic methylene derivative too; but once again we preferred not to use the drastic conditions such as the high pressure and TFOH catalysis, but other mild ones as devised by literature.

Furthermore, this choice is motivated by the future possibility to scale up the preparation of the compounds if they become drugs.

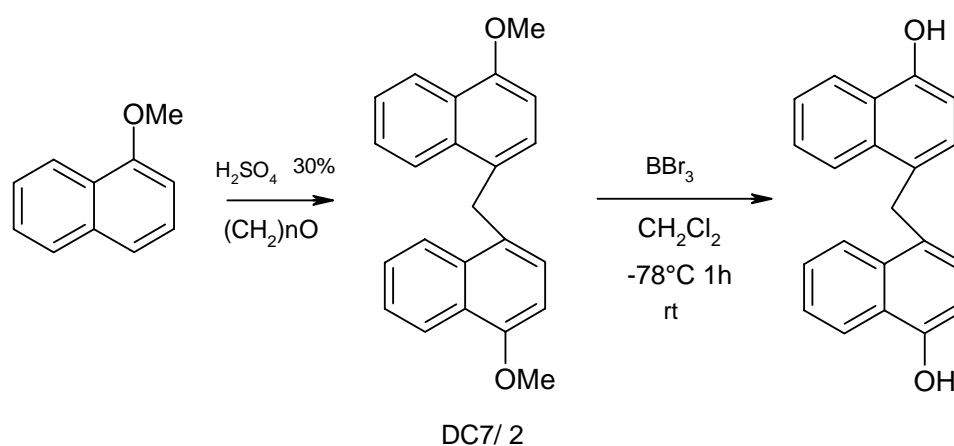
Several products have been synthesized by acid catalysis coupling, using HCl conc., CH<sub>3</sub>CO<sub>2</sub>H and different functionalised benzaldehydes<sup>78</sup>; they are reported in scheme H.

The other reported compounds (ST2282, ST2284 and ST2383) are available commercially.

- 1,1'-methylene- $\alpha$ -naphthol Compound

To indagate the effect of the phenolic hydroxyl group position on the interaction with the fibril model, an  $\alpha$ -bisnaphthtol derivative (DC7/2), as described in literature<sup>79</sup>, was synthesized (Scheme H'). The deprotection reaction of methoxy groups led to low yields (< 5%).

**Scheme H'**



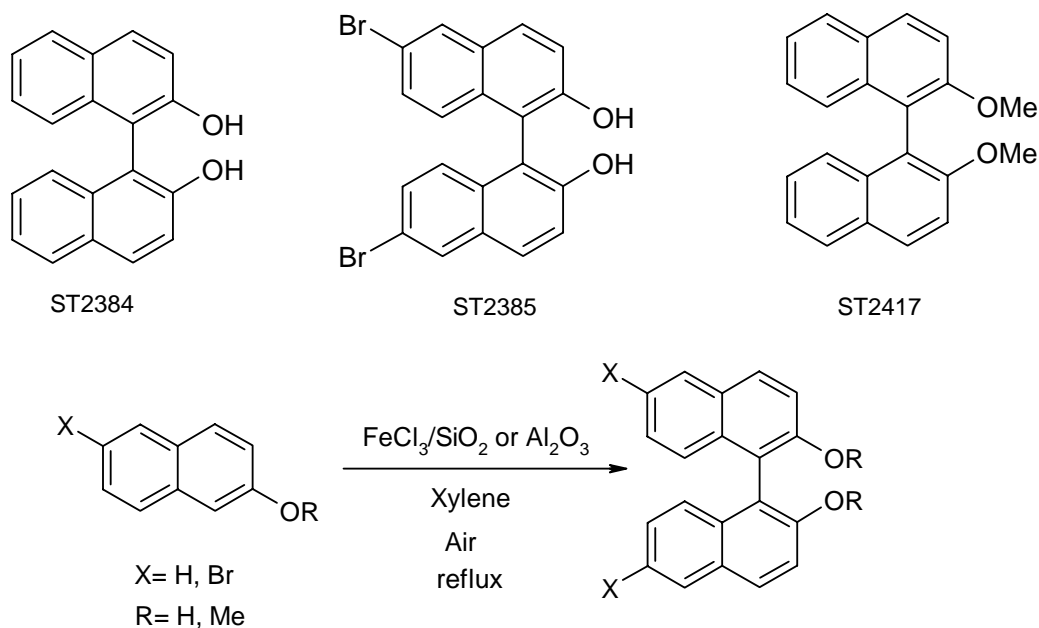
- 1,1'-binaphthalene Compounds

To analyze the real importance and influence of a methylene bridge between the two byaryl structures towards the A $\beta$  interactions, it was thought to eliminate it. The structure that agreed with our necessity were 1,1'-2-naphthol derivatives like racemic mixture<sup>80</sup>; these compounds remind us the famous chiral phospholigand inducing agent in asymmetric synthesis (Noyory 1986), and the most similar C-C coupling Suzuki products.

Using a catalytic oxidative coupling of 2-naphthols, catalysed by solid lewis acid in atmospheric oxygen as oxidant, according to the literature method (SEE SCHEME I) we used FeCl<sub>3</sub> on SiO<sub>2</sub> as catalyst, in a stoichiometric quantitative. The oxidative coupling reaction is carried out rapidly and simply by heating slurries containing the starting materials and the catalyst in xylene at refluxing temperature whilst bubbling air

through the mixture. The products have been obtained in high yield, short time, and further purification by treatment with active carbon or by simple crystallization (ST2384, ST2385, ST2417).

### Scheme I



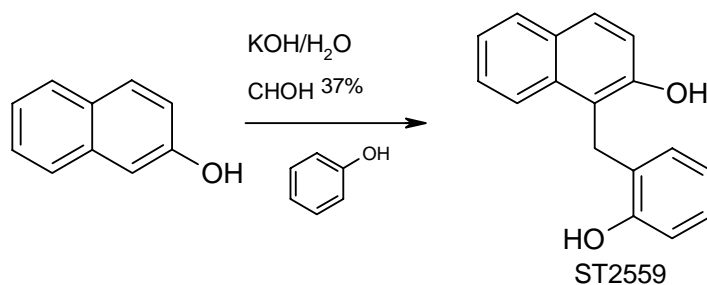
Furthermore the compound ST 2417 has been synthesized to study the effect of hydroxyl phenolic group protected.

The  $^1\text{H-NMR}$  and  $^{13}\text{C}$  analysis of ST 2384, 2385 and 2417 agree with the literature data and are reported in the experimental section.

- 1- (2-hydroxybenzyl)-2-naphthol Compound

In order to understand the importance of the biaryl structure in the interaction of the bis-naphthol towards the  $\text{A}\beta$ , the ST2559 was synthesized<sup>58</sup>. It can be considered a simple structural simplification of our lead compound (the hydroxylic function always occupies the H-2 position) (See SCHEME L).

Scheme L



It has been obtained by alkaline catalytic coupling settled up reaction with low yield (11.6%).

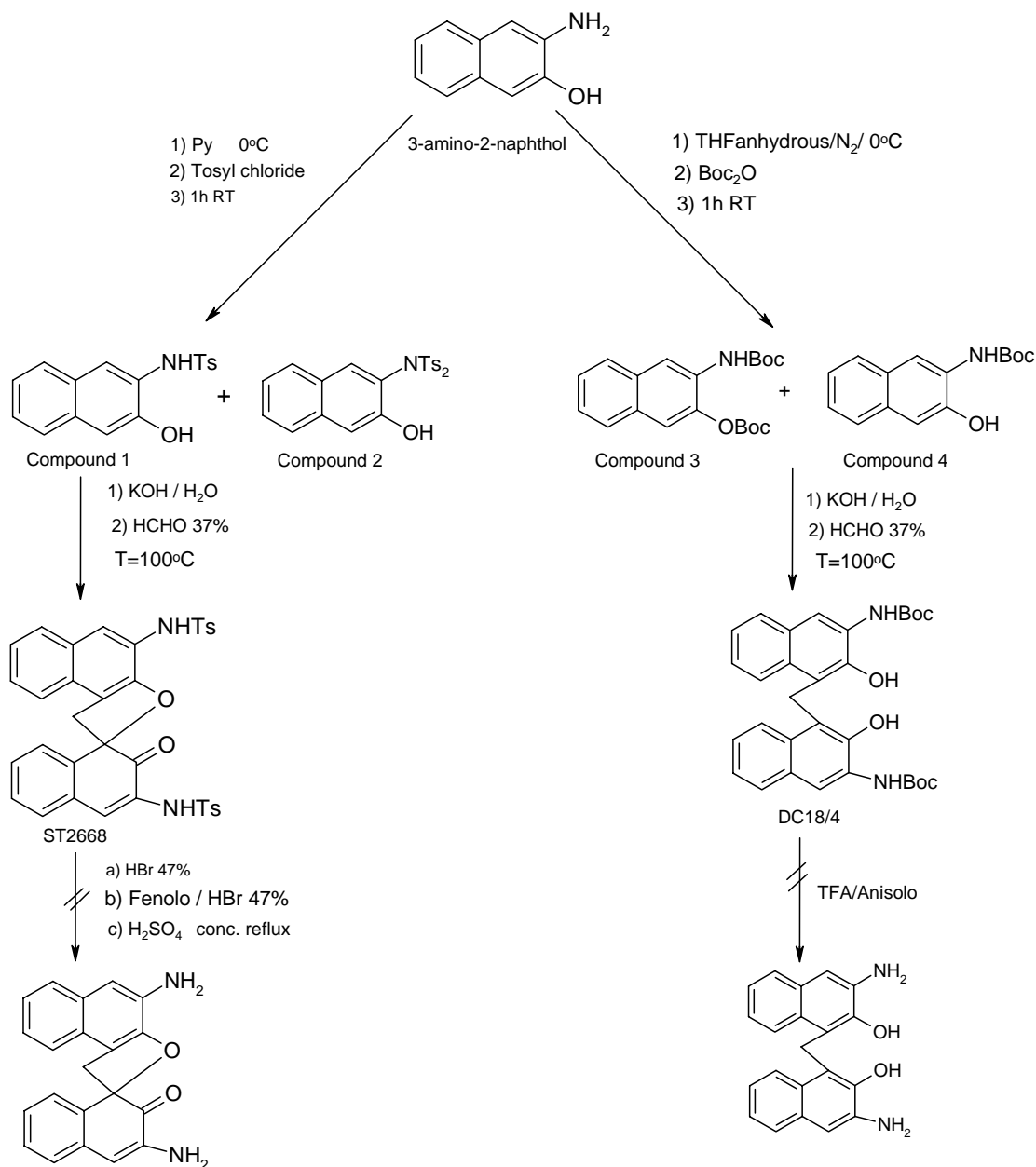
The structure was confirmed by analytical assays as IS, which shows up the molecular peak at 249m/z and by <sup>1</sup>H-NMR data, with the doublet at 4.4ppm relative to the methylene, and the two broad singlets at 4.70 and 5.00ppm.

- Amino Bis-Naphthol Derivatives

In order to resolve the solubility problems relative to the bis-naphthol derivatives, we proposed to insert an amino group on the bis naphthol scaffold.

To reach our item sulphonamide and tert-butoxyamide derivatives have been synthesized (See scheme M).

Scheme M



Two different selective protections of the amino group have been used<sup>81-82</sup> : selective tosylation of 3-amino-2-naphthol and anhydride butyl carbamide protection.

In the first case, both O- and N-Toluen p-sulphonil derivatives of o-aminophenol have been long known<sup>81</sup>. The same reaction conditions were applied to our aminonaphthol derivative. The tosylamide has been prepared by reaction of the naphthylamine with tosyl chloride in pyridine. The selectivity in the monotosylation was possible using a tertiary amine such as pyridine instead of Et<sub>3</sub>N. The tosylamide obtained (Compound 1)



underwent the alkaline catalyzed coupling reaction<sup>58</sup>, by HCHO 37% in KOH/H<sub>2</sub>O at 100 °C under stirring for 3h. The final product ST2668 has been obtained with low yield (17.3%).

The product was identified by IS analysis, which reveals the molecular peak at 635 m/z and by <sup>1</sup>H-NMR and <sup>13</sup>C NMR data; there are two doublets at 3.3-3.5ppm relative to the methylene protons not chemically and magnetic equivalent because of a non equivalent chemical environment. The H-4' shift to highfields (6.85ppm) and finally, but not least, the C = O at 192.2ppm.

The Boc pathway guaranteed the two amino boc derivatives<sup>82</sup> (Compound 3 and 4). It has been seen experimentally that there is not so much evidence of selectivity in this kind of protection, respect to literature data. The selectivity decrease is probably due to the work-up execution. After the (Boc)<sub>2</sub> O adding to the aminonaphthol in THF at room temperature, if the reaction mixture is quenched by evaporation under reduced pressure at 40°C, we obtain compound 3 (yield =62%) predominant to compound 4 (yield=17%); on the contrary, if the reaction is directly quenched by adding water, the main product becomes the monoderivative (yield=56%); probably, in the first experiment, the two derivatives have been obtained because of the drawing force of temperature using to quench the reaction in the work-up. However, these experimental conditions have been exploited by us and both of the two derivatives have been preferentially obtained and used in alkaline catalysed coupling reaction<sup>58</sup> to obtain the final product DC18/4, as highlighted by <sup>1</sup>H-NMR and <sup>13</sup>C analysis. The characteristic methylene singlet at 4.82 ppm by <sup>1</sup>H-NMR and at 28.3ppm by <sup>13</sup>C-NMR, highlights the bond formation between the biaryl structure, and the free hydroxyl groups appear again at low fields as broad singlet (9.40ppm). The major yield was obtained by the coupling of Compound 3 derivative.

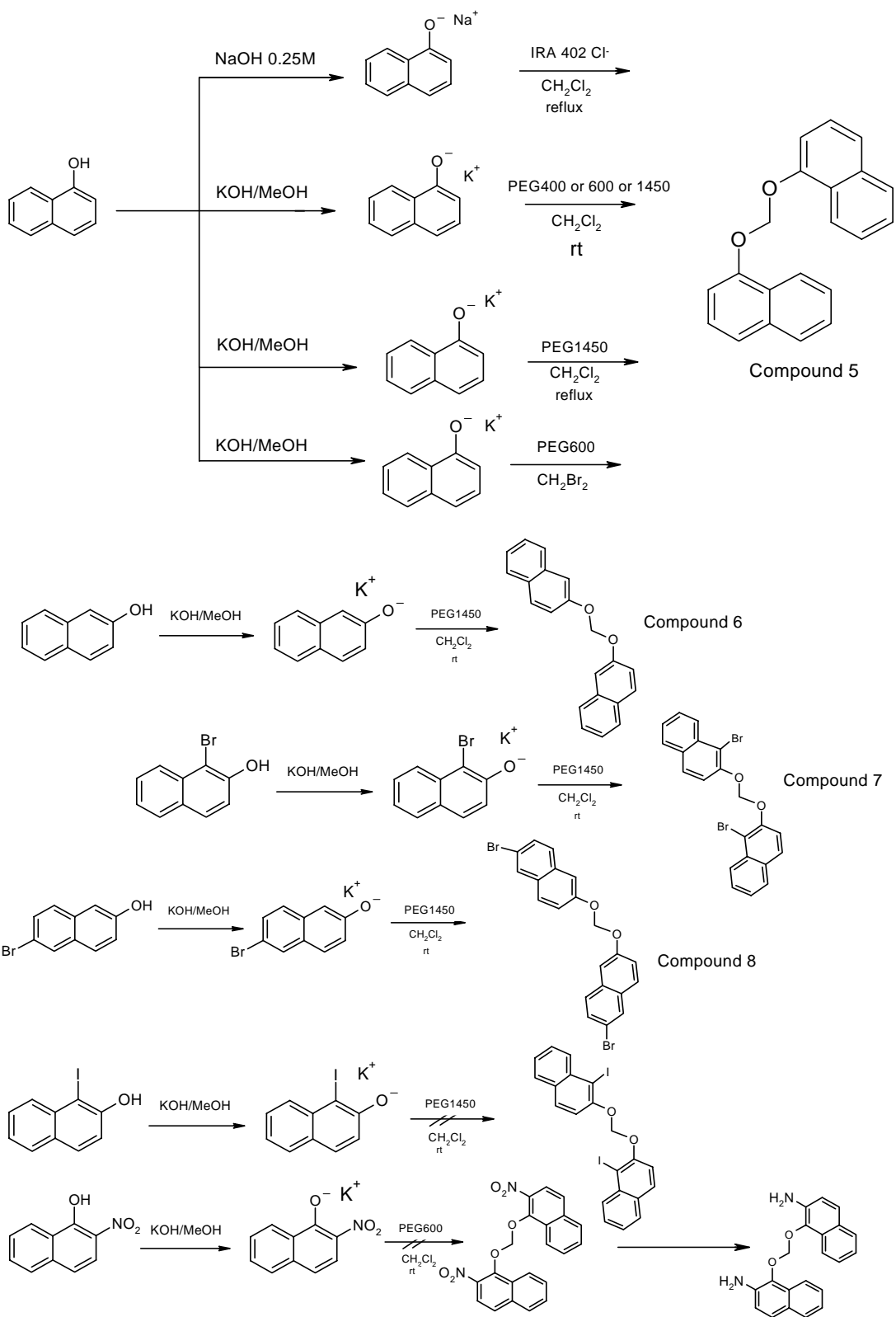
Our attempts in deblocking the amino group<sup>83</sup> have failed probably because of the intramolecular hydrogen bond interaction created between the amino Boc proton (donator) and the phenolic oxygen (acceptor), strong enough to inhibit the usual deprotection. An intramolecular nucleophilic substitution of the phenate, activated by NaH, at the amino boc, was proposed to make the amino group free. The amino tosyl deprotection<sup>84-86</sup> doesn't react probably because of a particular steric configuration, due to its final spiro structure.

- Diaryloximethane Compounds as Models for 1,1'-methylene-2-naphthol Derivatives

In order to obtain as much information as possible about structure and activity relationship, it was been proposed enhancing the space distance between the two naphthoic moieties. An answer to our necessity could be the diaryloxymethane compounds<sup>87-88</sup>, where the two biaryl structures were separated by a diether bond.

The 1-diaryloxymethane derivative was used as a model and to settle up also the methodology reported in literature, in order to apply this reaction to obtain compounds of our interest (see scheme **N**).

Scheme N



Starting from commercially available products, two synthetic ways were applied<sup>87-88</sup>; the first one consisted in a reaction of polymer supported phenoxide ions, where the activation of naphthol to naphthalate ion is due to its passing through the alkaline (OH<sup>-</sup>) activated resin IRA 402 (Cl<sup>-</sup>)<sup>87-88</sup>; This polymer supported reagent means the nucleophilic species, which substitutes the dichloromethane, the primary carbocation species, at reflux.

This kind of reaction was abandoned because of its low yield, probably due to the hard capacity of the starting material to form the sodium salt, especially in aqueous solution, hence its consequent low affinity for the ion exchange resin.

Other experimental conditions were adopted hoping they were more available for our substrate. The reaction always consists in a nucleophilic substitution, but phenate ion is formed in MeOH by KOH and the reaction is PEG catalysed, where the PEG is the phase transfer catalyst but also solvent. This kind of reaction represents an efficient method for the synthesis under solid –liquid phase transfer catalytic conditions<sup>88</sup>. The reactions yields were improved respect to the previously described method.

By the synthesis of our compounds, it was possible to extend the known synthetic methodology to different functionalized naphthol derivatives. It was also demonstrated that it is possible to use PEG with different molecular weight. The reaction was executed using not only PEG 600, but also 400 and 1450, to understand the influence of the molecular weight in the reaction. There is no difference from the yield obtained with PEG 400 and 1450, but they are better than 600, probably because these kind of PEG are more handy than the 600 one, in the reaction.

The several derivatives obtained are reported in Scheme N with satisfactory yields (35%). We have tried to substitute the dichloromethane by dibromomethane, in order to enhance the reactivity, using a more reactive substrate, but no improvement was registered; this means the low yields are due to less reactive naphthol structure respect to the phenolic one. As explained previously for halide derivatives, the best results were obtained with Bromide at C-6, respect to C-1, we think the reason is always in the electron withdrawing linked to the position of the halide.

These products show they are sparingly soluble in common organic solvents and especially in aqueous solutions, because of their large hydrophobic portion available for BBB passing but not for test assays. It was thought to enhance their hydrophilicity

moiety introducing an amino group, at C-2 to mimic the hydroxyl groups of bis-naphthol, on the biaryl scaffold; the amino group should come from a nitro group reduction, starting from the available commercial NO<sub>2</sub>-naphthol (2- NO<sub>2</sub> -1-naphthol). Making the nitration reaction directly on diaryloxymethane derivative is impossible because of the weak ether bond that undergoes easily the acidic hydrolysis, so it was thought to submit the nitro compound to the reaction; the reaction did not lead to the supposed final product, probably a cause of the strength of the intramolecular hydrogen bond formation between the phenolic hydroxyl group and the nitro substituent, which needs a stronger activating base to form the phenate ion. Actually 1,2-hydroxynaphthalene is the starting material that undergoes different synthetic attempts to be coupled after a selective protection of the two hydroxyl groups, in order to obtain diaryloxymethane derivative hydroxy functionalized at C-1 or/and C-2.

- Benzoamide Tetraline Compounds

Remounting the structure of the Congo Red, it was supposed that the aza bond in this dye could be substituted by an amidic one, recalling a similar planarity between the biaryl structure. It has been interesting also to study what would have happened if the biaryl structure had been simplified, leaving only an aromatic ring fused with a saturated one. Exploiting Sigma-Tau starting materials tetraline<sup>89</sup> derivatives could be used to reach our item, so they became the starting material in benzoamido derivatives synthesis. ST1683 turned out to be the most versatile in amidic reaction.

Several coupling agents have been used to reach our item (See scheme **O**), like as DCC, EDCI and EEDQ, also HOBt supported, and the directly amidation by benzoyl chloride derivatives<sup>90-91</sup>. The best yield has been obtained by the use of the benzoyl chloride on ST1683 giving the final product ST 2712 with 98% of yield.

Our attempts to obtain other derivatives, functionalised at the benzoamidic substituent, using the chloride derivative has not lead to good results.

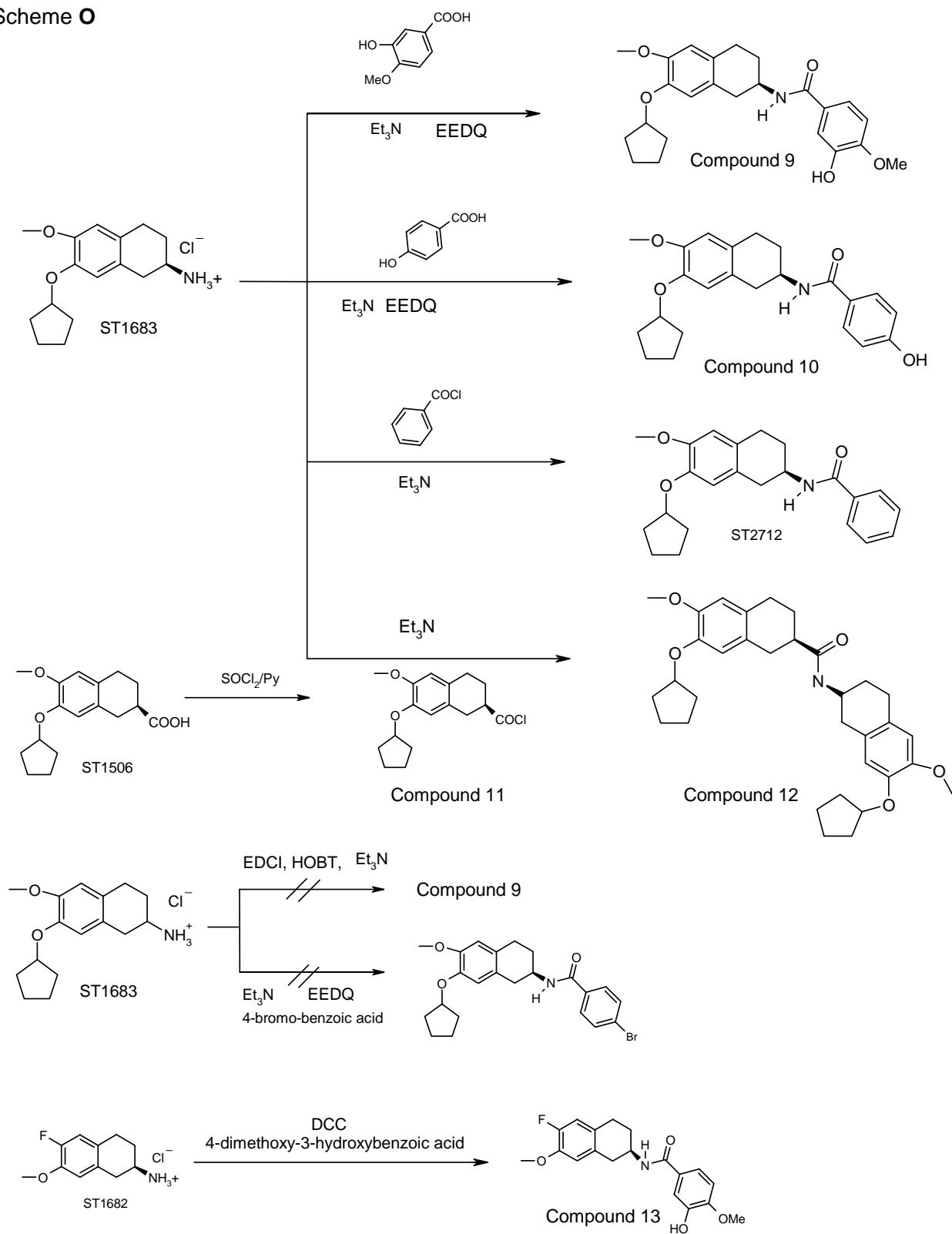
Starting from ST 1506, the acyl chloride derivative (Compound 11) was prepared, and was coupled with ST 1683, Et<sub>3</sub>N activated *in situ*; the final product (Compound 12) was obtained with low yield (5%) as highlighted by <sup>1</sup>H-NMR and IS analysis.

This compound could be useful to mimic two biphenilic rings linked by the amidic bond.

Using classical coupling agents as EEDQ led to Compound 9 (yield = 17%) and 10 (yield = 29%) against low yield obtained by DCC or non reaction for EDCI/HOBT as reacting agents (using the same ST1683 and benzoic acid). The ST1682 (another interesting starting tetraline because of a fluoride on its scaffold) submitted to coupling by DCC led to compound 13 still with low yield.

Probably all these differences depend on the lower reactivity of the benzoic acid derivatives used to form the acyl chloride or the complex with coupling agent; furthermore there is a low solubility of both starting material (tetraline and benzoic acid) in common organic solvents. The best results were obtained with activated methoxy or hydroxy benzoic acid instead of benzoic acid halide substituted (4-Br-benzoic acid), because of their electronic characteristics.

Scheme O



## II. Biology and SAR Analysis

Screening has been done to evaluate the drug capacity to inhibit the A $\beta$ 1-42 spontaneous aggregated formation during their coincubation with the peptide at 37°C for 24h. The amyloid fibril formation has been highlighted by the measurement of fluorescent emission signal, due to the specific bond between Thioflavine T and  $\beta$ -amyloid fibrils, by a spectrofluorimeter assay as explained previously in ThT test and in the experimental section. Drug activity has been expressed as the minor concentration capable of diminishing the A $\beta$  aggregation by 50% in experimental conditions (IC<sub>50</sub>). Based on good results, that this method have revealed if applied on Congo Red, the anti-amyloidogenic reference compound (IC<sub>50</sub> = 0.4mM), ThT assay has been evaluated good enough to be used as primary screening strategy of interference's capacity of our compounds in fibril formation.

It is possible to classify all the synthesized compounds in two main chemical classes: Pamoic derivatives and Bis naphthol ones<sup>35</sup>.

As highlighted by the IC<sub>50</sub> values, reported in the experimental section, the most active compounds among the pamoic acid derivatives, in ThT test, is the ST1641 (IC<sub>50</sub> = 38.1 $\mu$ M).

In this series, the lack of activity of 3-OH naphtoic acid is relevant, indicating the necessity of both parts of the pamoic acid to have a efficacious interaction. Moreover the functionalization of both carboxylic moieties, to produce a soluble prodrug (ST1800), results in a loss of activity in the in vitro test, nevertheless the esterification of hydroxylic group (ST1722) gives a molecule as active as pamoic acid. So in this series carboxylic groups, not hydroxylic ones, are important for the interaction with  $\beta$ A. Among the several bis naphthol derivatives the most active compounds have been ST1859 (IC<sub>50</sub>= 16.8 $\mu$ M), ST1913(15.4 $\mu$ M) and ST1745(IC<sub>50</sub>= 21.1 $\mu$ M). Also in this case the esterification of one hydroxylic group retains the activity of the compound, indicating that only one hydroxylic function in conjunction with the appropriate environment could be necessary. Docking results confirm this hypothesis and showed another site of interaction in respect to Pamoic acid (see Fig. in molecular modelling section) Instead the substitution of one of the naphtalene moieties with a phenyl ring



(ST2559) reverse the inhibition. Further conclusions are not possible due to lack of experimental data. In fact many bis naphthol derivatives have been tested with difficulty; the principal reason of that can be found in the main problem that we have faced and only partially resolved: their difficult solubilization in the aqueous medium used in the test. Their insolubility is clearly understood thinking of the large hydrophobic moiety, due to the biaryl planar ring, due to the scaffold functionalization by halides, and aryl or aliphatic substituent at the methylene bond, and also the methoxy derivatization of the phenolic hydroxyl groups.

So what can we deduce from these previous results? According to the biological data relative to ThT test and BBB permeability, and with the support of molecular modelling studies, it is possible to affirm that the pamoic acid itself is overcome by bis naphthol; in fact ST1859 is equipotent but more penetrating the BBB(see diagnostic target section). Further possible modifications of ST1859 will be made where the scaffold will be maintained and made more soluble not only leaving the phenolic hydroxy group free but also introducing nitrogen atoms on it. The  $IC_{50}$  values, where it has been possible to calculate, and the percentage of aggregation at relative drug concentration are reported in tables I, II, and III below.

Table I. Test ThT results - Chemical Class: Pamoic Acid

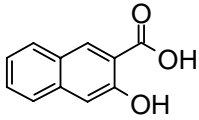
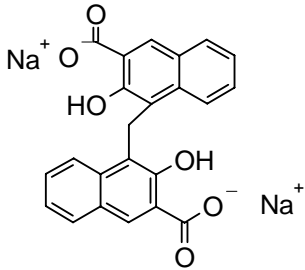
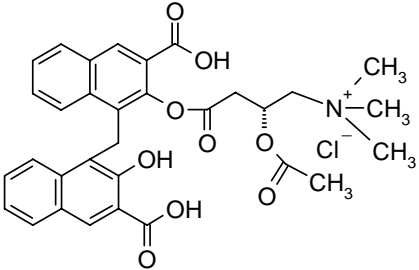
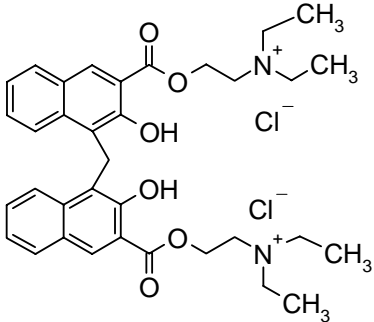
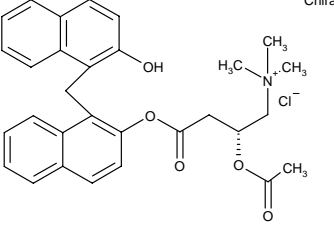
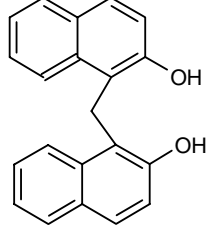
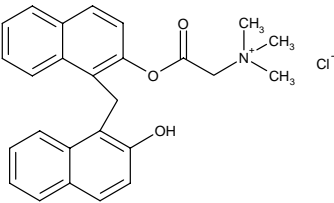
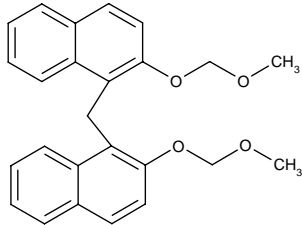
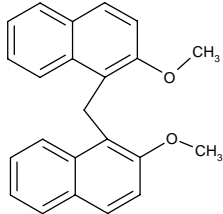
Name	STRUCTURE	IC50 (μM)	Source
3-hydroxy 2-naphtoic acid		> 500	Commercial product
ST1641		38,1	Commercial product
ST1722		90,5	
ST1800		82 (percentage of aggregation at 25.0μM)	

Table II. Test ThT results - Chemical Class :  $\beta$ -naphthols 1

NAME	STRUCTURE	IC50 ( $\mu$ M)	Source
ST1745		21,1	
ST1859		16,8	Commercial product
ST1913		15,4	
ST2164		70 (percentage of aggregation at 50.0 $\mu$ M)	
ST2165		84 (percentage of aggregation at 1.0 $\mu$ M)	

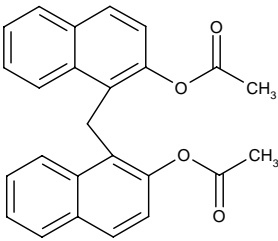
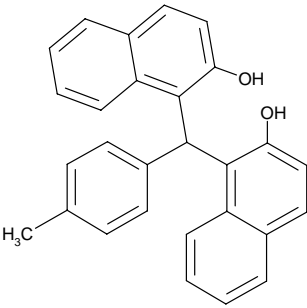
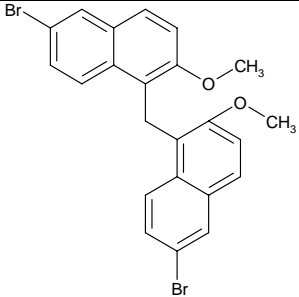
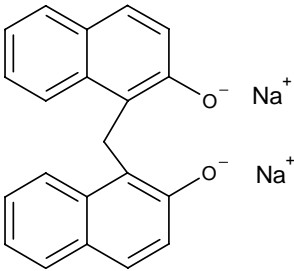
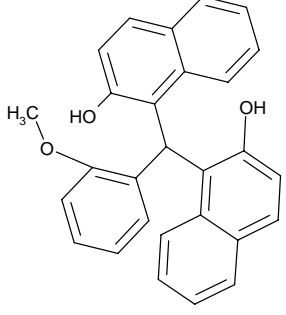
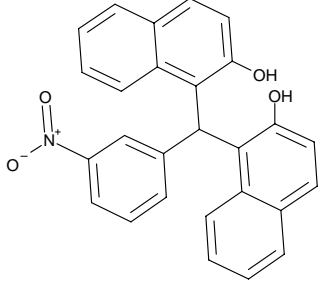
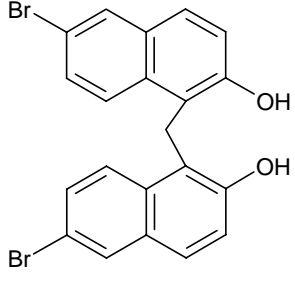
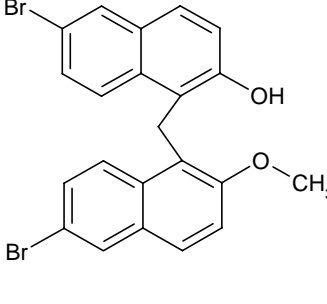
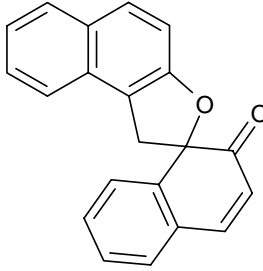
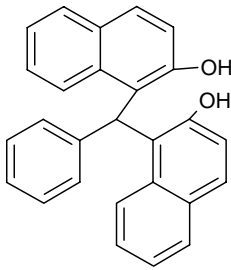
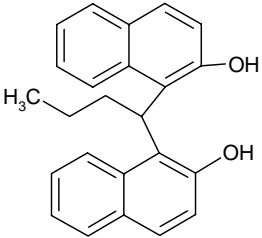
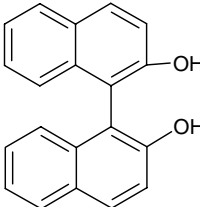
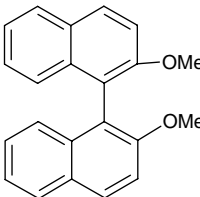
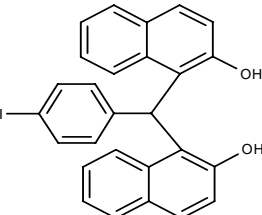
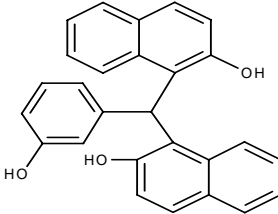
ST2166		75 (% aggregation at 1.0 μM)	
--------	---	------------------------------------	--

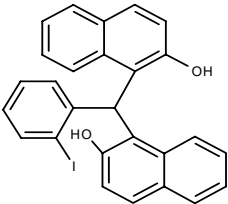
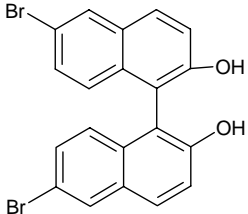
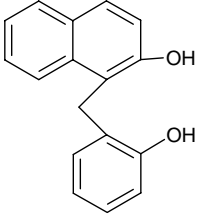
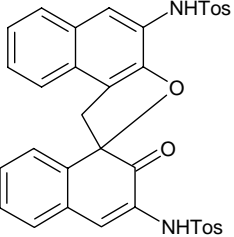
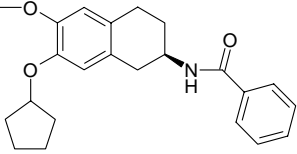
Table III: Test ThT results Chemical class: β-naphthol 2

NAME	STRUCTURE	% aggregation (assay concentration μM)	Source
ST2283		95 (50.0 μM)	Commercial product
ST2281		100 (100.0 μM)	Commercial product
ST2207		60 (20.0 μM)	

ST2282		105 (50.0 $\mu$ M)	Commercial product
--------	---	-----------------------	--------------------

ST2284		56 (40.0 $\mu$ M)	Commercial product
ST2305		75 (20.0 $\mu$ M)	
ST2342		60 (40.0 $\mu$ M)	
ST2383		75 (6.3 $\mu$ M)	

ST2386		84 (50.0 $\mu$ M)	Commercial product
ST2381		77 (6.3 $\mu$ M)	
ST2384		82 (50.0 $\mu$ M)	
ST2417		101 (0.4 $\mu$ M)	
ST2506		70 (100.0 $\mu$ M)	
ST2507		105 (1.0 $\mu$ M)	

ST2508		74 (100.0 $\mu$ M)	
ST2385		89 (70.0 $\mu$ M)	
ST2559		73 (100.0 $\mu$ M)	
ST2668		56 (50.0 $\mu$ M)	
ST2712		90 (50.0 $\mu$ M)	

### III. The Solubility Issue<sup>92-93</sup>

Many of the compounds that have been synthesized, have a low solubility in aqueous solution. This problem arises because of the generic structure of the drugs related to test typology, which has just been described previously. The test is executed in a buffer solution at pH = 7.4. The generic drug scaffold, adopted in our compounds, has a hydrophobic portion prevalent on the hydrophilic one, because of its biaryl or phenilic structure. This problem has been faced up following two different approaches: synthetic and pharmaceutical.

#### **Synthetic Approach**

We have focused on the insertion attempts of the amino group on the biaryl scaffold, in order to enhance the solubility exploiting the salt form, as it is described in the chemical results and discussion section.

#### **Pharmaceutical Approach**

Generally, water solubility of very few soluble compounds can be increased through these following methods: modifying the pH solution, if the compound is a weak base or acid; adding a cosolvent or a tensioactive or a complexant (in e.g. cyclodextrine, PVP) but also their suitable mixture.

Cosolvents: the most common cosolvents used pharmaceutically and practically for our interest are: dimethylsulphoxide (DMSO), benzilic alcohol, propylene glycol, transcutool P, PEG 200-400, ethanol.

Tensioactive: the tensioactive used to reach our aim are: pluronic F-127 (ethanolic solution 9%), gelucire 53/10, gelucire 44/14, solutol HS15, and polioxyethyl-ene-40-stearate. Some characteristic of less known solvents are reported above.

Pluronic F127 is a triblock copolymer consisting of propylene oxide and ethylene oxide. The propylene oxide (PO) is sandwiched between the ethylene oxide blocks. It is a non ionic surfactant, more versatile than the others. The pluronic surfactant is unique in that the hydrophobic and the hydrophilic portions of the molecule can be incrementally varied and manipulated to any molecular weight and hydrophilic/ lipophilic balance (HLB). As the numerical and alphabetical designation explains, it has a prevalent hydrophobic portion, which makes it available in order to dissolve our compounds.



TPGS (d- alpha-tocopheryl polyethylene Glycol-1000 succinate) is a water soluble form of natural source vitamin E. It is prepared by esterifying the acid group of crystalline d- a- tocopheryl acid succinate with polyethylene glycol 1000.

Because of its chemical functionality and water soluble characteristic, TPGS can emulsify lipophilic (fat soluble) drugs (HLB = 13).

Gelucire 44/14 is a well defined mixture of mono-, di- and tryglycerides and mono- and di- fatty acid esters of polyethyleneglycol, the lauric acid. It is synthesized by an alcoholysis (esterification reaction using hydrogenated palm korneil oil and PEG-1500 as starting material. Gelucire 50/13 is a stearyl macrogol- 32- glycerides. It has the same characteristic as the gelucire 44/14.

Solutol HS-15 is a polyethylene glycol mono- and di- esters of 12-hydroxystearic acid (its lipophilic part) and of about 30% of free polyethylene glycol ( its hydrophilic part). Based on this knowledge, the ST1859 has been used as drug model to choose and set up the best solvents system to reach our item. The ST1859 has been firstly dissolved in one or more solvents described previously; the resultant solution has been diluted with a phosphate buffer solution 50mM at pH=7.4, up to the suitable concentration used in ThT test, under stirring for 24h at room temperature. Suitable solvent systems have been considered all those that do not show any solid in suspension, and also do not interfere in biological test (ThT Test). To sum up, the only solvent that respects all rules described and adopted above, is that one consisting of triethanolamine (TEA) : ethanol 2:1p.p. diluted with phosphate buffer solution 50mM until final concentration 1,10,100 $\mu$ M. It means it has been necessary coming in and modifying pH solution characteristics, using a base and a cosolvent.

### **3. Conclusions**

In Alzheimer's disease, many efforts have been made to discover treatment for this devastating human disorder of complex etiology and pathogenesis. Following the A $\beta$  hypothesis of AD, which is focused on the pathogenic, neurotoxic role of A $\beta$  and the fibrillogenesis, aggregation process, our aim and our work has been focused on synthesizing and studying molecules, with potential antiamyloidogenic activity

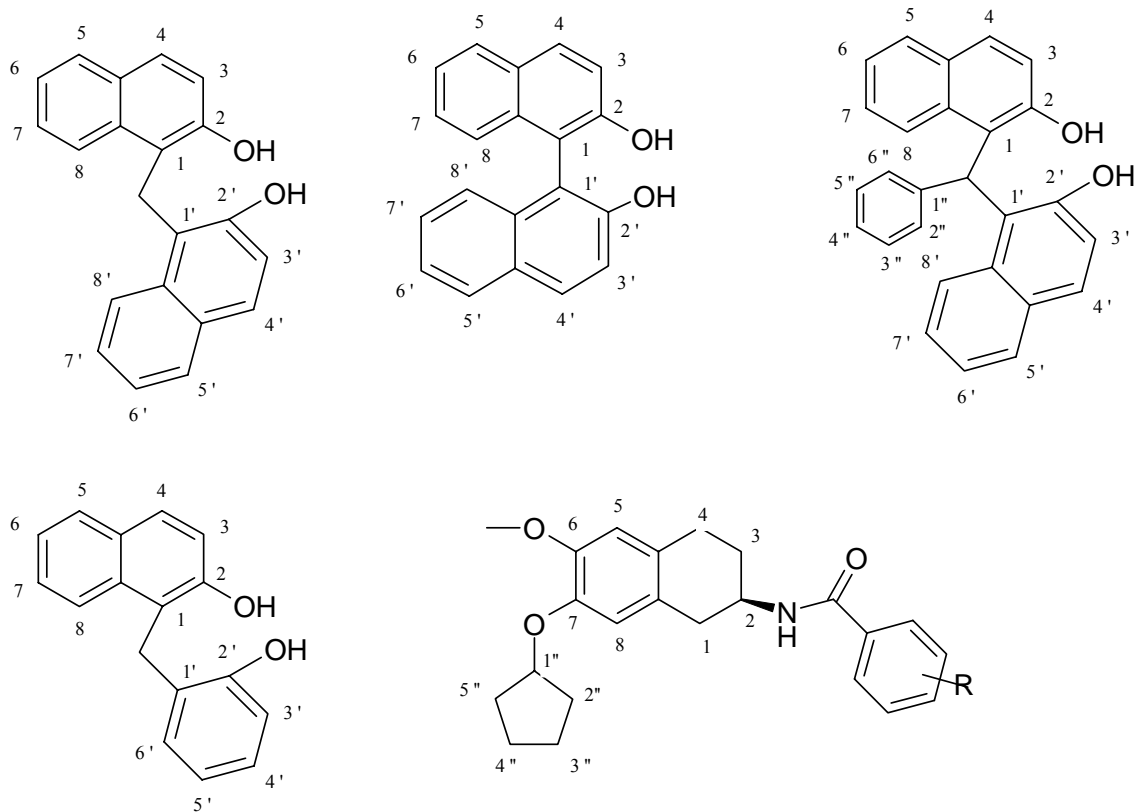
interfering in A $\beta$  fibrillogenesis and aggregation processes. Our efforts have been satisfied in finding in ST1859, according to the biological data relative to the ThT test and BBB permeability, with the support of molecular modelling studies, and some of its derivatives, probably prodrug (ST1913, ST1745), molecules with good antiaggregant activity (see biological and SAR results).

ST1859 is equipotent but more penetrating the BBB. Further possible modification of ST1859 are foreseen and will be made, maintaining its scaffold and making it more soluble, not only leaving the phenolic hydroxy group free, but also introducing nitrogen atoms into it. Our diagnostic target has been satisfied completely, succeeding in using ST1859 in PET studies (See diagnostic target section).

These compounds may provide the basis for the development of new aggregation inhibitors as a therapeutic strategy for developing or treating AD.

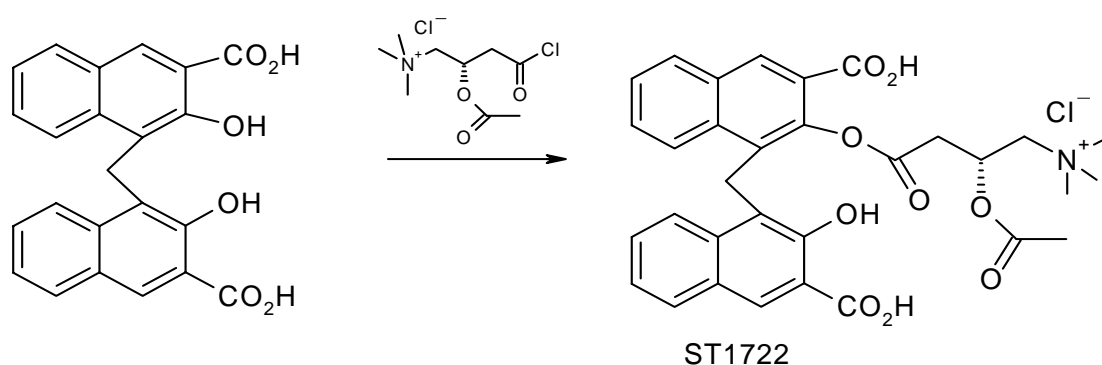
## 4. Experimental Section

### I. Chemistry



General:  $^1\text{H-NMR}$  and  $^{13}\text{C NMR}$  spectra were recorded on Varian Gemini 200 MHz and Varian XL 300 spectrometers, using TMS as internal standard; IS spectra were recorded on Mass Platform LC Micromas; chemical shifts are expressed in ppm downfield from TMS. – Products were purified by solid-liquid column and TLC chromatography on Merck 0.0623-0.20 mm silica gel; eluent mixtures were chosen case by case. – Elemental analyses gave satisfactory results for all the described compounds. – TLC on plates precoated with Kiesel-Gel 60 F<sub>254</sub> (Merck) was used to monitor the progress of the reactions; spots were developed by I<sub>2</sub>.

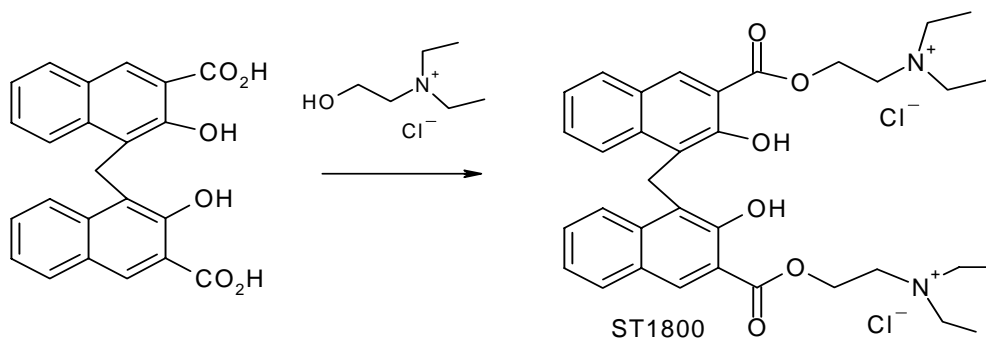
**Synthesis of (2R)-2-(acetyloxy)-4-({3-carboxy-1-[(3-carboxy-2-hydroxy-1-naphthyl)methyl]-2-naphthyl}oxy)-N,N,N-trimethyl-4-oxo-1-butanaminium chloride (ST1722)**



To L-acetyl carnitine (0.03mol, 7g) was added  $\text{SOCl}_2$  (0.045mol) in anhydrous  $\text{CH}_2\text{Cl}_2$  (6ml) and the mixture underwent stirring for 4h at room temperature. The mixture was washed with anhydrous  $\text{CH}_2\text{Cl}_2$  three times and the solvent was evaporated under reduced pressure, obtaining a yellow oil. This product was added to a suspension of pamoic acid (0.03mol, 11.6g) in  $\text{CH}_2\text{Cl}_2$  (30ml). The mixture underwent stirring overnight at room temperature. The crude product was treated with diethyl ether and filtered on gooch. The resultant solid was treated again with ether and dried under vacuum. The crude product was purified by chromatography, using as eluent  $\text{CHCl}_3/\text{MeOH}$  (90:10). The product was obtained as white powder (2.5g).

$^1\text{H-NMR}$  (300 MHz,  $\text{CDCl}_3$ )  $\delta$  2.02(3H, s), 2.90-3.10(2H, m), 3.29(9H, s), 3.54-3.69(2H, m), 4.86(2H, s,  $\text{CH}_2$ ), 5.50(1H, m), 7.50(1H, m), 7.70-7.90(3H, m), 8.10-8.20(6H, m), 9.00(4H, m);  $^{13}\text{C NMR}$  (300 MHz,  $\text{CDCl}_3$ )  $\delta$  20.8(1C), 30.2(1C), 37.1(1C), 56.2(3C), 60.1(1C), 98.3(1C), 113.7(1C), 123.1(1C), 124.3(1C), 125.4(1C), 126.4(1C), 126.5(1C), 127.5(1C), 127.8(1C), 129.8(1C), 129.9(1C), 130.1(1C), 130.5(1C), 130.6(1C), 132.3(1C), 132.5(1C), 133.1(1C), 138.6(1C), 140.5(1C), 141.6(1C), 145.4(1C), 156.8(1C), 162.8(1C), 169.5(1C), 170.2(1C); Anal. Calcd. For  $\text{C}_{32}\text{H}_{32}\text{NO}_9 \cdot \text{Cl}$ : C 63.00%, H 5.29%, N 2.30%, O 23.60%. Found: C 60.29%, H 7.20%, N 2.48%, O 20.60%.

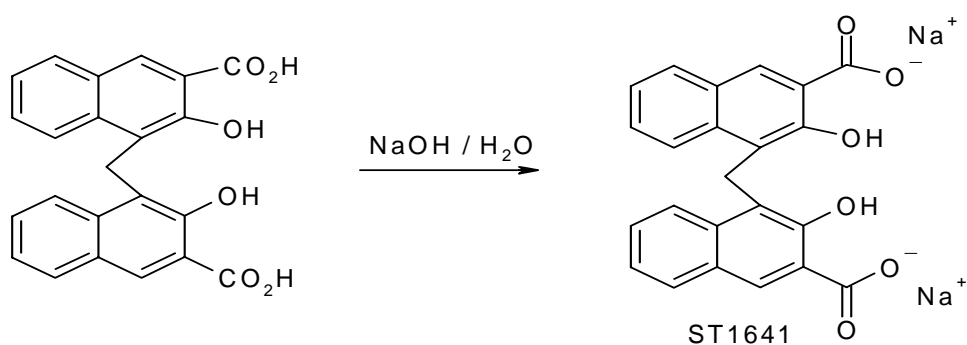
**Synthesis of 2-({4-[(3-{[2-(diethylammonio)ethoxy]carbonyl}-2-hydroxy-1-naphthyl)methyl]-3-hydroxy-2-naphthoyl} oxy)-N,N-diethylethanaminium dichloride (ST1800)**



To Pamoic acid (0.01mol, 3.88g) was added  $\text{SOCl}_2$ (0.045mol, 3.5ml) and the mixture underwent stirring overnight at reflux. The obtained sulphite (0.0021mol, 1g) was suspended in anhydrous  $\text{CH}_2\text{Cl}_2$  (10ml) and added of diethylamine ethanol (0.0053mol, 0.7ml). The mixture underwent stirring overnight at room temperature. At the end of the reaction, the mixture was filtered and the organic layer was evaporated under reduced pressure, obtaining a yellow solid (0.5g).

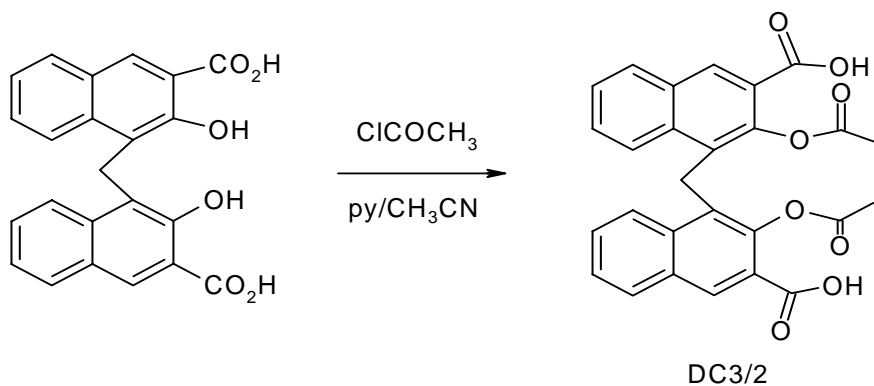
$^1\text{H}$ - NMR ( 300 MHz,  $\text{CDCl}_3$ )  $\delta$  1.50( 4H, m), 3.00-3.41 (8H, m), 4.10 (2H, m), 4.50 (3H, m), 4.84(2H, s,  $\text{CH}_2$ ), 7.50 (9H, m), 7.60-7.80 (9H, m), 8.50 (3H, m), 10.20 (4H, brs);  $^{13}\text{C}$  NMR ( 300 MHz,  $\text{CDCl}_3$ )  $\delta$  15.3(2C), 15.4(2C), 29.8(1C), 47.5(2C), 47.6(2C), 49.4(1C), 58.9(1C), 77.2(1C), 110.7(1C), 115.1(1C), 119.0(1C), 121.4(1C), 124.9(2C), 125.9(1C), 126.3(2C), 126.8(2C), 130.7(2C), 131.3(1C), 131.7(1C), 132.5(1C), 134.3(1C), 142.2(1C), 142.2(1C), 157.7(1C), 158.2(1C), 161.7(1C), 166.3(1C); Anal. Calcd. for  $\text{C}_{35}\text{H}_{44}\text{N}_2\text{O}_6\cdot 2\text{Cl}$ : C 63.73%, H 6.72%, N 4.25%, O 14.55%. Found: C 60.20%, H 7.80%, N 3.73%, O 15.00%.

**Synthesis of disodium 4-[(3-carboxylato-2-hydroxy-1-naphthyl)methyl]-3-hydroxy-2-naphthoate (ST1641)**



To a suspension of Pamoic acid (0.026mol, 10g) in H<sub>2</sub>O (10ml) was added NaOH (0.051mol, 2.04g). The resultant brown mixture was evaporated under vacuum and the brown solid obtained was treated by isopropilic alchool, and filtered on gooch. Analytical data according to commercial ones.

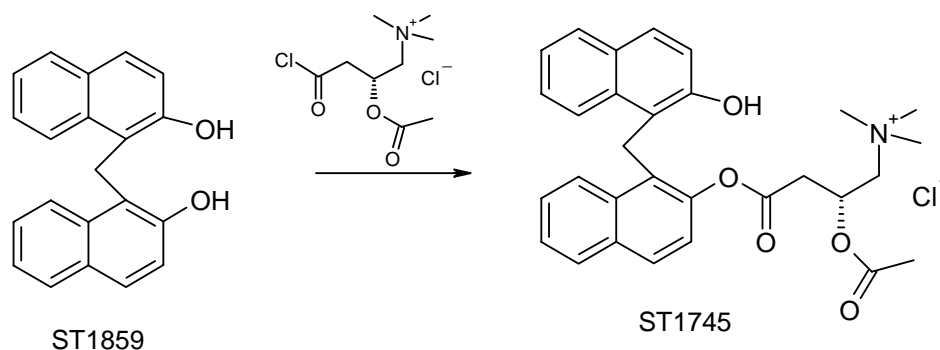
### Synthesis of 4,4'-methylenebis[3-(acetyloxy)-2-naphthoic acid] (DC3/2)



To a suspension of Pamoic acid (0.26mmol, 100mg) in anhydrous  $\text{CH}_3\text{CN}$  (1ml) was added pyridine (0.57mmol, 50 $\mu\text{L}$ ), and  $\text{ClCOCH}_3$  (0.57mmol, 43  $\mu\text{L}$ ) dropwise at  $0^\circ\text{C}$ . The resultant solution was left under stirring for 1h at room temperature. The solution was diluted with AcOEt and washed with  $\text{H}_2\text{O}$ , the organic layer was dried over anhydrous  $\text{Na}_2\text{SO}_4$ , and evaporated under vacuum. The crude product was purified by chromatography using as eluent  $\text{CH}_2\text{Cl}_2/\text{MeOH}/\text{CH}_3\text{CO}_2\text{H}$  (90:10:10). The final product was obtained as yellow solid (yield=15.6%).

$^1\text{H}$ - NMR ( 200 MHz,  $\text{CD}_3\text{OD}$ )  $\delta$  1.90( 6Hs), 5.40(2H, s,  $\text{CH}_2$ ), 7.40 (4H, m), 7.98 (2H, d), 8.20(2H, d), 8.40 (2H, m), 7.60-7.80 (9H, m), 8.50 (3H, m), 10.20 (4H, brs).

**Synthesis of (2R)-2-(acetyloxy)-4-( { 1-[(2-hydroxy-1-naphthyl)methyl]-2-naphthyl}oxy)-N,N,N-trimethyl-4-oxo-1-butanaminium chloride (ST1745)**

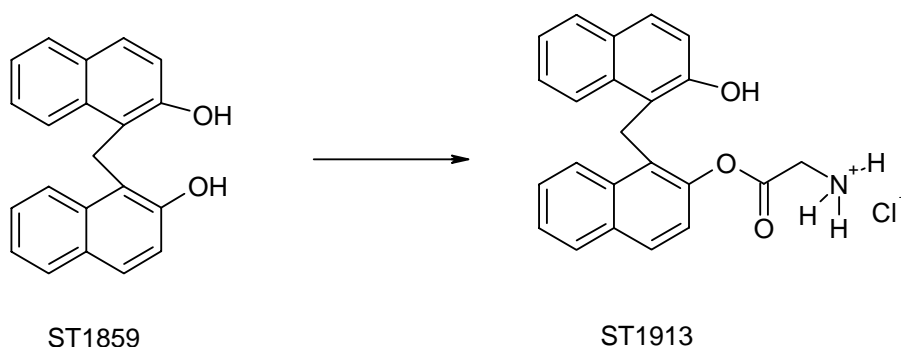


To L-acetyl carnitine (0.01mol, 2.39g) was added  $\text{SOCl}_2$ (0.015mol, 1.1ml) in anhydrous  $\text{CH}_2\text{Cl}_2$  (2ml) and the mixture underwent stirring for 4h at room temperature. The yellow mixture was washed with anhydrous  $\text{CH}_2\text{Cl}_2$  three times and the solvent was evaporated under reduced pressure, obtaining a yellow oil. This product was added to a suspension of ST1859 (0.01mol, 3g) in anhydrous  $\text{CH}_3\text{CN}$  (5ml). The mixture underwent stirring overnight at room temperature. The crude product was treated with diethyl ether and filtered on gooch. The organic layer was evaporated under vacuum and the crude product was purified by chromatography, using as eluent  $\text{CHCl}_3/\text{MeOH}$  (90:10). The product was obtained as pink solid.

$^1\text{H}$ - NMR ( 300 MHz, d-DMSO)  $\delta$  2.0( 2H, d), 3.10 (9H, s,  $\text{CH}_3\text{-N}$ ), 3.40 (3H, s,  $\text{CH}_3\text{-O}$ ), 3.60-4.00 (2H, m, N-  $\text{CH}_2\text{-CO}$ ), 4.60 (2H, s,  $\text{CH}_2$ ), 5.60 (1H, m), 7.00-7.40 (6H, m), 7.60-7.90 (5H, m), 8.40 (1H, m);  $^{13}\text{C}$  NMR ( 300 MHz, d-DMSO)  $\delta$  20.7(1C), 28.8(1C), 36.3(1C), 56.1(3C), 61.4(1C), 66.5(1C), 120.6(1C), 121.8(1C) 122.4(1C), 123.6(1C), 123.8(1C), 126.0(1C), 128.0(1C), 128.5(2C), 128.6(1C), 128.7(1C), 129.7(1C), 130.1(2C), 131.1(1C), 131.2(1C), 131.4(1C), 138.7(1C), 145.3(1C), 150.8(1C), 170.6(1C), 172.0(1C); Anal. Calcd. for  $\text{C}_{30}\text{H}_{32}\text{NO}_5\text{Cl}$ : C 69.02%, H 6.18%, N 2.68%, O 15.32%. Found: C 67.25%, H 7.40%, N 2.40%, O 13.20%.



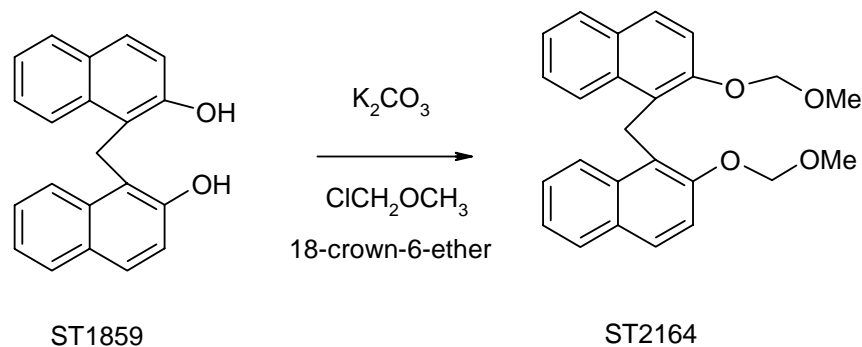
**Synthesis of 2-( {1-[(2-hydroxy-1-naphthyl)methyl]-2-naphthyl}oxy)-2-oxoethanaminium chloride (ST1913)**



To Bocglycine (0.016mol, 2.8g) in toluene (30ml) was added KOH (0.016mol, 0.9g) in H<sub>2</sub>O(3ml). The mixture underwent stirring at 180°C and the water was kept away. The mixture was added of N- methyl morpholine (1.5ml) and isobutyl chloroformate (2.36ml) in isobuthanol (1.2ml) at 0°C and left under stirring for 2h. To this mixture was added ST2207 (ST1859 was suspended in H<sub>2</sub>O(15ml) and added of KOH (0.02mol, 1.2g) in 10minutes. The mixture underwent stirring overnight at room temperature. The final solution washed with H<sub>2</sub>O and added with HCl 3N up to pH = 3, the organic layer was washed again with H<sub>2</sub>O and dried over anhydrous Na<sub>2</sub>SO<sub>4</sub>. The crude product was purified by chromatography using as eluent hexane/AcOEt (80:20). The final product (0.2g) was treated with TFA (2ml) under stirring for 2h at room temperature. The solution was treated with diethyl ether and the solid product was purified by chromatography using as eluent hexane/AcOEt (80:20). The resultant product was treated with A21(50ml) activated with HCl 5%, washed with H<sub>2</sub>O and MeOH, to obtain ST1913(1g).

<sup>1</sup>H- NMR ( 300 MHz, d-DMSO) δ 3.80 (2H, d, CH<sub>2</sub>-N), 4.75 (2H, s, CH<sub>2</sub>), 6.73(4H,m), 7.20-8.20 (12H, m); <sup>13</sup>C NMR(300 MHz, d-DMSO) δ 28.8(1C), 41.7(1C), 120.3(1C), 122.4(1C), 122.6(1C) 122.7(1C), 123.0(1C), 125.8(1C), 126.0(1C), 126.2(1C), 128.0(1C), 128.1(1C), 128.6(1C), 129.0(1C), 131.1(1C), 131.4(1C), 132.1(1C), 135.0(1C), 138.7(1C), 145.0(1C), 151.7(1C), 153.6(1C), 163.4(1C); Anal. Calcd. for C<sub>23</sub>H<sub>20</sub>NO<sub>3</sub>·Cl: C 70.15%, H 5.12%, N 3.56%, O 12.19%. Found: C 64.10%, H 6.40%, N2.58%,O10.0%.

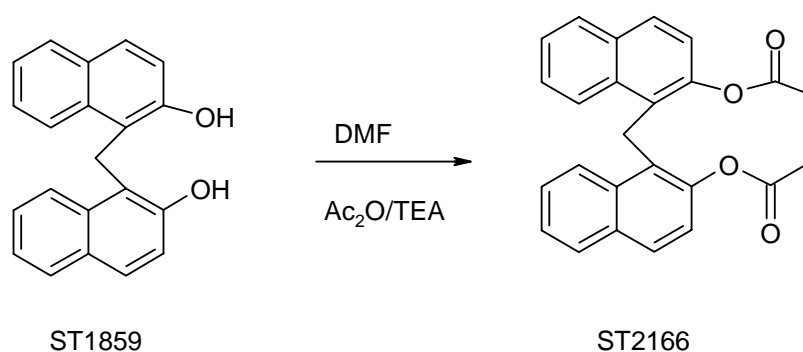
**Synthesis of 2-(methoxymethoxy)-1-[[2-(methoxymethoxy)-1-naphthyl]methyl]naphthalene (ST2164)**



To a suspension of ST1859 (0.005mol, 1.5g) in anhydrous CH<sub>3</sub>CN (30ml) was added K<sub>2</sub>CO<sub>3</sub> (0.025mol, 3.45g). The resultant mixture underwent stirring for 15minutes and it was added with ClCH<sub>2</sub>OCH<sub>3</sub> (0.025mol, 1.43ml) and 18-crown-6-ether(0.001mol, 0.264g). The mixture underwent stirring and diluted with H<sub>2</sub>O. The mixture was extracted with CH<sub>2</sub>Cl<sub>2</sub>. The organic layer was washed with H<sub>2</sub>O and dried over anhydrous Na<sub>2</sub>SO<sub>4</sub>. The product was obtained as white solid (1.9g).

<sup>1</sup>H- NMR ( 300 MHz, CDCl<sub>3</sub>) δ 3.25 (6H, brs), 4.10 (4H, q), 4.73(2H,bq), 5.52(1H, bd), 7.09(2H,d), 7.11(2H,t), 7.43-7.81(3H,m), 8.27(2H,t), 8.38(2H,d); <sup>13</sup>C NMR ( 300 MHz, CDCl<sub>3</sub>) δ 29.4(1C), 56.2(2C), 95.3(2C), 115.8(2C), 122.5(2C) 123.3(2C), 128.0(2C), 128.7(2C), 129.3(2C), 129.9(2C), 134.9(2C), 144.2(2C), 155.7(2C); Anal. Calcd. for C<sub>25</sub>H<sub>24</sub>O<sub>4</sub>: C 77.30%, H 6.23%, O 16.47%. Found: C 68.23%, H 5.20%, O 15.58%.

### Synthesis of 1-[[2-(acetyloxy)-1-naphthyl]methyl]-2-naphthyl acetate (ST2166)

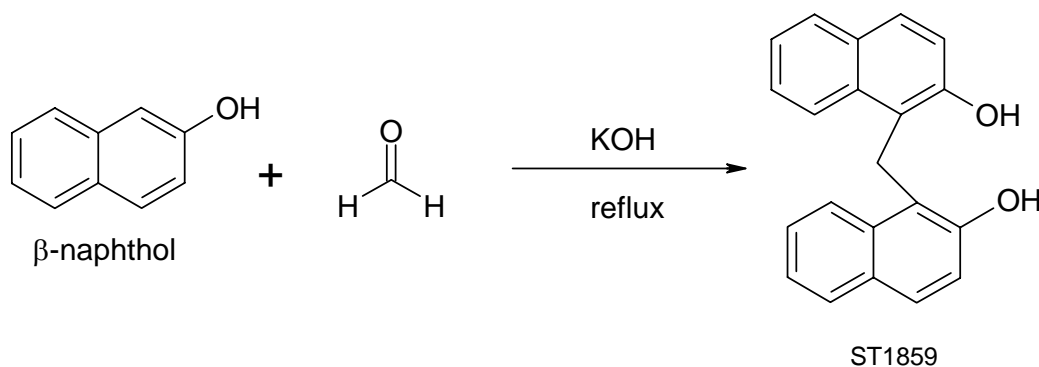


To a solution of ST1859 (0.006mol, 2g) in DMF (5ml) was added TEA (0.053mol, 7.4ml) and Ac<sub>2</sub>O (0.033mol, 3.1ml) dropwise at room temperature. The resultant mixture underwent stirring for 2h. The white solid was added filtered and dissolved in CH<sub>2</sub>Cl<sub>2</sub>. The organic layer was washed with HCl 2N. The organic layer was dried over anhydrous Na<sub>2</sub>SO<sub>4</sub> and the solvent evaporated under vacuum. The product was obtained as white solid (2g).

<sup>1</sup>H- NMR ( 300 MHz, CDCl<sub>3</sub>) δ 2.43 (6H, m), 4.80 (2H, s,CH<sub>2</sub>), 7.10(2H,d), 7.50(2H, m), 7.75(4H,d), 7.83(2H,m), 8.21(2H,m); ms : ei (m/z) 471(100%, M-1), 490 (M<sup>+</sup>+NH<sub>4</sub><sup>+</sup>).

## Diarylation of $\beta$ -naphthol

Scheme B



To a solution of  $\beta$ -naphthol (101 mg, 0.70 mmol), KOH (121 mg, 2.156 mmol) in H<sub>2</sub>O (2 ml, A or 0.55mL, B) were added HCOH 37% (26  $\mu$ l, 0.35 mmol) at room temperature. After stirring at reflux for 25 min. , the dark solution was cooled at room temperature and aqueous hydrochloric acid 2N was added dropwise until pH = 1. A pink precipitate was obtained. It was added of a mixture ethyl acetate / water to be transfer into a separatory funnel. The water was extracted with ethyl acetate (50 ml x 3). The combined organic extracts were washed with brine (10ml x 1), dried over sodium sulphate anhydrous, filtered, and the solvent removed in vacuo at 40°C. Purification was achieved by TLC chromatography (TLC 20x20cm, Merck) dissolving the crude product in ethyl acetate, as elution mixture was used hexane / ethyl acetate 70:30, to yield pure bis-naphthol (58 mg, 0.19 mmol) as a pallid yellow solid (yield = 55%). The reaction was checked by TLC using hexane/ethyl acetate (7:3) as eluent (R<sub>f</sub> = 0.36).

<sup>1</sup>H-NMR (200MHz, d-DMSO):  $\delta$  4.80 (s, 2H, CH<sub>2</sub>), 7.20 (m, 6H), 7.60 (m, 4H), 8.20 (d, 2H), 10.18 (2H, brs, OH); ms : ei (m/z) 299(100%, M-1), 301(100%, M+1).

<sup>13</sup>C- NMR and AE according to commercial data.

#### Scheme B'

To a solution of  $\beta$ -naphthol (100 mg, 0.694mmol), KOH (121 mg, 2.156 mmol) in H<sub>2</sub>O (0.55 ml) were added HCOH 37% (52  $\mu$ l, 0.694 mmol) at room temperature. After stirring at reflux for 25 min. , the dark solution was cooled at room temperature and aqueous hydrochloric acid 2N (1.1ml) was added dropwise up to pH = 1, to the solution. A pink precipitate was obtained, collected, washed with water and dried at 40°C, to provide pure ST1859 (120 mg, 0.4 mmol) as a pallid pink solid (yield 58%).

#### Scheme B''

To a solution of  $\beta$ -naphthol (100 mg, 0.694 mmol), KOH (121 mg, 2.156 mmol) in H<sub>2</sub>O (0.55 ml) were added (CH<sub>2</sub>O)<sub>n</sub> (20.8 mg, 0.694 mmol) at RT. After stirring at reflux for 25 min., the solution was cooled at RT.

2N aqueous hydrochloric acid (1.1ml) was added dropwise up to pH = 1.

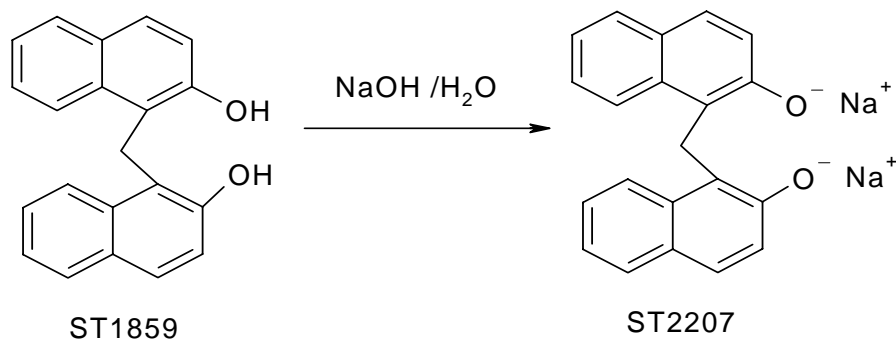
A pink precipitate was obtained, collected, washed with water. It was dissolved in ethyl acetate and checked by TLC hexane/ethyl acetate 7:3.

The bis-naphthol was obtained pure according to TLC evidence.

#### Scheme B'''

To a solution of  $\beta$ -naphthol (110 mg, 0.763mmol), in EtOH (1ml) were added HCHO 37% (57 $\mu$ l, 0.763 mmol) and 2N hydrochloric acid (0.5ml) at RT. After stirring at 63°C for 1h, the reaction was checked by TLC (hexane / ethyl acetate 7:3), which showed 50% of bis-naphthol and 50% of  $\beta$ -naphthol.

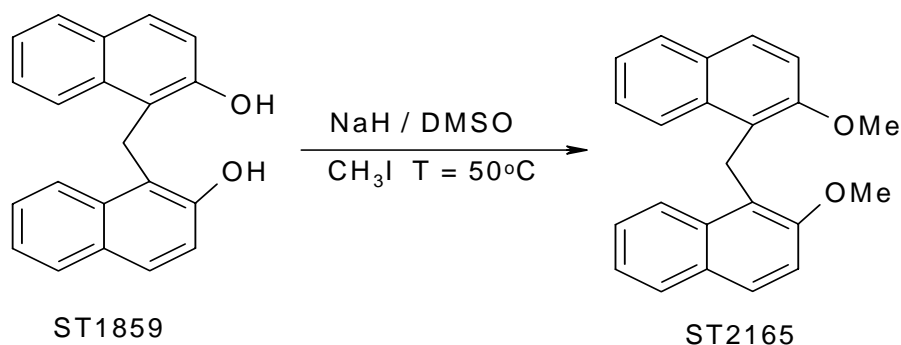
### Synthesis of disodium 1-[(2-oxido-1-naphthyl)methyl]-2-naphthalenolate (ST2207)



ST1859 (500mg, 1.67mmol) was suspended in water and NaOH (133.33mg, 2.34 mmol) was added to the suspension at 0°C under stirring. The resulting solution was filtered on a gooch funnel and the filtrate was evaporated in vacuo. The precipitate was recrystallized from 2-isopropanol. The product ST2207 was obtained as brown precipitate.

<sup>1</sup>H- NMR ( 200 MHz, d-DMSO) δ 4.60 ( 2H, s, -CH<sub>2</sub>), 7.10 ( 2H, t, H-6 and H- 6'), 7.2 (2H, t , H-7 and H-7'), 7.60 ( 4H, m, H-5, H-5', H-8, H-8'), 8.10 (4H, d, H-3 H-3', H-4, H-4').

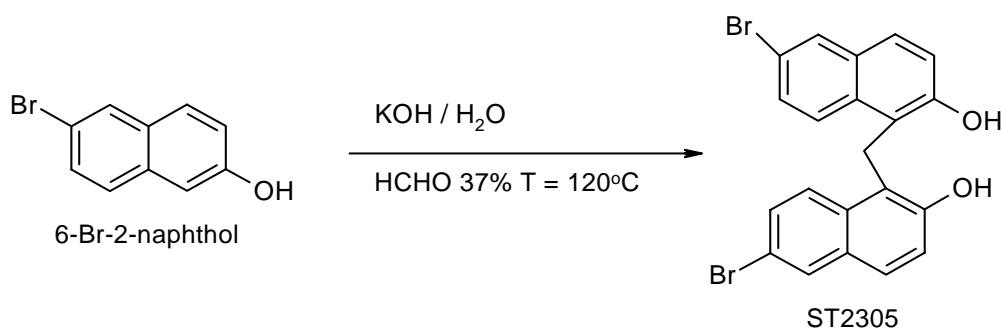
### Synthesis of 2-methoxy-1-[(2-methoxy-1-naphthyl)methyl]naphthalene (ST2165)



To a solution of ST 1859 (10g, 33mmol) in DMSO (50mL) were added NaH (2.4g, 99mmol) and CH<sub>3</sub>I (10.27mL, 165mmol) at room temperature. The mixture was stirred at 50°C, for 3h. The reaction was monitored by TLC using hexane / ethyl acetate (9:1) as eluent. The reaction was quenched adding water to the solution slowly. The aqueous phase was extracted with ethyl acetate and the organic layer was washed again with water and brine, the organic phase was dried with anhydrous Na<sub>2</sub>SO<sub>4</sub> and the solvent was evaporated in vacuo. The mixture was separated by chromatography using, hexane, hexane /ethyl acetate (95:5), hexane /ethyl acetate (9:1), hexane /ethyl acetate (8:2). The compound ST2165 was obtained as white powder (yield=70%).

<sup>1</sup>H- NMR ( 300 MHz, d-DMSO) δ 3.98 ( 6H, s, -OCH<sub>3</sub>), 4.70 ( 2H, s, -CH<sub>2</sub>-), 7.10-7.30 (4H, m), 7.49 ( 2H, d), 7.70-7.85 (4H, m), 8.10 (2H, d); <sup>13</sup>C NMR ( 300 MHz, d-DMSO) δ 34.3 (1C, -CH<sub>2</sub>-), 60.3 (2C, 2x -OCH<sub>3</sub>), 118.2 (2C, C-3 and C-3'), 122.4 (2C), 127.0 (2C), 128.0 (2C), 128.8 (2C), 130.0 (2C), 133.8 (2C), 144.6 (2C), 158.0 (2C, C-2 and C-2'); Anal. Calcd. for C<sub>23</sub>H<sub>20</sub>O<sub>2</sub> : C 84.12%, H 6.14%, O 9.74%. Found: C 70.15%, H 7.12%, O 6.94%.

**Synthesis of 6-bromo-1-[(6-bromo-2-hydroxy-1-naphthyl)methyl]-2-naphthol  
(ST2305)**



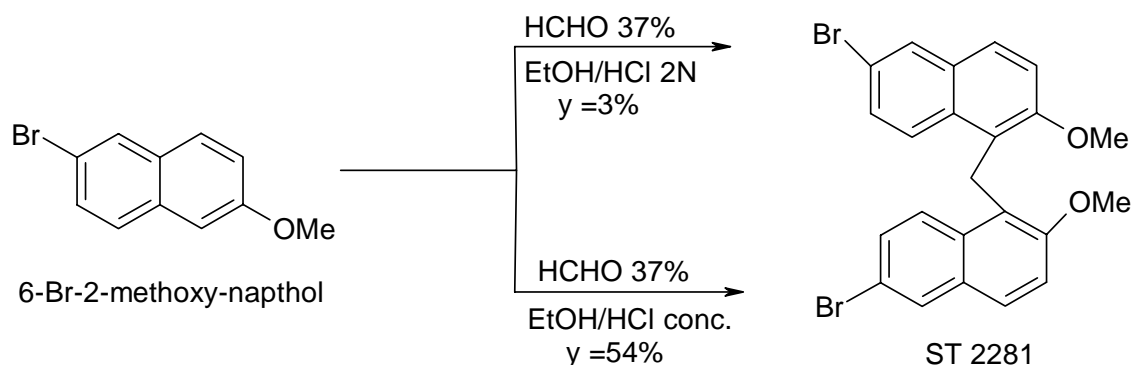
6-Br-2-naphthol (Aldrich, 610mg, 2.73mmol) was suspended in water (2ml) and KOH (546mg, 8.06mmol) was added. The mixture was stirred until complete dissolution of the starting material, at room temperature. HCHO 37% (200  $\mu$ L, 2.73mmol) was added to the solution. This mixture was left at 125°C for 3 h. Work-up consisted in neutralizing with HCl 2N until pH = 1, the aqueous layer was extracted with ethyl acetate; the organic phase was washed with water and brine up to pH = 7. The organic layer was dried with anhydrous Na<sub>2</sub>SO<sub>4</sub> and the solvent was evaporated in vacuo. The compound ST2305 was obtained directly as with powder (yield = 56% to the starting material).

The reaction was monitored by TLC using hexane / ethyl acetate (8:2) as eluent.

<sup>1</sup>H- NMR ( 200 MHz, d-DMSO)  $\delta$  4.62 ( 2H, d, -CH<sub>2</sub>-), 7.22 ( 4H, t, H-4,4' and H-8,8'), 7.60 (2H, d, H-3,3'), 7.90 ( 2H, d, H-7,7'), 8.08 (2H, d, H-5,5'), 10.40 (2H, brs);  
<sup>13</sup>C NMR ( 300 MHz , d-DMSO)  $\delta$  28.3 (1C, CH<sub>2</sub>), 118.7 (2C, C-Br), 122.5 (2C), 123.5 (2C, C-3,3'), 124.6 (2C), 127.4 (2C), 130.0 (2C), 130.3 (2C), 133.7 (2C), 136.3 (2C), 154.1 (2C, C-OH); ms : ei (m/z) 457 (100%, M-1); Anal. Calcd. for C<sub>21</sub>H<sub>14</sub>O<sub>2</sub>Br<sub>2</sub>: C 55.05%, H 3.08%. Found C 54.83%, H 4.10%.



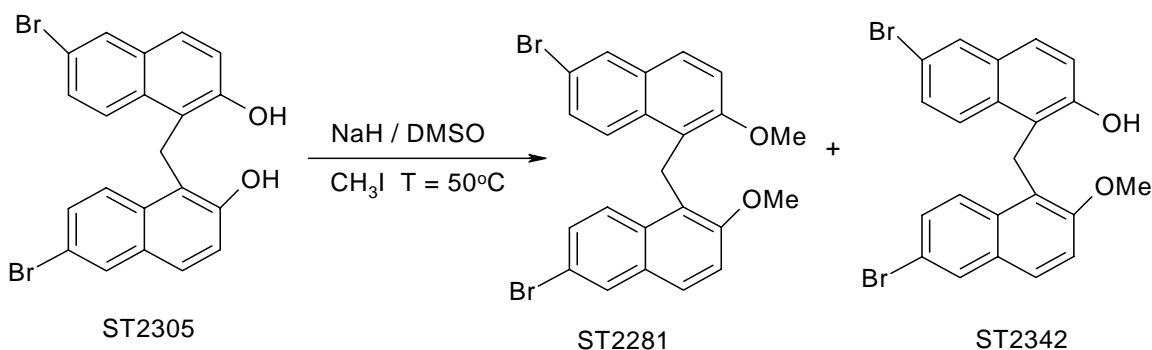
**Synthesis of 6-bromo-1-[(6-bromo-2-methoxy-1-naphthyl)methyl]-2-methoxynaphthalene (ST2281)**



6-Br-2-naphthol (Aldrich, 200mg, 0.9mmol) was suspended in ethanol 95% (2ml) and HCl 2N (1ml),(or HCl conc. 1ml) was added. The mixture was stirred until complete dissolution of the starting material, at room temperature. HCHO 37% (60  $\mu$ L, 0.9mmol) was added to the solution. This mixture was left at 120°C for 3 h. Work- up consisted in diluting water and neutralizing with saturated aq. NaHCO<sub>3</sub> solution, the aqueous layer was extracted with ethyl acetate; the organic phase was washed with water and brine up to pH = 7. The organic layer was dried with anhydrous Na<sub>2</sub>SO<sub>4</sub> and the solvent was evaporated in vacuo. The compound ST2281 was obtained as white powder (yield = 54% to naphthol, using HCl conc. the yield was 3%). The reaction was monitored by TLC using hexane / ethyl acetate (8:2) as eluent.

<sup>1</sup>H- NMR ( 300 MHz, d-DMSO)  $\delta$  3.98 ( 6H, s, -OCH<sub>3</sub>), 4.80 ( 2H, s, -CH<sub>2</sub> ), 7.40-7.58 (5H, m), 7.75 ( 2H, m), 8.00 (2H, m), 8.36 (1H, s); <sup>13</sup>C NMR ( 300 MHz , d-DMSO)  $\delta$  28.3 (1C), 117.7 (2C), 120.1 (1C), 121.2 (1C), 122.5 (2C), 124.5 (2C), 124.6 (2C), 127.4 (2C), 129.5 (2C), 130.3 (2C), 133.7 (2C),136.3 (2C), 154.1 (2C); ms : ei (m/z) 487 (100%, M<sup>+</sup>+1); Anal. Calcd. for C<sub>23</sub>H<sub>18</sub>O<sub>2</sub>Br<sub>2</sub>: C 56.82%, H 3.73%, O 6.58% . Found C 53.83%, H 6.10%, O 5.60%.

## Synthesis of ST2281 and 6-bromo-1-[(6-bromo-2-methoxy-1-naphthyl)methyl]-2-naphthol (ST2342)



To a solution of ST 2305 (67mg, 0.146mmol) in DMSO (1.5mL) were added NaH (24mg, 1mmol ) and CH<sub>3</sub>I (60μL, 0.06mmol) at room temperature. The mixture was stirred at 50°C, for 3h. The reaction was monitored by TLC using hexane / ethyl acetate (8:2) as eluent. The reaction was quenched adding water to the solution slowly. The aqueous phase was extracted with ethyl acetate and the organic layer was washed again with water and brine, the organic phase was dried with anhydrous Na<sub>2</sub>SO<sub>4</sub> and the solvent was evaporated in vacuo. The mixture was separated by TLC (Merck, 20X20 cm ,2mm,cod.1.05717.00) preparative chromatography, eluting with hexane /ethyl acetate (7:3). The compounds ST2281 (yield = 8%) and ST2342 (yield = 67%) were obtained as white powder.

ST2342:

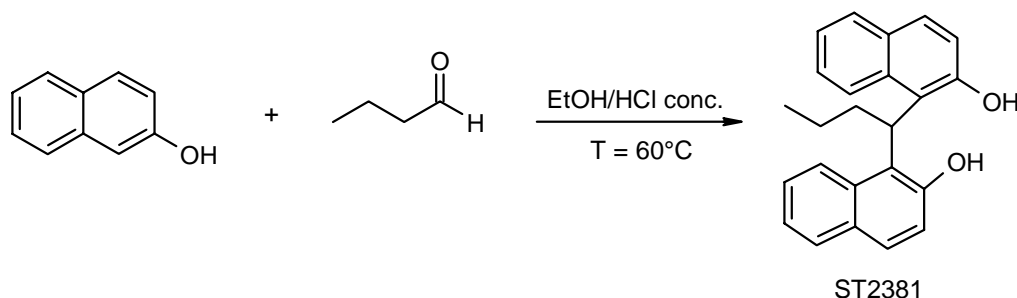
<sup>1</sup>H- NMR ( 300 MHz, d-DMSO) δ 4.10 ( 3H, s, -OCH<sub>3</sub>), 4.78 ( 2H, s, -CH<sub>2</sub>-), 7.40 (3H, t), 7.60 ( 2H, t), 7.80-7.98 (4H, m), 8.02 (1H, s), 8.20 (1H, s, OH); <sup>13</sup>C NMR ( 300 MHz, d-DMSO) δ 30.8(1C, -CH<sub>2</sub>-), 56.3(1C, CH<sub>3</sub>), 110.6(2C, C-Br), 118.3 (1C), 123.1(1C), 124.4(1C), 124.5(1C), 124.5(1C), 126.6(1C), 127.4(1C), 128.4(1C), 129.6(1C), 130.3 (2C), 131.1(1C), 132.4(1C), 133.4(1C), 137.5(1C), 142.5(1C), 155.0(1C, C-OH), 157.0(1C, OCH<sub>3</sub>); ms : ei (m/z) 471(100%, M<sup>+</sup>-1); Anal. Calcd. for

$C_{22}H_{16}O_2Br_2$ : C 55.96%, H 3.41%, Br 33.84%. Found: C 54.45%, H 4.62%, Br 35.84%.

ST2281:

$^1H$ - NMR ( 300 MHz, d-DMSO)  $\delta$  3.98 ( 6H, s,  $-OCH_3$ ), 4.80 ( 2H, s,  $-CH_2$  ), 7.40- 7.58 (5H, m), 7.75 ( 2H, m), 8.00 (2H, m), 8.36 (1H, s);  $^{13}C$  NMR ( 300 MHz , d-DMSO)  $\delta$  28.3 (1C), 117.7 (2C), 120.1 (1C), 121.2 (1C), 122.5 (2C), 124.5 (2C), 124.6 (2C), 127.4 (2C), , 129.5 (2C), 130.3 (2C), 133.7 (2C), 136.3 (2C), 154.1 (2C); ms : ei (m/z) 487.21 (100%,  $M^+ + 1$ ); Anal. Calcd. for  $C_{23}H_{18}O_2Br_2$ : C 56.82%, H 3.73%, O 6.58% . Found C 54.83%, H 4.10%, O 7.00%.

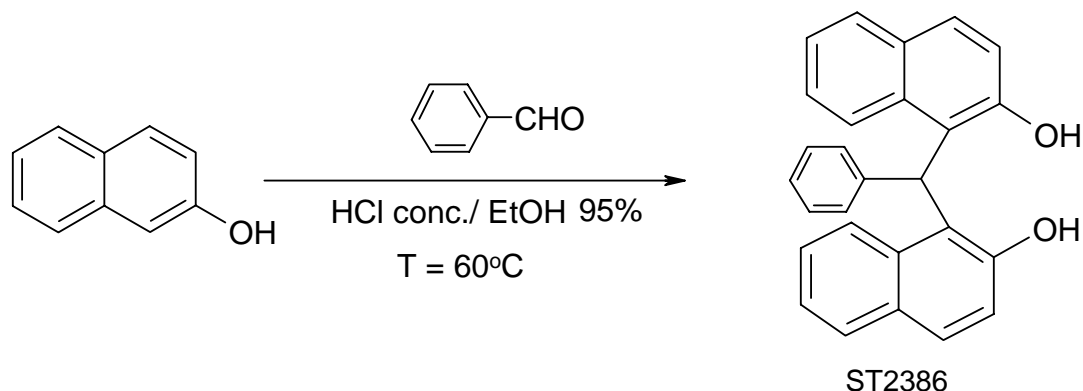
### Synthesis of 1-[1-(2-hydroxy-1-naphthyl)butyl]-2-naphthol (ST2381)



To 2-naphthol (Aldrich, 500mg, 3.47mmol) suspended in ethanol 95% (4ml), butyraldehyde (63 $\mu$ l, 0.694mmol) and HCl conc.(9.2 $\mu$ l) were added at room temperature. The mixture was stirred at 60°C for 3 h. The reaction was monitored by TLC using hexane / ethyl acetate (7:3) as eluent. Work-up involved diluting with water and neutralizing with saturated aq. NaHCO<sub>3</sub> solution. The pH value solution was corrected with HCl 2N to pH=1; the aqueous layer was extracted with ethyl acetate; the organic phase was washed with water and brine until pH = 7. The organic layer was dried with anhydrous Na<sub>2</sub>SO<sub>4</sub> and the solvent was evaporated in vacuo. The mixture was separated by chromatography, eluting with hexane, hexane /ethyl acetate (9:1). The compound ST2381 was obtained as a solid (yield = 4.1%).

<sup>1</sup>H- NMR ( 300 MHz, d-DMSO)  $\delta$  0.9 ( 3H, t, -CH<sub>3</sub>), 1.42 (2H, q, H-2''), 2.50 ( 2H, m, H-1''), 5.78 (1H, t, -CH), 7.02 ( 1H, t), 7.20 (4H, m), 7.60 (5H, dd), 8.40 (2H, m), 10.00 (2H, brs, OH) ; <sup>13</sup>C NMR ( 300 MHz, d-DMSO)  $\delta$  13.1(1C), 20.7 (1C), 38.69 (1C), 50.9(1C), 121.3(2C), 123.0(2C), 124.4 (2C), 127.3 (2C), 127.8(2C), 130.5(2C), 134.5 (2C), 135.6(2C), 135.6(2C), 148.9(2C, C-OH); ms : ei (m/z) 341(100%, M<sup>+</sup>-1); Anal. Calcd. for C<sub>24</sub>H<sub>22</sub>O<sub>2</sub>: C 84.18%, H 6.47%. Found: C 69.29%, H 7.39%.

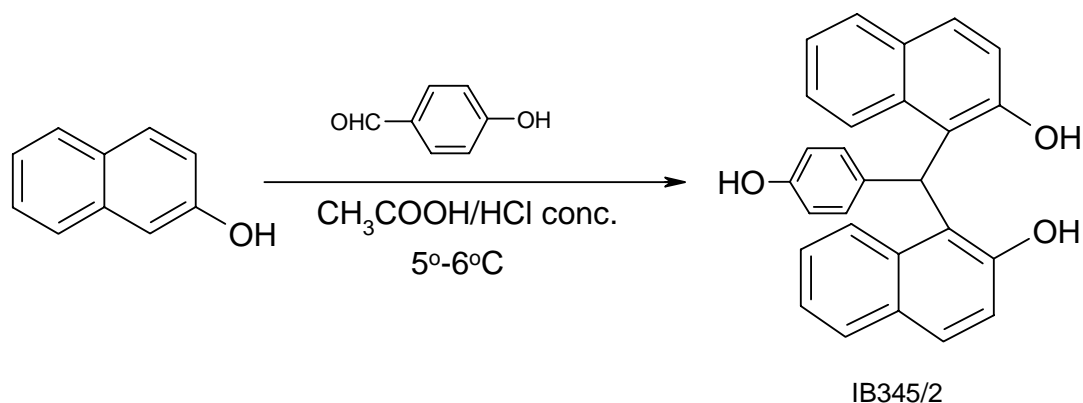
### Synthesis of 1,1 (benzylidene)di (2-naphthol) (ST2386)



To 2-naphthol (Aldrich, 300mg, 2.1mmol) suspended in ethanol 95% (2ml), benzaldehyde (42 $\mu$ l, 0.42mmol) and HCl conc.(3 drops) were added at room temperature. The mixture was stirred at 60°C for 1 night. The reaction was monitored by TLC using hexane / ethyl acetate (8:2) as eluent. Work-up involved diluting with water and neutralizing with saturated aqueous NaHCO<sub>3</sub> solution. The aqueous layer was extracted with ethyl acetate; the organic phase was washed with water and brine up to pH = 7. The organic layer was dried over anhydrous Na<sub>2</sub>SO<sub>4</sub> and the solvent was evaporated in vacuo. The mixture was separated by chromatography, eluting with hexane, hexane /ethyl acetate (85:15), hexane /ethyl acetate (9:1). The compound IB340 was obtained as white solid (yield = 7.9%).

<sup>1</sup>H- NMR (300 MHz, d-DMSO)  $\delta$  7.00 (3H, t), 7.12 (2H, d), 7.62 (1H, s, -CH-), 7.64 (3H, t), 8.10 (2H, d), 9.70 (2H, br s, -OH); <sup>13</sup>C NMR (300 MHz, d-DMSO)  $\delta$  42.1(1C, -CH-), 119.6(2C), 120.9(2C), 122.7(2C), 125.6(2C), 126.5(2C), 128.4(2C), 129.1 (2C), 129.2(2C), 129.3(2C), 134.9(2C), 144.7(4C), 153.4(2C); ms : ei (m/z) 375(100%, M-1); Anal. Calcd. for C<sub>27</sub>H<sub>20</sub>O<sub>2</sub>: C 86.14%, H 5.35%. Found: C 80.75%, H 5.61%.

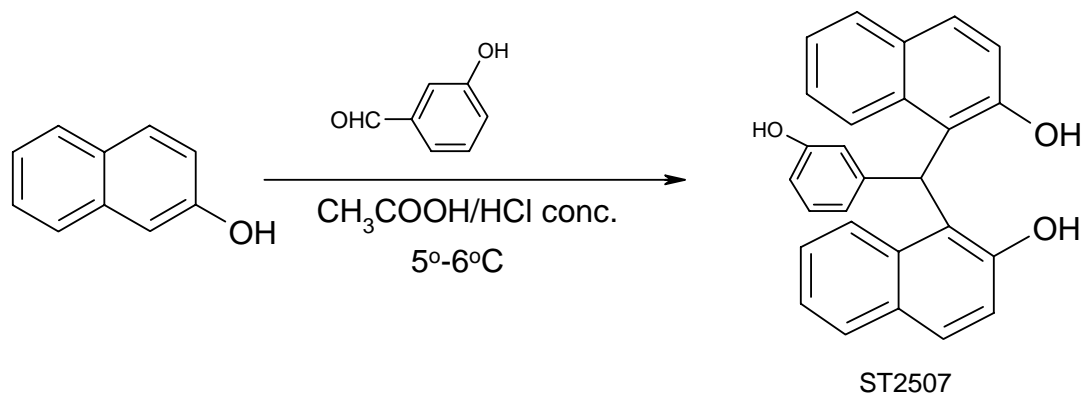
**Synthesis of 1-[(2-hydroxy-1-naphthyl)(4-hydroxyphenyl)methyl]-2-naphthol  
(IB345/2)**



To 2-naphthol (Aldrich, 200mg, 1.38mmol) and 4-hydroxybenzaldehyde (86.3mg, 0.69mmol) glacial acetic acid (0.7mL) and HCl conc. (0.11mL) dropwise were added at 10°C. The mixture underwent stirring at room temperature for 1h. The resulting solution was left at 4-5°C for 3-4days. The reaction was monitored by TLC using hexane / ethyl acetate (7:3) as eluent. Work-up consisted in triting the obtained solid, filtering and washing it on a gooch funnel, with glacial acetic acid. The precipitate was purified by TLC preparative chromatography, eluting with hexane /ethyl acetate (6:4). The compound IB345/2 was obtained as green solid (yield = 30%).

<sup>1</sup>H- NMR ( 300 MHz, CDCl<sub>3</sub>) δ 5.20 ( 1H, brs, -OH), 5.80 ( 1H, brs, -OH), 6.39 ( 1H, s, -CH), 6.56 (2H, d), 7.25-7.80 ( 12H, m), 8.30 (2H, d), 9.80 (2H, brs, OH); <sup>13</sup>C NMR ( 300 MHz , CDCl<sub>3</sub>) δ 40.3(1C, -CH), 119.0(2C), 122.0(2C), 123.4(2C), 124.3(2C), 128.3(2C), 128.5(2C), 131.2(2C), 133.7(2C), 134.2(2C), 134.8(2C), 136.2(2C), 149.5 (1C), 151.2(2C, C-OH), 154.0(1C; C-OH); ms : ei (m/z) 391 (100%, M-1); Anal. Calcd. for C<sub>27</sub>H<sub>20</sub>O<sub>3</sub>: C 82.63%, H 5.14%, O 12.23%. Found: C 69.13%, H 7.04%, O 9.05 %.

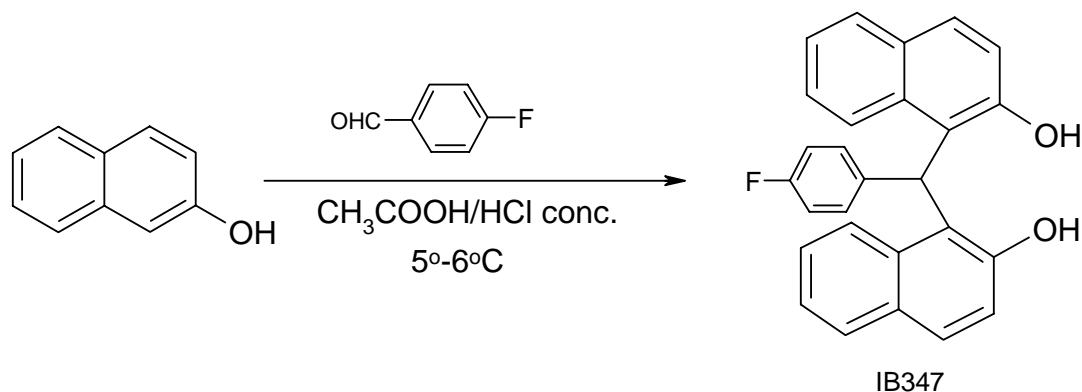
**Synthesis of 1-[(2-hydroxy-1-naphthyl)(3-hydroxyphenyl)methyl]-2-naphthol (ST2507)**



To 2-naphthol (Aldrich, 300mg, 2.1mmol) and 3-hydroxybenzaldehyde (128mg, 1.05mmol) glacial acetic acid (1.5mL) and HCl conc. (0.165mL) dropwise were added at  $10^\circ\text{C}$ . The mixture underwent stirring at room temperature for 1h. The resulting solution was left at  $4\text{-}5^\circ\text{C}$  for 3-4days. The reaction was monitored by TLC using hexane / ethyl acetate (7:3) as eluent. Work- up consisted in triting the obtained solid, filtering and washing it on a gooch funnel, with glacial acetic acid. The precipitate was purified by TLC preparative chromatography, eluting with hexane /ethyl acetate (6:4). The compound was obtained as green solid (yield = 31%).

$^1\text{H-NMR}$  ( 300 MHz, d-DMSO)  $\delta$  6.38 ( 1H, d), 6.60 (1H, s, -CH-), 6.82 ( 1H, s), 6.92 ( 1H, t), 7.18 (1H, d), 7.44 (2H, d, H-7,7'), 7.56 (2H, d, H-3,3'), 7.62 (2H, t, H-6,6'), 7.94 (4H, d, H-4,4' and H-5,5'), 8.62 (2H, d, H-8,8'), 9.18 (2H, brs, OH);  $^{13}\text{C NMR}$  ( 300 MHz, d-DMSO)  $\delta$  43.5(1C, -CH-), 112.8(1C), 114.7(1C), 122.4(2C), 123.1(2C), 124.2 (2C), 124.9(1C), 127.9(2C), 128.5(2C), 131.2(2C), 134.5(1C), 135.5(2C), 136.2(2C), 136.9(2C), 145.0(1C), 151.0(2C), 160.6(1C, C-OH); ms : ei (m/z) 391 (100%, M-1); Anal. Calcd. for  $\text{C}_{27}\text{H}_{20}\text{O}_3$ : C 82.63%, H 5.13%. Found: C 81.01%, H 4.78%.

### Synthesis of 1-[(2-hydroxy-1-naphthyl)(4-fluorophenyl)methyl]-2-naphthol (IB347)

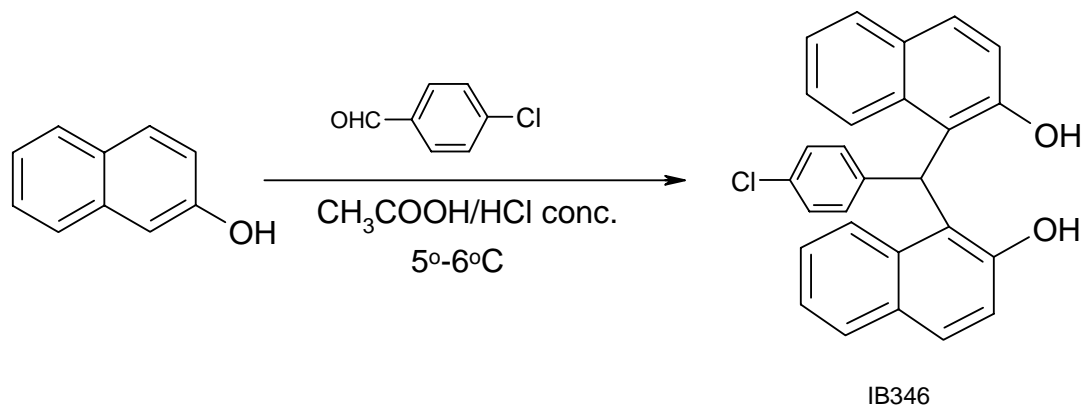


To 2-naphthol (Aldrich, 200mg, 1.4mmol) and 4-Fluoro-benzaldehyde (74 $\mu$ L, 0.69mmol) glacial acetic acid (0.1mL) and HCl conc. (0.165mL) dropwise were added at 10°C. The mixture underwent stirring at room temperature for 1h. The resulting solution was left at 4-5°C for 3-4days. The reaction was monitored by TLC using hexane / ethyl acetate (7:3) as eluent. Work- up consisted in triting the obtained solid, filtering and washing it on a gooch funnel, with glacial acetic acid. The precipitate was purified by TLC preparative chromatography, eluting with hexane /ethyl acetate (6:4). The compound was obtained as green solid (yield = 8%).

<sup>1</sup>H- NMR ( 300 MHz, d-DMSO)  $\delta$  6.78 ( 1H, s, -CH-), 6.88( 2H, t), 7.42 (2H, t), 7.50-7.70 ( 8H, m), 7.90 (4H, d), 8.62 (2H, d); <sup>13</sup>C NMR ( 300 MHz, d-DMSO)  $\delta$  37.4(1C, -CH-), 115.3(2C), 115.6(2C), 117.3(2C), 118.2(2C), 122.6(2C), 124.5(2C), 127.1(2C), 129.1(2C), 129.2 (2C), 129.9(2C), 131.3(1C), 140.9(1C), 141.9(1C), 148.5(1C), 159.7 (1C), 162.9(1C); ms : ei (m/z) 392.9 (100%, M-1); Anal. Calcd. for C<sub>27</sub>H<sub>19</sub>O<sub>2</sub>F: C 82.22%, H 4.86%, O 8.11%. Found: C 79.20%, H 7.00%, O 6.95%.



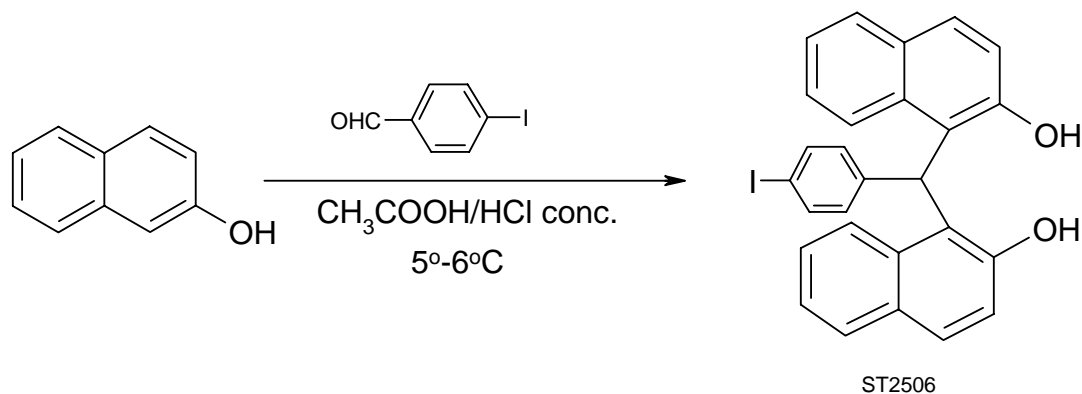
### Synthesis of 1-[(2-hydroxy-1-naphthyl)(4-chlorophenyl)methyl]-2-naphthol (IB346)



To 2-naphthol (Aldrich, 0.2g, 0.00138mol) and 4-chloro-benzaldehyde (0.097g, 0.0007mol) glacial acetic acid (1.1mL) and HCl conc. (0.165mL) dropwise were added at 10°C. The mixture underwent stirring at room temperature for 1h. The resulting solution was left at 4-5°C for 3-4days. The reaction was monitored by TLC using hexane / ethyl acetate (7:3) as eluent. Work- up consisted in triting the obtained solid, filtering and washing it on a gooch funnel, with glacial acetic acid. The precipitate was purified by TLC preparative chromatography, eluting with hexane /ethyl acetate (6:4). The compound was obtained as green solid (yield =30 %).

$^1\text{H-NMR}$  ( 300 MHz,  $\text{CDCl}_3$ )  $\delta$  6.45 ( 1H, s, -CH), 7.16 ( 3H, m), 7.4-7.54 (6H, m), 7.59 ( 2H, t), 7.80 (5H, t), 8.36 (2H, d);  $^{13}\text{C NMR}$  ( 300 MHz ,  $\text{CDCl}_3$ )  $\delta$  40.3(1C, -CH), 122.0(2C), 123.0(2C), 124.0(2C), 128.0(2C), 128.5(2C), 131.1(2C), 132.1(2C), 132.7(1C), 133.2(2C), 134.0(2C, C-1, 1'), 135.0(2C), 136.0(2C), 142.2(1C), 153.0(2C; C-OH); ms : ei (m/z) 409 (100%, M-1); Anal. Calcd. for  $\text{C}_{27}\text{H}_{19}\text{O}_2\text{Cl}$ : C 78.92%, H 4.65%, Cl 8.62%. Found: C 79.26%, H 4.45%, N 8.76 %.

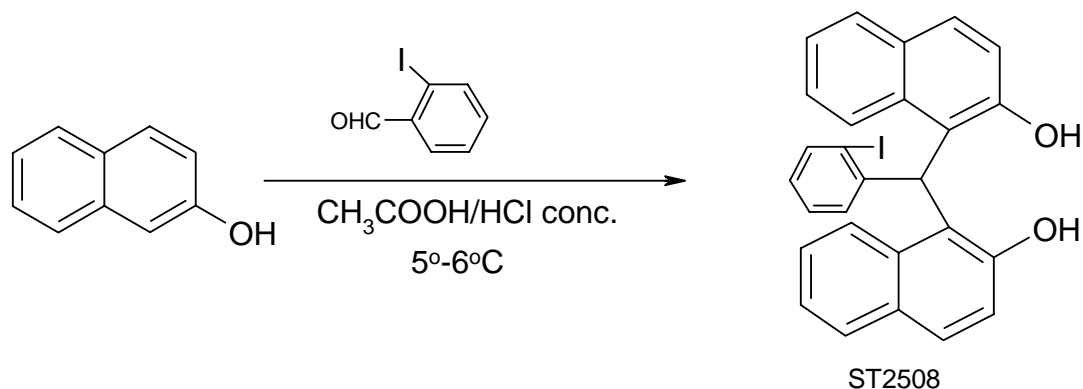
### Synthesis of 1-[(2-hydroxy-1-naphthyl)(4-iodophenyl)methyl]-2-naphthol (ST2506)



To 2-naphthol (Aldrich, 203mg, 1.408mmol) and 4-I-benzaldehyd (163mg, 0.704mmol), glacial acetic acid (1mL) and HCl conc. (0.11mL) dropwise were added at 10°C. The mixture underwent stirring at room temperature for 1h. The resulting solution was left at 4-5°C for 3-4 days. The reaction was monitored by TLC using hexane / ethyl acetate (8:2) as eluent. Work- up consisted in triting the obtained solid, filtering and washing it on a gooch funnel with glacial acetic acid. The precipitate was purified by TLC preparative chromatography, eluting with hexane /ethyl acetate (8:2). The compound ST2506 was obtained as white solid (yield = 38%).

<sup>1</sup>H- NMR ( 300 MHz, d-DMSO) δ 6.82 ( 2H, d), 7.00 (1H, s, -CH-), 7.20 ( 6H, m), 7.56 ( 2H, d), 7.76 (4H, m), 8.18 (2H, d), 9.98 (2H, brs, OH);<sup>13</sup>C NMR ( 300 MHz, d-DMSO) δ 40.3(1C, -CH-), 92.2(1C), 122.0(2C), 123.2(2C), 124.3(2C), 127.9(2C), 128.5(2C), 131.1(2C), 132.5(2C), 133.0(2C), 135.0(2C), 136.2(2C), 141.0(2C), 143.4(1C), 151.0(2C); ms : ei (m/z) 501(100%, M-1); Anal. Calcd. for C<sub>27</sub>H<sub>19</sub>IO<sub>2</sub>: C 64.55%, H 3.81%. Found: C 60.58%, H 4.33%.

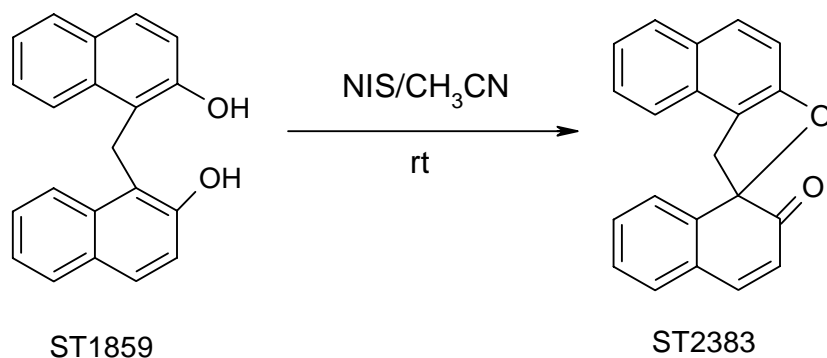
### Synthesis of 1-[(2-hydroxy-1-naphthyl)(2-iodophenyl)methyl]-2-naphthol (ST2508)



To 2-naphthol (Aldrich, 142mg, 0.989mmol) and 2-I-benzaldehyd (44.61mg, 0.494mmol), glacial acetic acid (0.8mL) and HCl conc. (0.08mL) dropwise were added at 10°C. The mixture was left under stirring at room temperature for 1h. The resulting solution was left at 4-5°C for 3-4 days. The reaction was monitored by TLC using hexane / ethyl acetate (8:2) as eluent. Work- up consisted in triting the obtained solid, filtering and washing it on a gooch funnel with glacial acetic acid. The precipitate was purified by TLC preparative chromatography, eluting with hexane /ethyl acetate (8:2). The compound ST2508 was obtained as white-yellow solid (yield = 38%).

<sup>1</sup>H- NMR ( 300 MHz, CDCl<sub>3</sub>) δ 7.00 ( 2H, d), 7.08 (2H, d), 7.10 ( 1H, s, -CH-), 7.42 ( 2H, t), 7.58 (2H, t), 7.70 (4H, d), 7.82-8.07 (4H, m); <sup>13</sup>C NMR ( 300 MHz, CDCl<sub>3</sub>) δ 45.2(1C, -CH-), 102.6(1C), 121.2(2C), 122.3(2C), 124.2(2C), 127.8(1C), 127.9(2C), 128.5(2C), 131.1(2C), 132.5(1C), 133.7(1C), 134.4(2C), 134.8(2C), 136.2(2C), 143.5(1C), 145.0(1C), 149.6(2C); ms : ei (m/z) 501(100%, M-1); Anal. Calcd. for C<sub>27</sub>H<sub>19</sub>IO<sub>2</sub>: C 64.56%, H 3.81%, O 6.37%, I 25.26%.

### Synthesis of 1'H, 2H-spiro[naphthalene-1-2'-naphtho[2,1-b]furan]-2-one (ST2383)

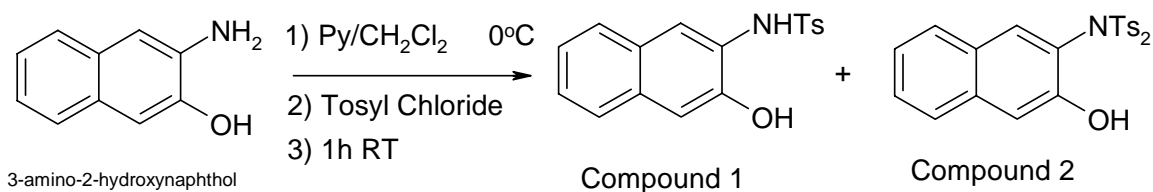


To a solution of ST1859 (200mg, 0.66mmol) in CH<sub>3</sub>CN (4mL), n- Iodo-succinimide (34mg, 1mmol) was added at room temperature. The solution was stirred over night at room temperature. The reaction was complete as highlighted by TLC hexane/ethyl acetate (8:2) and work-up consisted in evaporating the solvent, dissolving the crude product by diethyl ether, washing the organic layer with a 5% solution of sodium thiosulfate and water. The organic phase was dried over anhydrous Na<sub>2</sub>SO<sub>4</sub> and the solvent was evaporated under vacuum. The product was obtained as yellow solid (yield = 90%).

The same final product was obtained using temperature. The reaction underwent heating at 80°C.

<sup>1</sup>H- NMR ( 300 MHz, d-DMSO) δ 3.50 ( 1H, d, -CH<sub>a</sub>), 4.00 ( 1H, d, -CH<sub>b</sub>), 6.29 ( 1H, d, H-3'), 7.30 (2H, m ), 7.60 ( 2H, m ), 7.80 (2H, m), 7.90 (5H, m); <sup>13</sup>C NMR ( 300 MHz ,DMSO) δ 35.6(1C, -CH<sub>2</sub>), 100.1(1C, C-1'), 111.5(1C, C-3), 115.0(1C, C-1), 123.0(1C), 124.1(1C), 125.0(1C), 125.3(1C), 125.4(1C), 125.6(1C), 126.0(1C), 126.8 (1C, C-3'), 128.2 (1C), 128.8(1C), 128.9(1C), 134.1(1C), 136.0(1C), 138.0(1C), 140.8(1C), 153.2(1C, C-2), 186.5(1C, CO) ; ms : ei (m/z) 366(100%, M<sup>+</sup>+1), 388 (M<sup>+</sup>+Na); Anal. Calcd. for C<sub>21</sub>H<sub>14</sub>O<sub>2</sub>: C 84.54%, H 4.73%. Found: C 82.94%, H 4.77%.

## Synthesis of Compound 1 and 2



To a suspension of 3-amino-2-hydroxynaphthalene (165.1mg, 1.037mmol) in dry CH<sub>2</sub>Cl<sub>2</sub> (2 mL) at 0°C, was added dry pyridine (87μL, 1.037mmol) and then tosyl chloride (200mg, 1.049mmol). The solution was left at room temperature, under stirring for 1h. The reaction was complete as showed by TLC hexane/ ethyl acetate (7:3). Work-up consisted in eluting the reaction mixture with CH<sub>2</sub>Cl<sub>2</sub>, washing the organic layer with water, it was dried over anhydrous Na<sub>2</sub>SO<sub>4</sub> and the solvent was evaporated in vacuo. The crude brown oil was purified by chromatography eluting with hexane, hexane /ethyl acetate (9:1), hexane /ethyl acetate (8:2), hexane /ethyl acetate (7:3). The two compounds were obtained as yellow powder (yield = 51%).

### N-(3-hydroxy-naphthalen-2-yl)-4-methylbenzenesulfonamide (Compound 1)

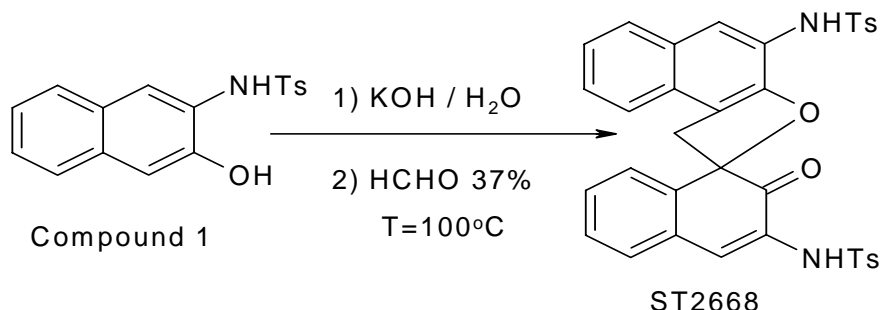
<sup>1</sup>H- NMR ( 300 MHz, d-DMSO) δ 2.38 ( 3H, s, -CH<sub>3</sub>), 7.02 ( 1H, s), 7.18-7.40 (4H, m), 7.56-7.80 ( 5H, m), 9.80 (1H, brs, OH); <sup>13</sup>C NMR ( 300 MHz , d-DMSO) δ 21.4(1C, -CH<sub>3</sub>), 110.7(1C), 114.7(1C), 124.7(1C, C-3), 125.0(1C), 125.2(1C), 125.4(1C), 128.0(2C), 129.4(1C), 130.1 (2C), 134.2 (1C), 141.0(1C), 143.3 (1C), 148.3(1C, C-2); ms : ei (m/z) 312 (100%, M<sup>+</sup>-1); Anal. Calcd. for C<sub>17</sub>H<sub>15</sub>O<sub>3</sub>NS: C 65.16%, H 4.82%, N 4.47%. Found: C 66.51%, H 5.60%, N 4.48 %.

### Toluene-4-sulfonic acid-3-hydroxynaphthalene (Compound 2)

<sup>1</sup>H- NMR ( 300 MHz, DMSO) δ 2.39 ( 3H, s, -CH<sub>3</sub>), 2.42 ( 3H, s, -CH<sub>3</sub> ), 7.38 (3H, d, H-1), 7.44 ( 5H, m), 7.60-7.78 (3H, m), 7.82 (3H, d), 10.00 (1H, brs, OH); <sup>13</sup>C NMR ( 300 MHz , DMSO) δ 21.5 (2C, -CH<sub>3</sub>), 112.3(1C), 114.7 (1C, CN), 116.0 (1C), 123.0

(1C), 123.4(1C), 125.4(1C), 128.2(4C), 130.0(4C), 140.0(1C), 143.0(2C), 143.6(2C), 150.2(1C); ms : ei (m/z) 466(100%, M<sup>+</sup>-1); Anal. Calcd. for C<sub>24</sub>H<sub>21</sub>O<sub>5</sub>NS<sub>2</sub>: C 61.65%, H 4.53%, N 3.00%. Found: C 62.00%, H 4.65%, N 2.80 %.

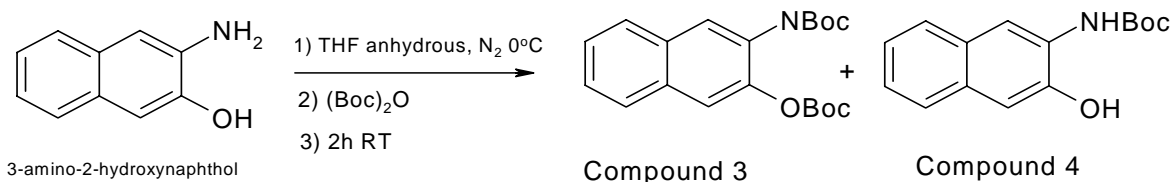
**Synthesis of 4-methyl-N-(3-[[[4-methylphenyl)sulfonyl]amino]-2-oxo-1'H, 2H-spiro[naphthalene-1-2'-naphthol[2,1-b]furan]-4'-yl]benzenesulfonamide (ST2668)**



Compound 1 (83.6mg, 0.27mmol) was suspended in water (0.7ml) and KOH (48.7mg, 0.86mmol) was added. The mixture was stirred until complete dissolution of the starting material, at room temperature. HCHO 37% (20  $\mu$ L, 0.27mmol) was added to the solution. This mixture was left at 100°C for 2 h. The reaction was monitored by TLC using hexane / ethyl acetate (7:3) as eluent. As showed by TLC, the starting compound disappeared, the mixture was left to go to room temperature. Work- up consisted in neutralizing with HCl 2N up to pH = 1, the aqueous layer was extracted with ethyl acetate; the organic phase was washed with water and brine. The organic layer was dried over anhydrous Na<sub>2</sub>SO<sub>4</sub> and the solvent was evaporated in vacuo. The crude mixture was purified by chromatography using as eluent hexane/AcOEt (70:30). ST2668 was obtained as yellow solid (yield = 17.3%).

<sup>1</sup>H- NMR ( 300 MHz, CDCl<sub>3</sub>)  $\delta$  2.40 ( 6H, d, -CH<sub>3</sub>), 3.30-3.50( 2H, dd,-CH<sub>2</sub>-), 4.70 (2H, br s, NH), 6.85 ( 1H, t), 7.18 (5H, t), 7.36 (5H, t), 7.56 (1H, s), 7.60-7.80 (5H, m), 7.90 (1H, s); <sup>13</sup>C NMR ( 300 MHz ,CDCl<sub>3</sub>)  $\delta$  21.7 (2C, CH<sub>3</sub>), 44.2(1C, CH<sub>2</sub>), 89.5 (1C), 115.8 (1C), 119.1(1C), 121.2(1C), 121.6(1C), 122.3(1C), 124.6(1C), 125.2(1C), 126.5(1C), 126.7(1C), 127.4 (1C), 127.5 (1C), 127.6(1C), 127.8(1C), 128.0(1C), 128.0 (1C), 128.7 (1C), 129.0 (1C), 129.6 (1C), 129.8 (1C), 129.8 (1C), 129.9 (1C), 130.2 (1C), 130.4 (1C), 130.5 (1C), 136.0 (1C), 136.5 (1C), 139.6 (1C), 144.1 (1C), 144.9 (1C),149.3 (1C), 192.2 (1C, CO); ms : ei (m/z) 635 (100%, M-1)<sup>-</sup>; Anal. Calcd. for C<sub>35</sub>H<sub>28</sub>N<sub>2</sub>O<sub>6</sub>S<sub>2</sub>: C 66.02%, H 4.43%, N 4.40%, S 10.07%. Found: C 64.20%, H 5.02%, N 4.33%, S 10.11%.

## Synthesis of Compound 3 and 4



To a solution of 3-amino-2-hydroxynaphthalene (300mg, 1.88mmol) in dry THF (4 mL) at 0°C, under N<sub>2</sub>, di-tert-butylidicarbonate (874mg, 3.77mmol) was added. The solution was stirred at room temperature for 2h. The reaction was complete as showed by TLC hexane/ ethyl acetate (7:3).

Work up 1:

the crude mixture was concentrated under vacuum at 40°C. A dark oil was obtained, it was diluted with ethyl acetate and washed with brine and water. The organic layer was dried over anhydrous Na<sub>2</sub>SO<sub>4</sub> and evaporated under vacuum.

Work up 2:

consisted in eluting the reaction mixture with ethyl acetate directly, washing the organic layer with water, drying over anhydrous Na<sub>2</sub>SO<sub>4</sub> and the solvent evaporated in vacuo.

The crude brown oil, obtained from both work-up operations, was purified by chromatography eluting with, hexane, hexane /ethyl acetate (9:1), hexane /ethyl acetate (95:5), hexane /ethyl acetate (9:1). The compound H was obtained as yellow powder with a yield of 17% from the work up 1, instead of 46% from work up 2. The compound G was obtained as yellow powder too, with a yield of 62% from the work-up 1.



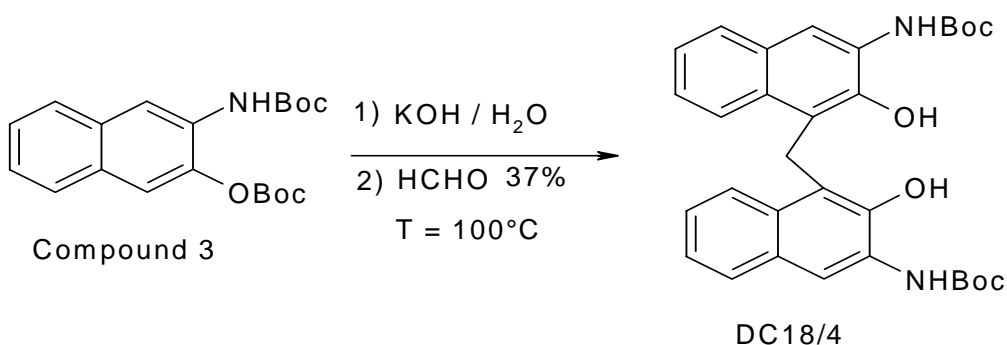
Carbonic acid 3-tert-butoxycarbonylamino-naphthalen-2-yl ester tert-butyl ester  
(Compound 3)

$^1\text{H}$ - NMR ( 300 MHz,  $\text{CDCl}_3$ )  $\delta$  1.58 ( 18H, m,  $-\text{OCH}_3$ ), 6.90 ( 1H, s,  $\text{H}_{-1}$  ), 7.40 (2H, m, H-7 and H- 8 ), 7.75 ( 1H, brs, NH), 7.80 (2H, m, H-5 and H-6'), 8.59 (1H, s, H-4);  $^{13}\text{C}$  NMR ( 300 MHz ,  $\text{CDCl}_3$ )  $\delta$  26.8 (3C,  $-\text{CH}_3$ ), 28.1 (3C,  $-\text{CH}_3$ ), 80.0 (1C, C-( $\text{CH}_3$ )<sub>3</sub>), 84.0 (1C, C-( $\text{CH}_3$ )<sub>3</sub>), 111.0 (1C, C-4), 112.3 (1C, C-1), 119.0 (1C), 123.0 (1C), 123.0 (1C), 124.1 (1C), 128.0 (1C), 131.0 (1C), 136.0 (1C), 138.1 (1C), 143.0 (1C, OCO), 153.0 (1C, NCO); ms : ei (m/z) 357 (20%, M-1), 382 (100%,  $\text{M}^+\text{Na}^+$ ); Anal. Calcd. for  $\text{C}_{20}\text{H}_{25}\text{O}_5\text{N}$ : C 66.84%, H 7.01%, N 3.90 %. Found: C 66.50%, H 6.89%, N 4.00 %.

Tert-butyl-3-hydroxy-2-naphthylcarbamate (Compound 4)

$^1\text{H}$ - NMR ( 300 MHz,  $\text{CDCl}_3$ )  $\delta$  1.50 ( 9H, s,  $-\text{OCH}_3$ ), 7.22 ( 1H, s), 7.35(2H, m, H-7 and H- 8 ), 7.60-7.79 ( 2H, m, H-6 and H-5), 7.84 (1H, s, H-1), 8.22 (1H, s, H-4);  $^{13}\text{C}$  NMR ( 300 MHz ,  $\text{CDCl}_3$ )  $\delta$  28.1 (3C,  $-\text{CH}_3$ ), 80.0 (1C,  $-\text{C}(\text{CH}_3)_3$ ), 109.0 (1C, C-1), 112.2 (1C, C-4), 119.8 (1C), 120.2 (1C), 122.0 (1C, C-2), 123.5 (1C), 130.0 (1C), 131.0 (1C), 133.0 (1C), 142.0 (1C, C-2), 153.0 (1C, CO); ms : ei (m/z) 257.93 (50%, M-1), 516.88 (100%, 2 x M); Anal. Calcd. for  $\text{C}_{15}\text{H}_{17}\text{O}_3\text{N}$ : C 69.48%, H 6.61%, N 5.40%. Found: C 68.50%, H 6.70%, N 4.48 %.

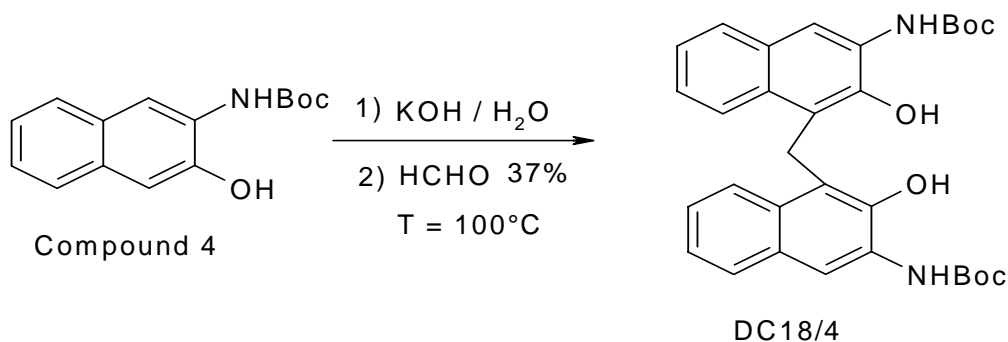
**Synthesis of di-tert-butyl(methylenebis(2-hydroxynaphthalene-1,3-diyl))bis carbamate (DC18/4)**



To Compound 3 (233mg, 0.9mmol) suspended in water (0.7ml) and KOH (124mg, 2.2mmol), HCHO 37% (60  $\mu$ L, 0.9mmol) was added. The mixture was stirred until complete dissolution of the starting material, at room temperature. This mixture was left at 100°C for 3 h. The reaction was monitored by TLC using hexane / ethyl acetate (8:2) as eluent. As showed by TLC, at the end of starting material, the mixture was left to go to room temperature. Work- up consisted in neutralizing with HCl 2N until pH = 1, the aqueous layer was extracted with ethyl acetate; the organic phase was washed with water and brine. The organic layer was dried over anhydrous Na<sub>2</sub>SO<sub>4</sub> and the solvent was evaporated in vacuo. The crude mixture was purified by chromatography Hexane, hexane /ethyl acetate (9:1), hexane / ethyl acetate (8:2). The relative compound was obtained as brown solid (yield = 25%).

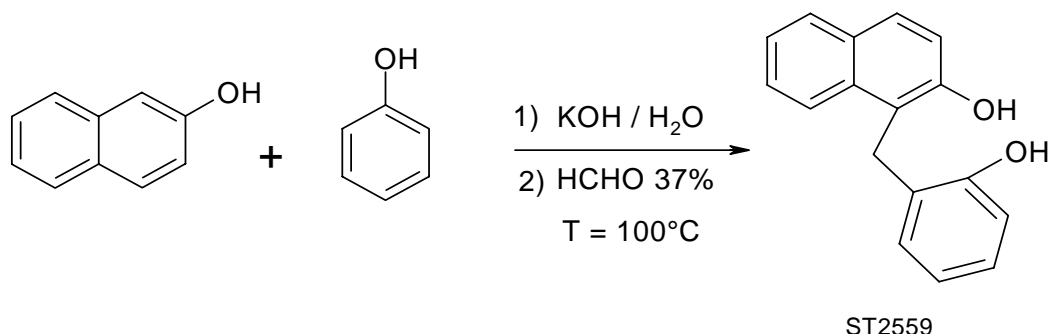
<sup>1</sup>H- NMR ( 300 MHz, CDCl<sub>3</sub>)  $\delta$  1.20 ( 9H, s, -OCH<sub>3</sub>), 1.60 ( 9H, s, -OCH<sub>3</sub>), 4.82 ( 2H, s, -CH<sub>2</sub>-), 7.56 (4H, m, H-6, 6' and H-7, 7' ), 7.70 ( 2H, d, H-5 and H-8), 7.80 (2H, s, H-5' and H-8'), 8.20 (2H, d, H-4, 4'), 9.40 (2H, brs, OH); <sup>13</sup>C NMR ( 300 MHz , CDCl<sub>3</sub>)  $\delta$  28.0 (6C, -CH<sub>3</sub>), 28.3 (1C, -CH<sub>2</sub>), 80.0 (2C, C-(CH<sub>3</sub>)<sub>3</sub>), 111.4 (2C, C-4,4'), 114.0 (2C), 119.0 (2C), 121.0 (2C), 123.0 (2C), 125.3 (2C, C-N), 128.0 (2C), 131.0 (2C), 140.0 (2C), 146.2 (2C, C-2,2'), 153.0 (2C, CO); ms : ei (m/z) 529 (100%, M-1); Anal. Calcd. for C<sub>31</sub>H<sub>34</sub>O<sub>6</sub>N<sub>2</sub>: C 70.17%, H 6.45%, N 5.28 %. Found: C 67.98%, H 5.89%, N 8.30 %.

## Synthesis of DC18/4



To Compound 4 (25mg, 0.1mmol) suspended in water (0.7ml) and KOH (18mg, 0.6mmol), HCHO 37% (8  $\mu$ L, 0.1mmol) was added. The mixture was stirred until complete dissolution of the starting material, at room temperature. This mixture was left at 100°C for 3 h. The reaction was monitored by TLC using hexane / ethyl acetate (1:1) as eluent. As showed by TLC, at the end of starting material , the mixture was left to go to room temperature. Work- up consisted in neutralizing with HCl 2N up to pH = 1, the aqueous layer was extracted with ethyl acetate; the organic phase was washed with water and brine. The organic layer was dried over anhydrous Na<sub>2</sub>SO<sub>4</sub> and the solvent was evaporated in vacuo. The crude mixture was purified by TLC chromatography using hexane /ethyl acetate (1:1)as eluent. The relative compound was obtained as brown solid (yield = 9%).

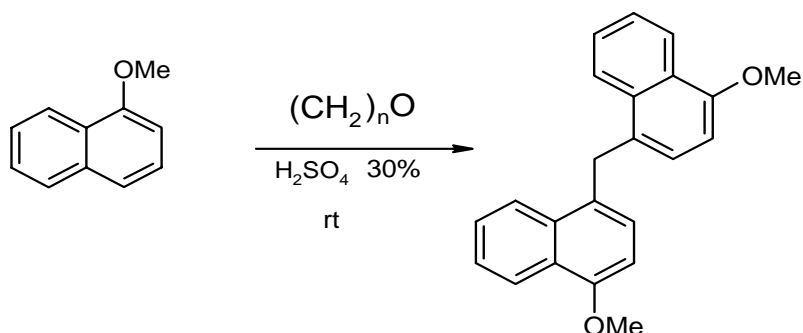
### Synthesis of 1-(2-hydroxybenzyl)-2-naphthol (ST2559)



To a solution of  $\beta$ -naphthol (100 mg, 0.7mmol), phenol (aldrich, 160mg, 1.7mmol), KOH (121 mg, 2.156 mmol) in H<sub>2</sub>O (0.55 ml), HCOH 37% (52  $\mu$ l, 0.7mmol) was added at room temperature. After stirring at reflux for 1h, the green solution was cooled at room temperature and aqueous hydrochloric acid 2N (1.1ml) was added dropwise up to pH = 1, to the solution. The aqueous phase was extracted with ethyl acetate and the organic layer was washed with brine, collected and dried over anhydrous Na<sub>2</sub>SO<sub>4</sub>. The organic phase was evaporated in vacuo at 40°C to provide the crude product, which was purified by chromatography, using hexane, hexane/ethyl acetate (9:1), hexane/ethyl acetate (8:2). The ST2559 was obtained as red oil (yield = 11.6%).

<sup>1</sup>H- NMR ( 300 MHz, CDCl<sub>3</sub>)  $\delta$  4.40 ( 2H, d, -CH<sub>2</sub>-), 4.70 ( 1H, br s, -OH), 5.00 (1H, br s, -OH), 6.75 ( 25H, d), 7.10 (2H, d), 7.30-7.89 (6H, m); <sup>13</sup>C NMR ( 300 MHz ,CDCl<sub>3</sub>)  $\delta$  22.2 (1C, CH<sub>2</sub>), 28.1 (1C), 33.3 (1C), 109.9 (1C), 119.9 (1C), 122.9 (1C), 123.7 (1C), 126.0 (1C), 127.3 (1C), 128.2 (1C), 128.4 (1C), 128.7 (1C), 129.0 (1C), 131.6 (1C), 145.0 (1C), 152.2 (1C, C-2'), 170.1 (1C, C-2'); ms : ei (m/z) 249 (100%, M-1), 308.65 (M<sup>+</sup>+ NH<sub>4</sub><sup>+</sup>); Anal. Calcd. for C<sub>17</sub>H<sub>14</sub>O<sub>2</sub>: C 81.58%, H 5.64%, O 12.78%. Found: C 80.20%, H 6.64%, O 10.78%.

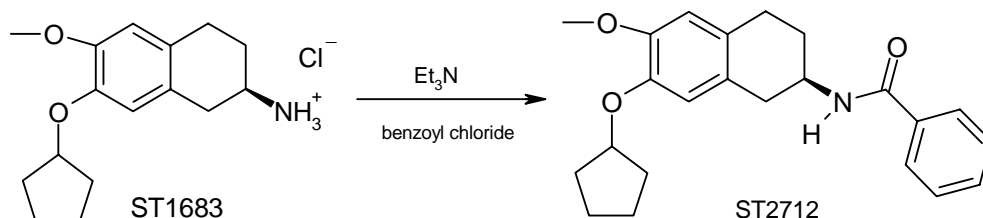
## Synthesis of 1,1'-bis-methoxynaphthalene (DC7/2)



To a solution of 1-methoxynaphthalene (120mg, 0.759mmol) and paraformaldehyde (27.6mg, 0.92mmol) in 0.8mL of dioxane was added 0.15mL of 30% H<sub>2</sub>SO<sub>4</sub> dropwise at room temperature for 48h. The reaction was followed by TLC hexane / ethyl acetate (95:5). The resulting white precipitate was filtered, washed with several portions of petroleum ether and dried under vacuum to give the compound DC7/2 as white powder (yield = 25%); if the work-up consisted in eluting the mixture reaction with CH<sub>2</sub>Cl<sub>2</sub>, washing with a saturated solution of NaHCO<sub>3</sub>, and brine, the organic layer dried over Na<sub>2</sub>S<sub>2</sub>O<sub>4</sub> anhydrous, evaporated under vacuum, and the yield came up as far as 61%.

<sup>1</sup>H- NMR ( 300 MHz, CDCl<sub>3</sub>) δ 3.90 ( 6H, s, -OCH<sub>3</sub>), 4.62 ( 2H, s, -CH<sub>2</sub>), 6.60 (2H, dd, H-3, 3'), 6.92 ( 2H, dd, H-2,2'), 7.40 (4H, m, H-6,6' and H-7,7'), 7.90 (2H, m, H-8,8'), 8.28 (2H, m, H-5,5'); <sup>13</sup>C NMR ( 300 MHz, CDCl<sub>3</sub>) δ 36.7 (1C, -CH), 56.0 (2C, CH<sub>3</sub>), 107.1 (2C, C-3,3'), 120.3 (2C), 123.1 (2C), 123.6 (2C), 128.2 (2C), 128.6 (2C), 130.0 (2C, C-1,1'), 131.2 (2C), 136.0 (2C), 158.0 (2C, C-4,4'); ms : ei (m/z) 329 (100%, M<sup>+</sup>+1); Anal. Calcd. for C<sub>23</sub>H<sub>20</sub>O<sub>2</sub>: C 84.12%, H 6.14%, O 9.74%. Found: C 83.80%, H 5.95%, O 8.95 %.

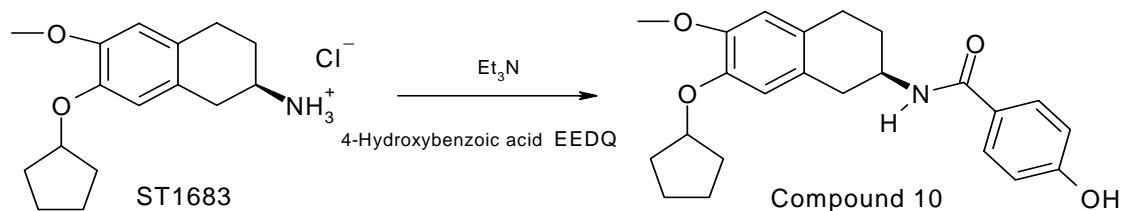
### Synthesis of N-[7-(cyclopentyloxy)-6-methoxy-1,2,3,4-tetrahydronaphthalen-2-yl]benzamide (ST 2712)



To (2R)-7-cyclopentyloxy-6-methoxy-1,2,3,4-tetrahydronaphthalen-2-aminium chloride (ST1683, 74mg, 0.25mmol) suspended in CH<sub>2</sub>Cl<sub>2</sub> anhydrous at 0°C, Et<sub>3</sub>N dry (69μL, 0.5mmol) was added. When the starting material was completely dissolved, benzoyl chloride ( 32μL, 0.27mmol) in 0.8mL of CH<sub>2</sub>Cl<sub>2</sub> dry was added dropwise to the solution. The reaction mixture was left at room temperature for 3h until the finish of the starting material, as highlighted by TLC hexane /ethyl acetate (1:1). The work up consisted in eluting the reaction mixture with CH<sub>2</sub>Cl<sub>2</sub> , which was washed with a solution of HCl 5% and neutralized by a saturated solution of NaHCO<sub>3</sub> until pH = 7. The organic layer was washed with brine and dried over Na<sub>2</sub>S<sub>2</sub>O<sub>4</sub> anhydrous, evaporated in vacuo. The crude product was purified by chromatography using CH<sub>2</sub>Cl<sub>2</sub>, CH<sub>2</sub>Cl<sub>2</sub> /ether (6:4) as eluent. The ST2712 was obtained as white powder (yield = 98%).

<sup>1</sup>H- NMR ( 300 MHz, CDCl<sub>3</sub>) δ 1.90 ( 8H, m, H-2'', H-3'', H-4'', 11', H-5''), 2.10 (1H, m, H-1''), 2.62 ( 2H, dd, H-1a), 2.82 (2H, q, H-4), 3.12-3.18 ( 1H, dd, H-1b), 3.82 (3H, s, -OCH<sub>3</sub>), 4.52 (1H, m, H-2), 4.74 (1H, m, H-3c), 6.18 (1H, d, H-3d), 6.60 (2H, d, H-5, H-8), 7.42 (3H, q, H-3', H-4', H-5'), 7.78 (2H, d, H-2', H-6'); <sup>13</sup>C NMR ( 300 MHz, CDCl<sub>3</sub>) δ 24.2 (1C), 26.7 (1C), 28.8 (1C), 33.0 (1C), 33.0 (1C), 35.5 (1C), 45.8 (1C), 56.3 (1C), 80.7 (1C), 112.6 (1C), 116.2 (2C), 125.8 (2C), 127.0 (2C), 127.5 (2C), 128.7 (2C), 129.9 (2C), 131.6 (2C), 135.0 (2C), 146.3 (2C), 148.9 (2C), 167.3 (2C) ; ms : ei (m/z) 366 (100%, M<sup>+</sup>+1), 388 (M<sup>+</sup>+ Na); Anal. Calcd. for C<sub>23</sub>H<sub>27</sub>NO<sub>3</sub>: C 75.58%, H 7.44%, N 3.83%. Found: C 75.42%, H 7.54%, N 4.40%.

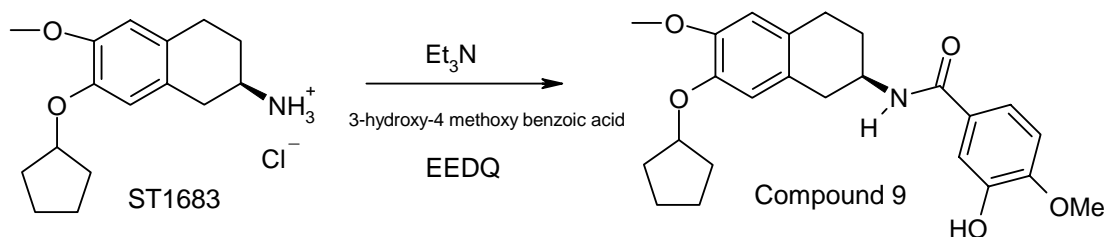
## Synthesis of N-(7-cyclopentyloxy-6-methoxy-1,2,3,4-tetrahydro-naphthalen-2-yl)-4-hydroxy-benzamide (Compound 10)



To ST1683 (25mg, 0.08mmol) dissolved in water at 0°C, Et<sub>3</sub>N dry (27μL, 0.16mmol) was added. When the starting material was completely dissolved, 4-hydroxy benzoic acid (11mg, 0.08mmol) in 200μL of CH<sub>3</sub>CN / 1mL of H<sub>2</sub>O was added dropwise to the solution, after 10 min under stirring EEDQ (22mg, 0.08mmol) was added to the solution too. The reaction mixture was left at 60°C for 3h until the starting material was finished, as highlighted by TLC hexane /ethyl acetate (8:2). The work up consisted in evaporating the reaction solution in vacuo, eluting the residue with a mixture of ethyl acetate and water, the organic layer was washed with brine and dried over Na<sub>2</sub>S<sub>2</sub>O<sub>4</sub> anhydrous, evaporated in vacuo. The crude product was purified by chromatography using CH<sub>2</sub>Cl<sub>2</sub>, CH<sub>2</sub>Cl<sub>2</sub> /ether (95:5) as eluent. The Compound **10** was obtained as white powder (yield = 29.5%).

<sup>1</sup>H- NMR (300 MHz, CDCl<sub>3</sub>) δ 1.00 – 1.90 (8H, m, H-2', H-3', H-4', H-5'), 2.00 - 2.20 (1H, m), 2.40-2.80 (3H, m, H-4, H-1a), 3.00-3.20 (2H, m), 3.75 (3H, s, OCH<sub>3</sub>), 4.20-4.40 (1H, m, H-2), 4.60-4.80 (1H, m, H-1''), 6.85 (2H, d, H-5 and H-8), 7.50 (2H, m, H-2, H-6'), 8.25 (2H, d, H-3', H-5'); <sup>13</sup>C NMR (300 MHz, CDCl<sub>3</sub>) δ 23.7 (2C), 27.3 (1C), 32.0 (1C), 33.0 (1C), 34.4 (2C), 46.5 (1C, C-2), 56.0 (1C, CH<sub>3</sub>), 86.0 (1C), 111.0 (1C), 112.5 (1C), 114.7 (2C), 126.9 (1C), 127.4 (1C), 127.7 (1C), 129.0 (2C), 146.6 (1C), 147.1 (1C), 160.4 (1C, C-OH), 166.2 (1C, CO); ms : ei (m/z) 380 (100%, M-1); Anal. Calcd. for C<sub>23</sub>H<sub>27</sub>NO<sub>4</sub>: C 72.42%, H 7.13%, N 3.67%. Found: C 75.42%, H 7.54%, N 4.40%.

**Synthesis of N-(7-cyclopentyloxy-6-methoxy-1,2,3,4-tetrahydro-naphthalen-2-yl)-3-hydroxy-4-methoxy-benzamide (Compound 9)**

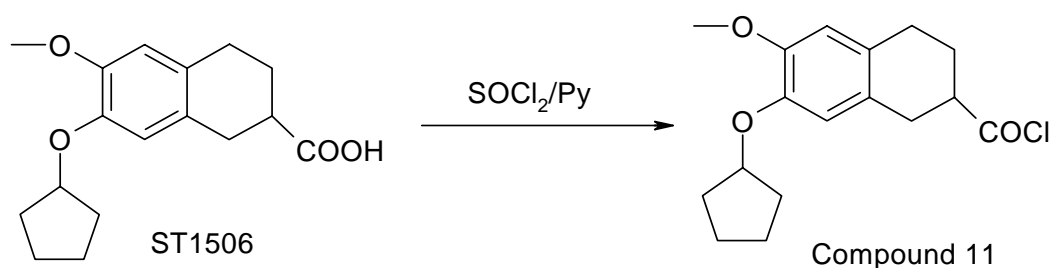


To a solution of ST1683 (50mg, 0.17mmol) in water, Et<sub>3</sub>N (50μL, 0.34mmol) was added at 0°C, after 10 min. 3-hydroxy-4-methoxy benzoic acid (30mg, 0.17mmol) in H<sub>2</sub>O / CH<sub>3</sub>CN (0.5:1) and EEDQ (46mg, 0.18mmol) in CH<sub>3</sub>CN were added dropwise. The reaction mixture was left at 50°C for 3h. The solvent was evaporated in vacuo and the residue was diluted with ethyl acetate and washed with a 5% solution of HCl, brine to pH 7. The organic layer was dried on Na<sub>2</sub>HSO<sub>4</sub> anhydrous, and evaporated in vacuo. The crude product was purified by TLC chromatography, using ethyl acetate as eluent. The product Compound 9 was obtained as white product (yield =17%).

<sup>1</sup>H- NMR ( 300 MHz, CDCl<sub>3</sub>) δ 1.02 – 2.00 ( 8H, m, H-2'', H-3'', H-4'', H-5''), 2.50 - 2.60 (1H, m, H-1a), 2.62-2.80 ( 2H, m, H-4), 3.00-3.20 (1H, dd, H-1b), 3.60 ( 3H, s, OCH<sub>3</sub>), 3.80 (3H, s, OCH<sub>3</sub>), 4.40 (1H, m, H - 2), 4.60 (1H, m, H-1''), 6.00 (1H, d), 6.50 (2H, d), 6.80 (1H, d), 7.00 (1H, d), 7.80 (1H, s), 8.00 (1H, d); <sup>13</sup>C NMR ( 300 MHz, CDCl<sub>3</sub>) δ 23.7 (2C), 27.3 (2C), 31.9 (1C), 32.7 (2C), 34.4 (2C), 46.3 (1C), 56.1 (1C, CH<sub>3</sub>), 60.0 (1C, CH<sub>3</sub>), 88.0 (1C,C-1), 114.0 (2C), 114.8 (1C), 118.2 (1C), 127.2 (1C), 130.4 (1C), 134.3 (1C), 146.5 (1C), 151.0 (1C), 158.2 (1C), 170.2 (1C, CO); ms : ei (m/z) 410 (100%, M-1); Anal. Calcd. for C<sub>24</sub>H<sub>29</sub>NO<sub>5</sub>: C 70.05%, H 7.10%, N 3.40%. Found: C 64.00%, H 9.00%, N 2.40%.

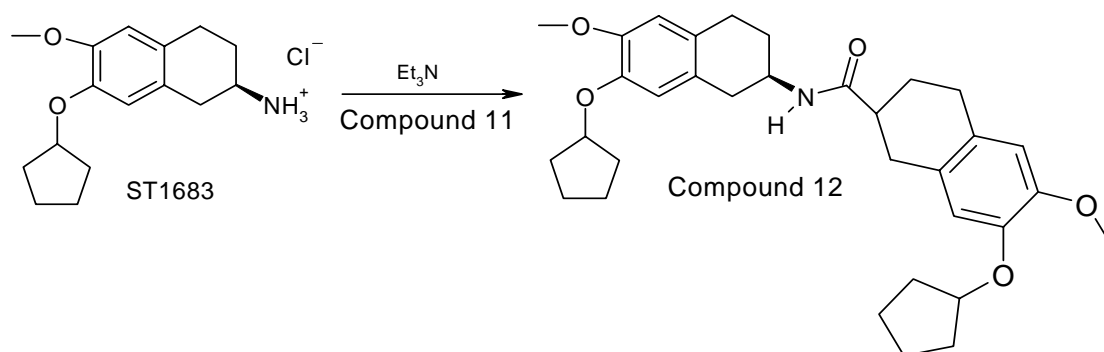


**Synthesis of (2R)-7-(cyclopentyloxy)-6-methoxy-1,2,3,4-tetrahydronaphthalene-2-carbonyl chloride (Compound 11)**



To a solution of (2R)-7-(cyclopentyloxy)-6-methoxy-1,2,3,4-tetrahydronaphthalene-2-carboxylic acid (ST1506, 50mg, 0.17mmol) in  $\text{CH}_2\text{Cl}_2$  dry, pyridine (30 $\mu\text{L}$ , 0.34mmol) and thionyl chloride (70  $\mu\text{L}$ , 0.85mmol) were added at 0°C. The solution was left at room temperature, for 1h. The reaction mixture was evaporated in vacuo, the residue was washed a number of times with  $\text{CH}_2\text{Cl}_2$ .

**Synthesis of 7-cyclopentyloxy-6-methoxy-1,2,3,4-tetrahydro-naphthalen-2-carboxylic acid-(7-cyclopentyloxy-6-methoxy-1,2,3,4-tetrahydro-naphthalen-2-yl)amide (Compound 12)**

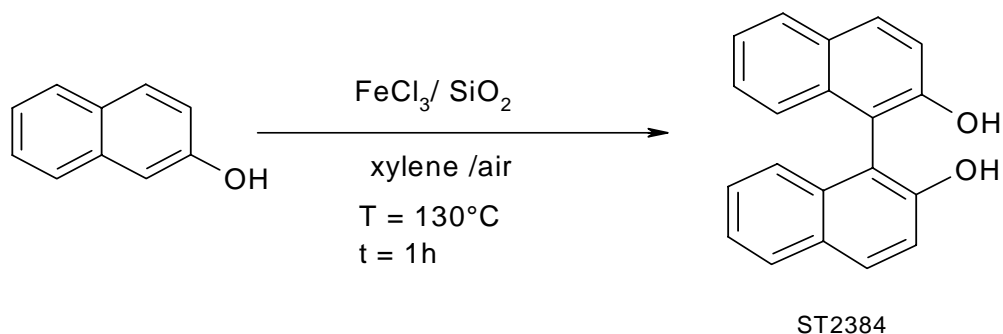


To ST1683 (50mg, 0.2mmol) suspended in  $\text{CH}_2\text{Cl}_2$  anhydrous at 0°C,  $\text{Et}_3\text{N}$  dry (47 $\mu\text{L}$ , 0.34mmol) was added. When the starting material was completely dissolved, the

intermediate D ( 0.2mmol) in 0.8mL of CH<sub>2</sub>Cl<sub>2</sub> dry was added dropwise to the solution. The reaction mixture was left at room temperature for 3h. Even though the reaction was not complete , as highlighted by TLC hexane /ethyl acetate (8:2), it was quenched . The work up consisted in eluting the reaction mixture with CH<sub>2</sub>Cl<sub>2</sub> , which was washed with a solution of HCl 5% and neutralized by a saturated solution of NaHCO<sub>3</sub> up to pH = 7. The organic layer was washed with brine and dried over Na<sub>2</sub>S<sub>2</sub>O<sub>4</sub> anhydrous, evaporated in vacuo. The crude product was purified by chromatography using CH<sub>2</sub>Cl<sub>2</sub>, CH<sub>2</sub>Cl<sub>2</sub> /ether (6:4) as eluent. The product was obtained as white powder (yield < 5%).

<sup>1</sup>H- NMR ( 300 MHz, CDCl<sub>3</sub>) δ 0.98–1.80 ( 16H, m, H-2 and H-2'', H-3',3'', H-4',4'', H-5', 5''), 2.00-2.20 (1H, m, H-3), 2.40-2.90 (12H, m, H-1', H-3', H-4', H-1, H-4, H-3), 3.70 (6H, s, OCH<sub>3</sub>), 4.00-4.20 ( 1H, m, H-2), 4.60 (2H, m, H-1'' and H-1'''), 6.60 (2H, m, H – 5 and H- 8), 7.40 (1H, m), 7.60 (1H, m), 8.02 (1H, brs); <sup>13</sup>C NMR ( 300 MHz, CDCl<sub>3</sub>) δ 20.1 (4C), 24.5 (1C), 27.9 (1C), 30.1 (1C), 31.9 (1C), 34.3 (1C), 38.4 (4C), 43.2 (1C), 46.2 (2C), 65.0 (2C,CH<sub>3</sub>), 90.2 (2C), 111.5 (1C), 111.8 (1C), 112.2 (1C), 112.4 (1C), 125.5 (1C), 126.7 (1C), 127.4 (1C), 129.4 (1C), 143.2 (1C), 143.4(1C), 143.8 (1C), 149.3 (1C), 170.2 (1C, CO); ms : ei (m/z) 543 (100%, M<sup>+</sup>+1); Anal. Calcd. for C<sub>33</sub>H<sub>43</sub>NO<sub>5</sub>: C 74.27%, H 8.12%, N 2.62%. Found: C 70.43%, H 9.00%, N 2.40%.

## Synthesis of 1,1'-binaphthalene-2,2'-diol (ST2384)



A three-necked round bottom flask was charged with  $\text{FeCl}_3/\text{Al}_2\text{O}_3$  (650mg, 4mmol), beta-naphthol (288mg, 1.99mmol), and xylene (15mL). The mixture was stirred vigorously at refluxing temperature for 20 min whilst bubbling air through the mixture. TLC showed that the starting material was completely converted to the product. After cooling, the catalyst was removed by filtration and washed with hot toluene and then with  $\text{CH}_2\text{Cl}_2$ . The solvent of the recombined filtrate was evaporated under reduced pressure to give the product as grey solid. This was treated with active carbon and crystallised from toluene to provide the ST2384 (yield = 49%).

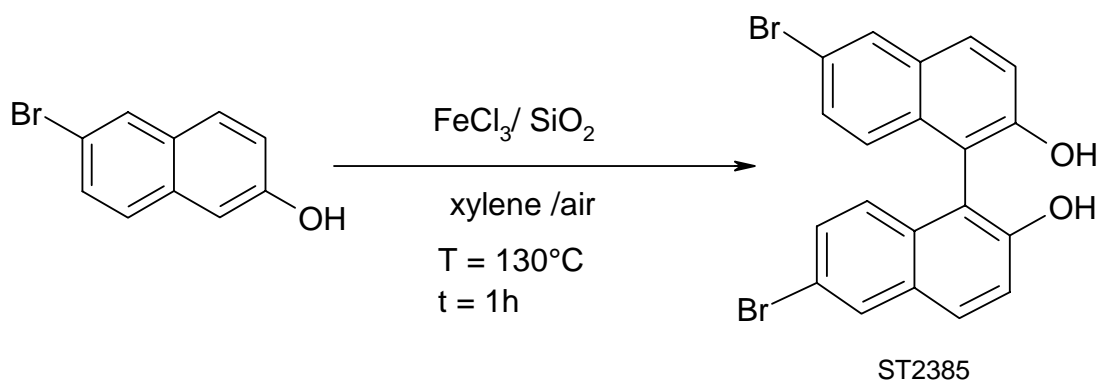
$^1\text{H-NMR}$  (300 MHz,  $\text{CDCl}_3$ )  $\delta$  5.03 (2H, br s, -OH-), 7.15 (2H, d, H-3 – H-3'), 7.31 (2H, dd, H-6 – H-6'), 7.7.38 (2H, d, H-7 - H-7'), 7.39 (2H, d, H-4 – H-4'), 7.89 (2H, d, H-8 – H-8'), 7.98 (2H, d, H-5 – H-5');  $^{13}\text{C NMR}$  (300 MHz,  $\text{CDCl}_3$ )  $\delta$  110.7 (2C), 117.71 (2C), 124.02 (2C), 124.16 (2C), 127.38 (2C), 128.3 (2C), 129.4 (2C), 131.40 (2C), 133.35 (2C), 152.70 (2C, -OH); ms : ei (m/z) 285.5 (100%, M-1); Anal. Calcd. for  $\text{C}_{20}\text{H}_{12}\text{O}_2$ : C 81.72%, H 5.00%. Found: C 83.89%, H 4.92%.

### Preparation of $\text{FeCl}_3$ adsorbed on $\text{SiO}_2$ :

To a solution of  $\text{FeCl}_3 \cdot 6\text{H}_2\text{O}$  (16.7g, 61.7mmol) in acetone (250ml) was added silica gel (90g, 200-300mesh), and the slurry was stirred at room temperature for 30min. The

solvent was removed by a rotary vapor at 40°C and then 80°C under reduced pressure. The resulting yellow powder was obtained (95g).

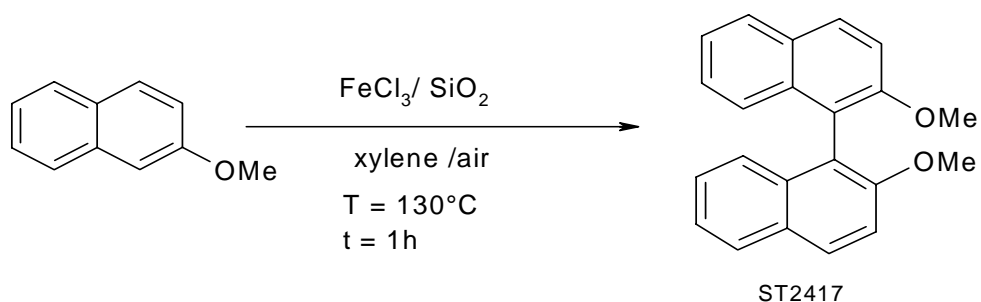
### Synthesis of 6,6'-dibromo-1,1'-binaphthalene-2,2'-diol (ST2385)



A three-necked round bottom flask was charged with FeCl<sub>3</sub>/ Al<sub>2</sub>O<sub>3</sub> (418mg, 2.5mmol), 6-Br- 2-naphthol (288mg, 1.99mmol), and xylene (15mL). The mixture was stirred vigorously at refluxing temperature for 20 min whilst bubbling air through the mixture. TLC showed that the starting material was completely converted to the product. After cooling, the catalyst was removed by filtration and washed with hot toluene and then with CH<sub>2</sub>Cl<sub>2</sub>. The solvent of the recombined filtrate was evaporated under reduced pressure to give the product as grey solid. This was treated with active carbon and crystallised from toluene to provide the ST2385 as white powder (yield = 23%).

<sup>1</sup>H- NMR ( 300 MHz, CDCl<sub>3</sub>) δ 5.01 ( 2H, br s, -OH-), 6.95( 2H, d, H-3 – H-3'), 7.38 (2H, dd, H-7 –H- 7'), 7.40 ( 2H, d, H-4 - H-4'), 7.87 (2H, d, H-8– H-8'), 7.98 (2H, d); <sup>13</sup>C NMR ( 300 MHz, DMSO) δ 113.2 (2C, C-1 and 1'), 119.2 (2C, C-6,6'), 120.8 (2C, C-3,3'), 124.6 (2C, C-8,8'), 127.3 (2C), 131.2 (2C, C-4,4'), 132.0 (2C, C-7,7'), 132.8 (2C, C-5,5'), 132.4 (2C), 152.3 (2C, C-2,2'); ms : ei (m/z) 442 (100%, M-1); Anal. Calcd. for C<sub>20</sub>H<sub>12</sub>O<sub>2</sub>Br<sub>2</sub>: C 54.08%, H 2.72%, Br 35.98%. Found: C 55.52%, H 3.66%, Br 41.89%.

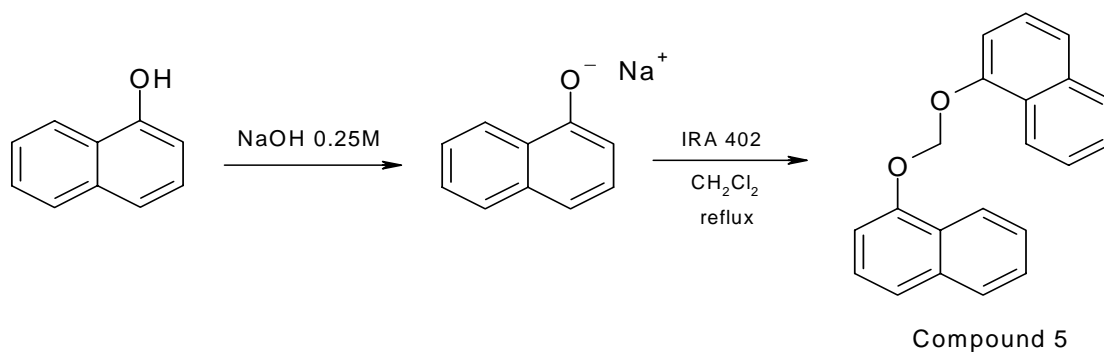
### Synthesis of 2,2'-dimethoxy-1,1'-binaphthlene (ST2417)



A three-necked round bottom flask was charged with  $\text{FeCl}_3/\text{Al}_2\text{O}_3$  (678mg, 4mmol), 2-methoxynaphthalene (300mg, 1.99mmol), and xylene (15mL). The mixture was stirred vigorously at refluxing temperature for 20 min whilst bubbling air through the mixture. TLC showed that the starting material was completely converted to the product. After cooling, the catalyst was removed by filtration and washed with hot toluene and then with  $\text{CH}_2\text{Cl}_2$ . The solvent of the recombined filtrate was evaporated under reduced pressure to give the product as grey solid. This was treated with active carbon and crystallised from toluene to provide the ST2417 (yield = 23%).

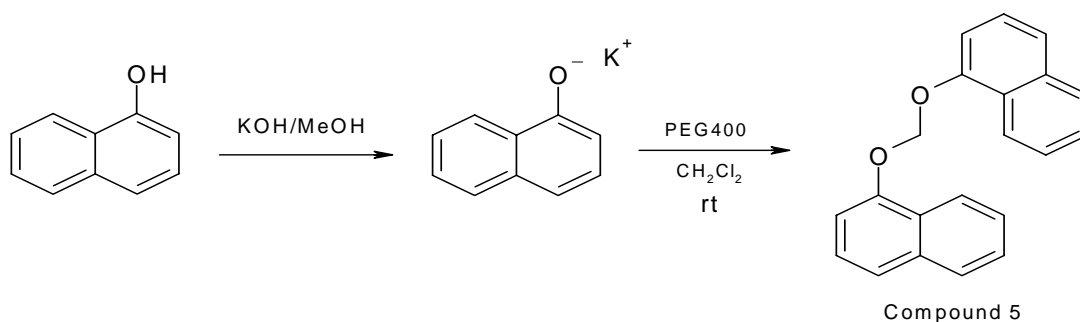
$^1\text{H-NMR}$  (300 MHz, d-DMSO)  $\delta$  3.70 (6H, s, 2x  $-\text{OCH}_3$ ), 6.90 (2H, d, H-3 – H-3'), 7.20 (2H, t, H-6 – H-6'), 7.30 (2H, t, H-7 – H-7'), 7.59 (2H, d, H-4 – H-4'), 7.90 (2H, d, H-5 – H-5'), 8.08 (2H, d, H-3 – H-3');  $^{13}\text{C-NMR}$  (300 MHz, d-DMSO)  $\delta$  56.0 (2C,  $\text{CH}_3$ ), 108.7 (2C, C-1,1'), 115.5 (2C, C-3,3'), 123.6 (2C, C-6,6'), 126.4 (2C), 127.5 (2C), 127.7 (2C, C-8 and 8'), 129.2 (2C, C-5,5'), 132.5 (2C, C-4,4'), 136.7 (2C), 158.0 (2C, C- $\text{OCH}_3$ ); ms : ei (m/z) 314 (100%,  $\text{M}^+ + 1$ ), 331 ( $\text{M}^+ + \text{NH}_4^+$ ); Anal. Calcd. for  $\text{C}_{22}\text{H}_{18}\text{O}_2$ : C 84.05%, H 5.35%. Found: C 82.52%, H 6.22%.

### Synthesis of 1-[(1-naphthyloxy)methoxy]naphthalene (Compound 5)



A column packed with Amberlite IRA 402 (Cl<sup>-</sup>) was washed with 0.25M aqueous sodium salt of a-naphthol (prepared by dissolving 133mg of a-naphthol in 3.68ml of NaOH 0.25M) until the complete removal of chloride ions. The resin was then washed successively with water, ethanol and ether. The amberlite IRA402 conditioned with sodium salt of naphthol and 1ml of dichloromethane was refluxed overnight. The reaction was followed by TLC, using as eluent hexane/ethyl acetate (8:2). The mixture was cooled at room temperature, the red resin was filtered and washed with more dichloromethane. The organic layer was evaporated under vacuum. The crude product was purified by flash chromatography, using hexane/ethyl acetate (9:1) as eluent. The final product was obtained as white powder (yield = 1.7%).

### Diaryloximetane derivate by peg methodology: Synthesis of Compound 5



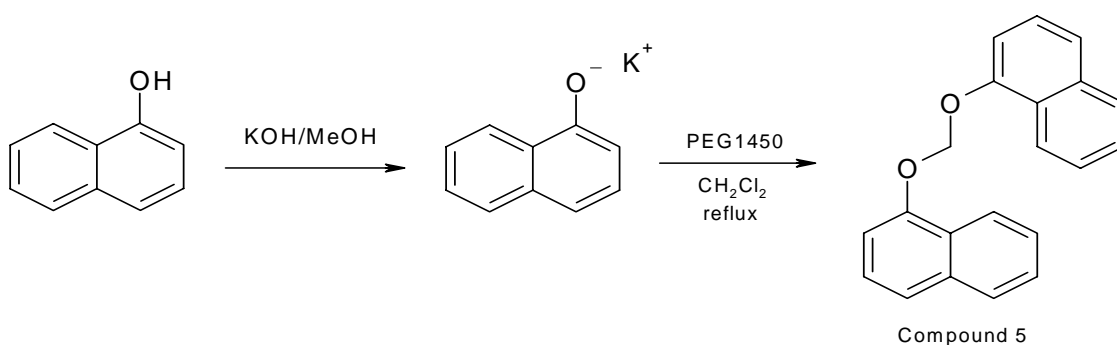
A mixture of the potassium salt of the 1-naphthol (1mmol, 500mg), (prepared by dissolving phenol 1mmol and potassium hydroxide 1mmol, in methanol 3.77ml and evaporating the solvent under reduced pressure) PEG-400 (96mg) and dichloromethane(5ml) was stirred at room temperature for 27h. The reaction was followed by TLC hexane/ethyl acetate (8:2). The reaction was quenched by diluting dichloromethane and washing it with water; the organic layer was dried over anhydrous Na<sub>2</sub>SO<sub>4</sub>. The solvent was evaporated under reduced pressure and the crude product was purified by Flash chromatography, using as eluent hexane/ethyl acetate (9:1). The product was obtained as white powder (yield = 20%).

The same reaction was reprepared using PEG1450 as catalyst, obtaining the same product with the same yield, and using PEG 600 (8%).

The same reaction was reprepared using PEG600 as catalyst, and CH<sub>2</sub>Br<sub>2</sub> at room temperature for 27h, obtaining the same product, Compound 5, (20%).



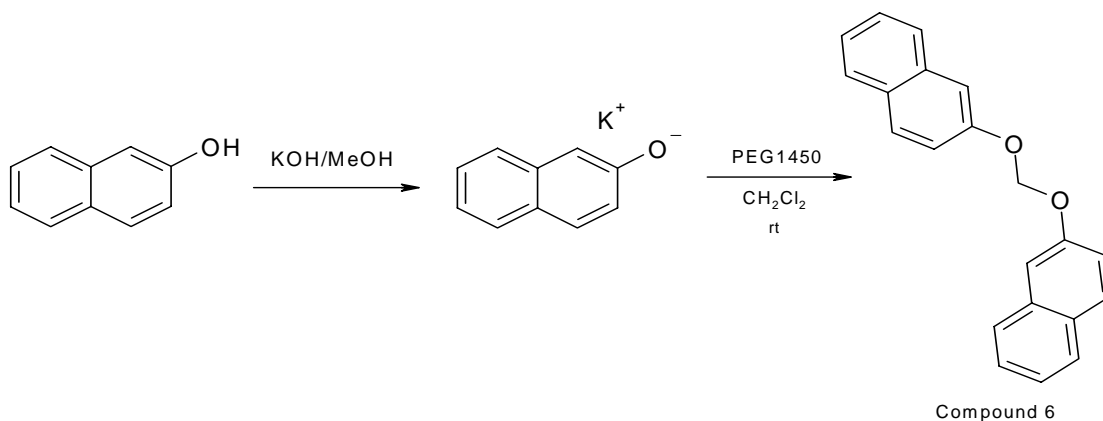
## Synhtesis of Compound 5



A mixture of the potassium salt of the 1-naphthol (1mmol, 500mg), (prepared by dissolving phenol 1mmol and potassium hydroxide 1mmol, in methanol 3.77ml and evaporating the solvent under reduced pressure) PEG-1450 (0.2mmol, 1g) and dichloromethane (15ml) was stirred at reflux for 27h. The reaction was followed by TLC hexane/ethyl acetate (8:2). The quenching of the reaction consisted in cooling the mixture at room temperature, the dichloromethane was washed with water and dried over anhydrous Na<sub>2</sub>SO<sub>4</sub>. The solvent was evaporated under reduced pressure and the crude product was purified by Flash chromatography, using as eluent hexane/ethyl acetate (9:1). The product was obtained as white powder (yield = 35%).

<sup>1</sup>H- NMR ( 300 MHz, CDCl<sub>3</sub>) δ 6.10 ( 2H, s, CH<sub>2</sub>), 7.19-7.45 (10H, m), 7.70-7.80 (2H, m, H-3,3'), 8.19-8.22 (2H, m ,H-2,2'); <sup>13</sup>C NMR ( 300 MHz, CDCl<sub>3</sub>) δ 100.2 (1C, CH<sub>2</sub>), 105.7 (2C), 120.1 (2C), 122.1 (2C), 127.3 (2C), 127.5 (2C), 128.3 (2C), 128.8 (2C), 140.1 (2C), 150.6 (2C), 140.1 (2C); ms : ei (m/z) 301 (100%, M<sup>+</sup>+1); Anal. Calcd. for C<sub>21</sub>H<sub>16</sub>O<sub>2</sub>: C 83.98%, H 5.37%, O 10.65%. Found: C 70.43%, H 3.48%, O 8.35%.

## Synthesis of 2-[(2-naphthyloxy)methoxy]naphthalene (Compound 6)

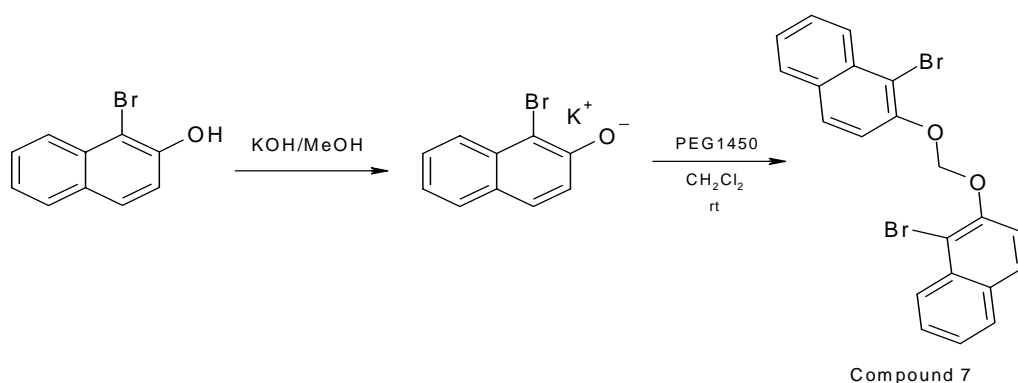


A mixture of the potassium salt of the 2-naphthol (0.7mmol, 100mg), (prepared by dissolving phenol 0.7mmol and potassium hydroxide 0.7mmol, in methanol 1ml and evaporating the solvent under reduced pressure) PEG-1450 (0.14mmol, 230mg) and dichloromethane (2.2ml) was stirred at room temperature for 27h. The reaction was followed by TLC hexane/ethyl acetate (8:2). The quenching of the reaction was done by diluting the dichloromethane and washing it with water. The organic layer was dried over anhydrous Na<sub>2</sub>SO<sub>4</sub>. The solvent was evaporated under reduced pressure and the crude product was purified by Flash chromatography, using as eluent hexane/ethyl acetate (8:2). The product was obtained as white powder (yield = 16.6%).

<sup>1</sup>H- NMR ( 300 MHz, CDCl<sub>3</sub>) δ 5.97 ( 2H, s, CH<sub>2</sub>), 7.17-7.42 (2H, m, H-1,1'), 7.47-7.59 (4H, m, H-3,3'), 7.73-7.80 (6H, m), 8.15-8.19 (2H, m); <sup>13</sup>C NMR ( 300 MHz, CDCl<sub>3</sub>) δ 105.7 (1C, CH<sub>2</sub>), 110.0 (1C), 104.1 (1C, CH<sub>2</sub>), 110.5 (2C), 118.2 (2C), 123.4 (12C), 125.4 (2C), 126.9 (2C), 127.1 (2C), 127.9 (2C), 134.5 (2C), 138.5 (2C), 155.4 (2C, C-2,2'); ms : ei (m/z) 301 (100%, M<sup>+</sup>+1); Anal. Calcd. for C<sub>21</sub>H<sub>16</sub>O<sub>2</sub>: C 83.98%, H 5.37%, O 10.65%. Found: C 70.43%, H 3.48%, O 8.35%.

## Synthesis of 1-bromo-2-[[1-(1-bromo-2-naphthyl)oxy]methoxy]naphthalene

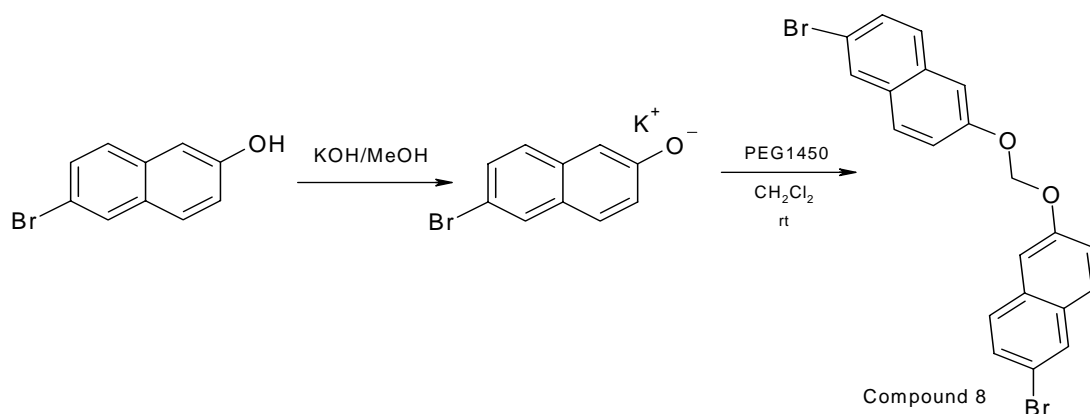
### (Compound 7)



A mixture of the potassium salt of the 1-Br-2-naphthol (0.45 mmol, 100mg), (prepared by dissolving phenol 0.45mmol and potassium hydroxide 0.45mmol, in methanol 1ml and evaporating the solvent under reduced pressure) PEG-1450 (0.09mmol, 130mg) and dichloromethane (2.2ml) was stirred at room temperature for 27h. The reaction was followed by TLC hexane/ethyl acetate (8:2). The reaction was quenched by diluting the dichloromethane and washing it with water and dried over anhydrous Na<sub>2</sub>SO<sub>4</sub>. The solvent was evaporated under reduced pressure and the crude product was purified by Flash chromatography, using as eluent hexane/ethyl acetate (8:2). The product was obtained as white powder (yield = 15.5%).

<sup>1</sup>H- NMR ( 300 MHz, CDCl<sub>3</sub>) δ 5.99( 2H, s, CH<sub>2</sub>), 7.39-7.57(7H, m, H-3,3'), 7.91-7.83 (5H, m, H-4,4', H- 8,8'); <sup>13</sup>C NMR ( 300 MHz, CDCl<sub>3</sub>) δ 102.0 (1C, CH<sub>2</sub>), 105.1 (2C), 115.5 (2C), 125.0 (2C), 126.8 (2C), 128.5 (2C), 128.8 (2C), 130.0 (2C), 130.8 (2C), 140.3 (2C), 155.1 (2C); ms : ei (m/z) 459 (100%, M<sup>+</sup>+1); Anal. Calcd. for C<sub>21</sub>H<sub>14</sub>O<sub>2</sub> Br<sub>2</sub>: C 55.05%, H 3.08%, O 6.98%. Found: C 50.20%, H 6.20%, O 4.78%.

**Synthesis of 2-bromo-6-[[[(6-bromo-2-naphthyl)oxy]methoxy]methoxy]naphthalene  
(Compound 8)**



A mixture of the potassium salt of the 6-Br-2-naphthol (0.45 mmol, 100mg), (prepared by dissolving phenol 0.45mmol and potassium hydroxide 0.45mmol, in methanol 1ml and evaporating the solvent under reduced pressure) PEG-1450 (0.09mmol, 130mg) and dichloromethane (2.2ml) was stirred at room temperature for 27h. The reaction was followed by TLC hexane/ethyl acetate (8:2). The reaction was quenched diluting the dichloromethane, washing it with water and dried over anhydrous Na<sub>2</sub>SO<sub>4</sub>. The solvent was evaporated under reduced pressure and the crude product was purified by Flash chromatography, using as eluent hexane/ethyl acetate (9:1). The product was obtained as white powder (yield = 33.33%).

<sup>1</sup>H- NMR ( 300 MHz, CDCl<sub>3</sub>) δ 5.98( 2H, s, CH<sub>2</sub>), 7.28-7.32 (2H, dd, H-1,1'), 7.51-7.54 (4H, dd, H-3,3', H- 8,8'), 7.64 (1H, s, H-4'), 7.67 (2H, d, H-5,5'), 7.71 (1H, s, H-4), 7.94 (2H, d, H-6,6'); <sup>13</sup>C NMR ( 300 MHz, CDCl<sub>3</sub>) δ 100.9 (1C, CH<sub>2</sub>), 107.4 (2C), 115.2 (2C, C-6,6'), 125.3 (2C), 130.2 (6C), 130.4 (2C), 134.5 (2C), 139.6 (2C), 153.42 (2C); ms : ei (m/z) 459 (100%, M<sup>+</sup>+1); Anal. Calcd. for C<sub>21</sub>H<sub>14</sub>O<sub>2</sub> Br<sub>2</sub>: C 55.05%, H 3.08%, O 6.98%. Found: C 50.20%, H 3.48%, O 5.98%.

## II. Biology

### **The Preparation of Samples**

A mother liquor of drugs, to test as fibrillogenesis inhibitors, was prepared, dissolving them in DMSO. This solution was diluted with water up to the final concentration of 10 and 100 $\mu$ M. The drugs, which showed they were active, were tested again at available concentration to calculate the IC<sub>50</sub> value. The total percentage of DMSO in the drug solution had to be less than 10%.

#### **A $\beta$ - not aggregated Sample Preparation (A $\beta$ -NA):**

The peptide A $\beta$  (1-42) was dissolved in H<sub>2</sub>O/CH<sub>3</sub>CN (1:1) mixture at final concentration of 1mg/ml. The solution was fractionized in 2ml samples and stored at  $-80^{\circ}$ C until its use. These samples would have been further diluted with water (per 5 time) up to the final concentration of 44.3 $\mu$ M at the test execution time.

#### **A $\beta$ - aggregated Sample Preparation (A $\beta$ -A):**

The peptide A $\beta$  (1-42) was dissolved in H<sub>2</sub>O/CH<sub>3</sub>CN (1:1) mixture at a final concentration of 1mg/ml. An aliquot sample (2ml) of this solution was lyophilized overnight in order to eliminate TFA eventually due to the peptide synthesis. The lyophilized A $\beta$  (1-42) was successively dissolved in DMSO (0.1mL) and PBS 2x (double concentration) (5mL) at pH = 7.4 (86.9 $\mu$ M). After the dissolution, the A $\beta$  (1-42) was incubated at 37 $^{\circ}$ C for 8 days; at the end of incubation the sample was sonicated and further diluted by PBS 2x until final concentration of 17.4 $\mu$ M. The A $\beta$  (1-42) aggregated was fractionated and stored at  $-80^{\circ}$ C until its use.

### Screening of inhibitor activity of A $\beta$ aggregation:

Into the wells of a 96-well plate, the sample drugs to test at the right concentration, was pipetted on A $\beta$  aggregated [(A $\beta$ -A), final concentration of 5.8 $\mu$ M]; after 15 minutes, the A $\beta$  not aggregated [(A $\beta$ -NA), final concentration of 11.1 $\mu$ M] was added on (see the table 4). The 96-well plate was incubated at 37°C under stirring for 24h.

### Scheme of well-plate loading: table IV

	<b>PBS</b>	<b>H<sub>2</sub>O</b>	<b>Vehicle</b> (H <sub>2</sub> O)	<b>A<math>\beta</math>-A</b>	<b>Sample</b>	<b>A<math>\beta</math>-NA</b>
<b>Control</b>	40 $\mu$ L	30 $\mu$ L	50 $\mu$ L			
<b>Control+Sample</b> (high concentration)	40 $\mu$ L	30 $\mu$ L			50 $\mu$ L	
<b>A<math>\beta</math></b> (control)			50 $\mu$ L	40 $\mu$ L		30 $\mu$ L
<b>A<math>\beta</math>+Sample</b>				40 $\mu$ L	50 $\mu$ L	30 $\mu$ L

At the end of daily incubation, 200 $\mu$ L of a buffer solution composed of ThT 10 $\mu$ M and Na<sub>2</sub>PO<sub>4</sub> x 2H<sub>2</sub>O (50 $\mu$ M) at pH = 6.5 was pipetted into each well-plate.

VICTOR 2(WALLAC) was used as spectrofluorimeter at 450nm in excitation and 486 nm in emission spectra for 60 seconds.

The data relative to the inhibition activity of A $\beta$  aggregation are reported as IC50. These values come from an elaboration (GraphPad Prism, Version 3.0) of the aggregation percentage data, which are calculated by the following formula:

$$\frac{V(\beta\text{- amyloid + sample}) - V(\text{Bianco + sample})}{V(\beta\text{-Amyloid control}) - V(\text{control})} \times 100$$

$$V(\beta\text{-Amyloid control}) - V(\text{control})$$

V means the medium fluorescence value, in particular, V( $\beta$ -Amyloid control) represents the medium fluorescence value relative to 100% of aggregation; V(control) means medium fluorescence value relative to 0% of aggregation. Low percentage of aggregation corresponds to high inhibition drug activity.

The IC<sub>50</sub> values are reported in biology and SAR analysis section (See Results and Discussion).

## 5. Bibliography

1. D. B. Teplow, Amyloid: *Int. J. Exp. Clin. Invest*, **1998**, 5, 121-142.
2. Soo Borson MD, and Murray A. Raskind, MD, *Neurology*, May **1997**, 48, (suppl. 6), 517.
3. M. S. Wolfe, *J. Med. Chem.*, **2001**, vol. 44, 13.
4. D. J. Selkoe, *Science*, **1997**, 275, 630–631.
5. M. C. Chartier-Harlin, F. Crawford, H. Houlden; A. Warren et al., *Nature*, **1991**, 353, 844-6.
6. J. Murrell, M. Farlow; B. Ghetti, M. D. Benson, *Science*, **1991**, 254, 97-9.
7. J. K. Teller; C. Russo, L. M. De Busk, G. Angelini et al., *Nat. Med.*, **1996**, 2, 93-5.
8. C. A. Lemere, T. J. Grenfell; D. J. Selkoe; *Am. J. Pathol.*, **1999**, 155, 29-37.
9. R. Sherrington et al., *Nature*, **1995**, 375, 754–60.
10. E. Levy-Lahad et al., *Science*, **1995**, 269, 937-7.
11. E. H. Corder et al., *Science*, **1993**, 261, 921–3.
12. K. R. Bales et al., *Proc. Natl. Acad. Sci. U.S.A.*, **1999**, 96, 15233-8.
13. A. B. Clippingdale, J. D. Wade and C. J. Barrow, *J. Peptide Sci.*, **2001**, 7, 227-249.
14. D. A. Kirschner et al., *Proc. Natl. Acad. Sci. U.S.A.*, **1986**, 83: 503-507.
15. K. S. Kosik, *Science*, **1992**, 256, 780-783.
16. R. E. Tanzi, J. F. Gusella et al., *Science*, **1987**, 235, 880-884.
17. M. P. Matson, *Physiol. Rev.*, **1997**, 77, 1081-1182.
18. M. Lalowski et al., *J. Biol. Chem.*, **1996**, 271, 33623-33631.
19. T. Dyrks et al., *J. Biol. Chem.*, **1992**, 267, 18210–18217.
20. C. Mc Keon – O'Malley et al., *Emerging Therapeutic Targets*, **1998**, 2 (2): 157–179.
21. D. H. Small, C. A. McLean, *Neurochem.*, **1999**, 73, 443–449.
22. C. J. Pike et al., *S. Neurosci.*, **1993**, 13, 1676-87.
23. A. Lorenzo, B. Yanker, *Proc. Natl. Acad. Sci. U.S.A.*, **1994**, 91, 12243-7.
24. C. J. Pike et al., *J. Neurochem.*, **1995**, 64: 253-265.
25. A. S. Cohen and E. Calkins, *Nature*, **1959**, 183, 1202-1203,.
26. R. D. Terry Gonatas NK and Weiss M.; *Am. J. Pathol.*, **1964**, 44, 269-297,.
27. D.A. Kirschner, C. Abraham and D. J. Selkoe, *Proc. Natl. Acad. Sci. U.S.A.*, **1986**, 83, 503-507.



28. H. A. Lashuel et al., *JBC papers in Press* 06/08/02.
29. C. Mc Keon – O'Malley, Sauwders, Bush, Tanzi, *Emerging Therapeutic Targhets*, **1998**, 2 (2).
30. M. N. Sabbagh, D. Galasko, and L. J. Thal; *Alzheimer's Disease Rewiew*, **1997**, 3, 1-19.
31. T. Bandiera, J. Lansen, C. Pest and M. Varasi, *Current Medicinal Chemistry*, **1997**, 4, 159-170.
32. C. Soto, *Molecular Medicine Today*, **1999**, 5, (8), 343-5.
33. M. A. Findeis, *Bioch. et Bioph. Acta*, **2000**, 1502, 76-84.
34. W.E. Klunk et al., *J. Histochem Cytochem*, **1989**, 37(8): 1273-1281.
35. SIGMA-TAU Patent EP1301463.
36. M. Hamdam, B. Masi, L. Rovatti, *Rapid Commun. Mass Spectrometry*, **1996**, 110, 1739-1742.
37. K. Watanabe et al. , *J. Peptide Res.*, **2001**, 8, 342-346.
38. T. Gunilla et al., *Methods in Enzymology*, **1999**, 309, 3.
39. H. Le Vine III, *Methods in Enzymology*, **1999**, 309, 274.
40. H. Puchtler and F. Sweat, *J. Histochem. Cytochem.*, **1965**, 13, 693.
41. H. Le Vine III, *Arch. Biochem. Biophys.*, **1997**, 342, 306.
42. H. I. Le Vine, *Arch. Biochem. Biophys.*, **1997**, 342, 306.
43. H. I. Le Vine III, *Prot. Sci.*, **1993**, 2, 404.
44. Mark A. Findeis, S. M. Molineaux, *Methods in Enzymology*, **1999**, 309 , 476.
45. J. Wall and A. Solomon, *Methods in Enzymology*, **1999** , 309, 28.
46. C. Hilbich et al., *J. Mol. Biol.*, **1991**, 218, 149-163.
47. E. Terzi et al, *Biochemistry*, **1994**, 33, 1345-1350.
48. S. Pollack et al., *Neurosciences Letter*, **1995**, 184, 113-116.
49. W. E. Klunk et al., *Neurobiol Aging* , **1994**, 15(6), 691-698.
50. <http://www.Alzforum.org/home.asp>
51. F. Iannone, O. I. Ursini, *J. Radioanal. Nucl. Chem.*, **2002**, 251, 363-368.
52. G. Angelini, O. Ursini, P. Minetti, D. Celona and F. De Angelis; *J. Label Comp. Radiopharm.*, **2004**, 47: 543-556.
53. C. Pascali, A. Bogni, F. Crippa, E. Bombardieri, *Concetti generali sulla produzione di radiofarmaci emettitori di positroni.*

54. M. W. Nader, S. K. Zeisler, A. Theobald and F. Oberdofer, *App. Radiat. Isot.*, **1998**, 49(12), 1599-1603,.
55. G. Berger et al., *J. of Labelled Compounds and Radiopharmaceuticals*, **1978**, vol XVII, (1), 59.
56. M. Maziera et al., *J. of Radioanalytical Chem.*, **1981**, 62, n. 1-2, 279-284.
57. D. Roeda, C. Crouzel, *Appl. Radiat. Isot.*, **2001**, 54 (6), 935-9.
58. Robinson and Weygand, *J. Chem. Soc.*, **1941**, 386.
59. J. March, *Advanced Organic Chemistry*, III edition, 493.
60. T. R. Kasturi, S. K. Jayaram et al., *Tetrahedron*, **1993**, 49, (32), 7145-7158.
61. T. R. Kasturi et al., *J. Chem. Soc. Perkin Trans 1*, **1984**, 2375.
62. T. R. Kasturi and K. A. Kumar, *Indian Journal of Chem.*, 34B, **1995**, 6-11.
63. J. Oliver, C. N. Lamb, R. H. Smith, *J. Agric. Food. Chem.*, **1983**, 31, 1178-1183.
64. Z. Bao Y. Chen; R.B. Cai; L. Yu, *Macromolecules*, **1993**, 26, 5281.
65. K. A. Bach ; F. Foubelo, Yusi M., *Tetrahedron*, **1994**, 50, 5139-5146.
66. K. Orito T. Hatakcyame; M. Takeo, H. Suginome, *Synthesis*, **1995**, 10, 1273.
67. S. G. Young ; Y. H. Kim., *Tetrahedron lett.*, **1999**, 40, 6051-6054.
68. M. C. Carreno, J. L. G. Ruano, M.A. Toledo, A. Urbano, *Tetrahedron Lett.*, **1996**, 37, ( 23), 4081-4084.
69. A. B. Font and T. de Mas Rocabarera, *J. Chem. Soc. Perkin Trans 1*, (3), 84, 81.
70. G. Casiraghi, G. Casnati, A. Pochini, G. Puglia, R. Ungaro, G. Sartori, *Synthesis*, **1981**, 143-145.
71. Yongchun Pan and Zhonghua Peng, *Tetrahedron Letter.*, **2000**, 41, 4537-4540.
72. N. G. Andersen, S. P. Maddaford and B. A. Keay, *J. Org. Chem.*, **1996**, 61, 26, 9556-9599.
73. *J. Org. Chem.*, **1991**, 56, (18), 5451-5456.
74. Y. Pan and Z. Peng, *Tetrahedron Letter.*, 41 (2000), 4537-4540.
75. *J. Org. Chem.*, vol. 56, n. 18, 1991.
76. T. Ohishi et al., *Tetrahedron Letter.*, **2001**, 42, 2493-2496.
77. T. R. Kasturi, K. A. Kumar, P. V. P. Pragnacharyulu, *Tetrahedron*, **1993**, 49, 1.
78. J. P. Poupelin, G. Saint. Ruf, O. F. Blanpin, G. Narcisse, G. U. Ernoui et R. Lacroix, *Eur. J. Med. Chem, Chimica terapeutica*, J. February, **1978-13**, 1, 67-71.

79. P. E. Georghiou, M. Ashram, Z. Li, S. G. Chaulk, *J. Org. Chem.*, **1995**, *60*, 7284-7289.
80. T. S. Li H. Y. Duan, B. Z. Li, Porij B. Tewari, S. H. Li, *J. Chem., Soc. Perkin Trans I.*, **1999**, 291-293.
81. K. Kurita, *Chem. Ind. (London)*, **1974**, 345.
82. C. Buoh et al., *Tetrahedron*, **2000**, *56*, 605-614.
83. Green, *The Protective Groups in Organic Synthesis*, II edition, 64.
84. M. L. Wolfrom, E. W. Koos, H. B. Bhat, *J. Org. Chem.*, **1967**, *32*, 1058.
85. R. C. Roemmele and H. Rapoport, *J. Org. Chem.*, **1988**, *53*, 2367-2371.
86. R. Compagnone, H. Rapoport, *J. Org. Chem.*, **1986**, *51*, 1713-1719.
87. M. M. Salunkhe, B. P. Salunkhe, A. S. Kanade, R. B. Mane and P. P. Wadgaonkar, *Synthetic Commun.* *20* (8), 1143-1147 (1990).
88. M. M. Salunkhe, B. P. Kavitate, S. V. Patir and P. P. Wadgaonkar, *J. Chem. Research* (8), 1995, 503.
89. SIGMA-TAU Patent WO02/00609.
90. S. V. D'Andrea, J. P. Freemon, P. F. Van Voigtlander, *Tetrahedron*, **1991**, *47* (32), 6157-6162,.
91. F. Mu, S. L. Coffing et al., *J. Med. Chem.*, **2001**, *44*, 441-452.
92. R. G. Strickley, *Pharmaceutical Research*, **2004**, *21*, 2.
93. Ping Li, S. E. Tabibi and S. H. Yalkowsky, *J. of Pharmaceutical Sciences*, **1998**, *87*, 12.